TUNNELLING EXPERIMENTS IN HIGH T_c SUPERCONDUCTORS: INTRINSIC AND HEATING EFFECTS

THÈSE N^{O} 3346 (2005)

PRÉSENTÉE À LA FACULTÉ SCIENCES DE BASE

Institut de physique de la matière complexe

SECTION DE PHYSIQUE

ÉCOLE POLYTECHNIQUE FÉDÉRALE DE LAUSANNE

POUR L'OBTENTION DU GRADE DE DOCTEUR ÈS SCIENCES

PAR

Thomas GEIGES

physicien diplômé EPF
de nationalité suisse et originaire de Zurich (ZH)

acceptée sur proposition du jury:

Prof. L. Forro, directeur de thèse
Prof. L. Mihaly, rapporteur
Prof. F. Mila, rapporteur
Prof. A. Schilling, rapporteur

Lausanne, EPFL
2005

Abstract

Tunnelling experiments have played an essential role in the development and verification of theories for superconductivity. They are usually interpreted within the so-called semiconductor model, in which the tunnelling current is given by the convolution of the density of states of the tunnelling electrodes.

With a break junction technique, we have measured the current-voltage characteristics $I(V)$ in the high T_c superconductor $Bi_2Sr_2Ca_{n-1}Cu_nO_{2(n+2)}$ at different temperatures and doping levels. The derivative dI/dV shows the well-known peak-dip-hump structure. These results, including their dependence on temperature and doping, are similar to that of other tunnelling experiments like scanning tunnelling microscopy, grain boundary junction or mesa structure experiments.

In mesa structures it is known that self-heating of the structure is a severe problem. At a bath temperature of 4.2 K, temperatures as high as T_c were measured in the mesa stack already when a voltage comparable to the dip-position was applied. The typical current-voltage characteristics can be described with a heating model, in which all the non-linearities are explained by only the temperature dependence of the junction resistance. It seems that the peak-dip-hump structure is an artefact of Joule heating.

This heating model can in principle also explain the peak-dip-hump structure of our break junction measurements. Many features like the temperature or doping dependence of the $I(V)$ characteristics are described naturally. Furthermore we realised that the so-called Kohlrausch relation gives an estimate of the junction temperature in function of the voltage that is consistent with the heating model. The typical features of our spectra are independent of the contact area between the broken parts: this observation has often been used as a proof against heating. The Kohlrausch relation shows that this argument does not hold.
For low bath temperatures the relation predicts that a voltage $U = 3.6\,k_B T/e$ has to be applied to reach the contact temperature T. This similarity to the BCS relation $2\Delta = 3.52\,k_B T_c$ makes clear that care has to be taken when an experimental feature appears at twice the BCS gap energy Δ: it might be caused by heating.

Due to problems of thermal dilatation of the sample holder, the validity of the heating model could only be tested qualitatively for our break junction technique. However, data of grain boundary structures allowed a more precise verification. These results are in very good agreement with the model predictions: the heating model is a valid alternative to the semiconductor model.

This work opens many questions concerning the validity of the semiconductor model. We argue that further investigation of heating effects in tunnelling experiments is important.

Version abrégée

Les expériences d'effet tunnel ont joué un rôle essentiel dans le développement de théories de la supraconductivité. On les interprète habituellement dans le cadre du "modèle semi-conducteur", dans lequel le courant est donné par la convolution de la densité d'états des électrodes.

Avec une technique de "break junction" (jonction de cassure), nous avons mesuré la caractéristique courant-tension $I(V)$ à différentes températures et niveaux de dopage dans le supraconducteur à haute T_c $Bi_2Sr_2Ca_{n-1}Cu_nO_{2(n+2)}$. La dérivée dI/dV présente la structure bien connue de "peak-dip-hump". Ces résultats, ainsi que la dépendance en température et dopage, sont similaires à ceux d'autres expériences, comme celles de microscopie à effet tunnel, de jonctions à joints de grains ou de structures Mesa.

Dans les structures Mesa, on sait que le réchauffement est un sérieux problème. A une température extérieure de 4.2 K, des températures aussi élevées que T_c ont été mesurées près de l'échantillon lorsque des tensions comparables à la position du "dip" sont appliquées. La caractéristique courant-tension typique peut être décrite au moyen d'un modèle de réchauffement, dans lequel toutes les non-linéarités sont expliquées par la dépendance en température de la résistance de la jonction uniquement. Il semble que la structure "peak-dip-hump" soit un artefact dû au réchauffement par effet Joule.

Ce modèle de réchauffement peut en principe aussi expliquer la structure "peak-dip-hump" de nos mesures de "break junction". Plusieurs caractéristiques telles que la dépendance en température ou en dopage de la relation $I(V)$ sont décrites de manière naturelle. En outre, nous nous sommes rendu compte que la relation de Kohlrausch, qui relie la tension appliquée et la température du contact, prédit une température qui est consistante avec le modèle de réchauffement. Les caractéristiques typiques de nos spectres sont indépendantes de la surface de contact entre les extrémités de la jonction: cette observation a souvent été utilisée en guise de preuve contre le réchauffement. La relation de Kohlrausch montre que cet argument n'est pas valable.
Pour des températures extérieures basses, la relation prédit qu'une tension $U = 3.6\,k_B T/e$ doit être appliquée pour atteindre la température du contact T. Le fait que cette expression ressemble à la relation $2\Delta = 3.52\,k_B T_c$ de la théorie BCS met en évidence qu'il faut considérer avec prudence les caractéristiques expérimentales apparaissant autour du double du gap Δ: il pourrait en effet s'agir d'effets de réchauffement.

A cause de problèmes de dilatation thermique du porte-échantillon, la validité du modèle n'a pu être testée que qualitativement pour notre technique de "break junction". En revanche, des données de structures de joints de grains ont permis une vérification plus précise du modèle. Ces résultats sont en très bon accord avec les prédictions: ce modèle de réchauffement est donc une alternative valide au modèle semi-conducteur.

Ce travail pose de nombreuses questions concernant la validité du modèle semi-conducteur. Nous jugeons nécessaire d'entreprendre une étude approfondie des effets de réchauffement dans les expériences d'effet tunnel.

Kurzfassung

Tunnelexperimente spielten eine entscheidende Rolle bei der Entwicklung einer Theorie für Supraleitung. Diese Experimente werden normalerweise mit dem so genannten Halbleiter Modell erklärt. Der Tunnelstrom ist dabei durch die Faltung der Zustandsdichten der Tunnelelektroden bestimmt.

Mit einer Bruch-Übergang (break junction) Technik haben wir die Strom-Spannungs Kurve $I(V)$ im Hochtemperatur Supraleiter $Bi_2Sr_2Ca_{n-1}Cu_nO_{2(n+2)}$ in Abhängigkeit von Temperatur und Dotierung gemessen. Die Ableitung dI/dV zeigt die bekannte „peak-dip-hump“ (Scheitelpunkt-Minimum-Buckel) Struktur. Diese Resultate, einschliesslich deren Temperatur- und Dotierungsabhängigkeit gleichen denjenigen von anderen Tunnelexperimenten wie Rastertunnelmikroskop (STM), Korngrenzen-Übergang oder Mesa Struktur Experimente.

Es ist bekannt, dass Selbstheizung ein ernst zu nehmendes Problem in Mesa Strukturen ist. Wenn eine Spannung vergleichbar mit derjenigen vom „dip“ über der Struktur angelegt wird, können in der Nähe des Mesas Temperaturen so hoch wie T_c gemessen werden, auch wenn die Badtemperatur nur gerade 4.2 K beträgt. Die typische Strom-Spannungs Kurve kann mit einem Heizmodell beschreiben werden, bei welchem alle Nichtlinearitäten einzig durch die Temperaturabhängigkeit des Widerstandes des Übergans erklärt werden. Es scheint, dass die „peak-dip-hump“ Struktur ein Artefakt von Joule-Heizung ist.

Dieses Heizmodell kann prinzipiell auch die „peak-dip-hump“ Struktur unserer Bruch-Übergang Messungen erklären. Viele Eigenheiten, wie die Temperatur- oder Dotierungsabhängigkeit werden in natürlicher Weise beschrieben. Wir haben zudem gemerkt, dass die so genannte Kohlrausch-Relation eine spannungsabhängige Kontakttemperatur voraussagt, die recht gut mit derjenigen übereinstimmt, die man vom Heizmodell erwarten würde. Gleichzeitig wird daraus auch klar, dass die Unabhängigkeit unserer Spektren von der Kontaktfläche zwischen den gebrochenen Teilen nicht als Beweis gegen ein Heizmodell gelten kann. Bei tiefen Temperaturen besagt diese Relation, dass eine Spannung von $U = 3.6\,k_BT/e$ eine Kontakttemperatur T hervorruft. Aus der Ähnlichkeit zur BCS-Relation $2\Delta = 3.52\,k_BT_c$ geht hervor, dass man sehr vorsichtig umgehen muss mit Merkmalen, die nahe der doppelten Energielückenenergie Δ auftreten: Sie können von Heizeffekten stammen.

Da wir in unseren Experimenten Probleme mit der thermischen Ausdehnung des Probenhalters haben, kann die Anwendbarkeit des Heizmodells auf unsere Bruchübergangsstrukturen nur qualitativ überprüft werden. Messungen in Korngrenzen-Übergängen erlaubten eine genaue Überprüfung des Heizmodells. Unsere Voraussagen wurden bestätigt: Das Heizmodell kann als gültige Alternative zum Halbleitermodell betrachtet werden.

Diese Arbeit stellt viele Fragen zur Gültigkeit des Halbleitermodells in den Raum. Wir schlagen vor, dass eine vertiefte Untersuchung von Heizeffekten in Tunnelexperimenten nötig ist.

Contents

Κινδυνεύει μὲν γὰρ ἡμῶν οὐδέτερος
οὐδὲν καλὸν κἀγαθὸν εἰδέναι,
ἀλλ' ουτος μὲν οἴεταί τι εἰδέναι οὐκ εἰδώς,
ἐγὼ δέ, ὡσπερ οὖν οὐκ οἶδα, οὐδὲ οἴομαι.
ἔοικα γοῦν τούτου γε σμικρῷ τινι
αὐτῷ τούτῳ σοφώτερος εἶναι,
ὅτι, ἃ μὴ οἶδα, οὐδὲ οἴομαι εἰδέναι.
(Je sais que je ne sais rien.)

Platon, *ΑΠΟΛΟΓΙΑ ΣΩΧΡΑΤΟΥΣ*, [21d]

ARPES	angle resolved photoemission spectroscopy
BCS	Bardeen-Cooper-Schrieffer
BSCCO	$Bi_2Sr_2Ca_{n-1}Cu_nO_{2(n+2)}$
BSCCO-2212	$Bi_2Sr_2Ca_1Cu_2O_8$
BSCCO-2223	$Bi_2Sr_2Ca_2Cu_3O_{10}$
dI/dV	derivative of the current with respect to the voltage
e	electron charge: $e = 1.60217653(14) \cdot 10^{-19}\,\mathrm{C}$
E_F	Fermi energy
$f(E)$	Fermi-Dirac distribution function $1/(e^{\frac{E-E_F}{k_B T}} + 1)$
$\hbar$	Planck's constant: $\hbar = 1.05457168(18) \cdot 10^{-34}\,\mathrm{Js}$
H	magnetic field
H_{c2}	upper critical field
I	current
I_c	critical current
$I(V)$	current measured as a function of the voltage
k_B	Boltzmann's constant: $k_B = 1.3806505(24) \cdot 10^{-23}\,\mathrm{J/K}$
L	Lorenz number: $L = (\pi k_B)^2/(3e^2) \approx 2.4 \cdot 10^{-8}\,\mathrm{W\Omega/K^2}$
$N(E)$	density of states
p	doping level
R	resistance
$R_{V\to 0}$	resistance at a low voltage $R = (dV/dI)_{V\to 0}$
STM	Scanning Tunnelling Microscope (Microscopy)
SIN	Superconductor-Insulator-Normal Metal
SIS	Superconductor-Insulator-Superconductor
SNS	Superconductor-Normal Metal-Superconductor
T	temperature
T_c	critical temperature of a superconductor
T_m	contact temperature
T_0	bath temperature
T^*	pseudogap temperature
U	voltage
V	voltage
Δ	superconducting gap energy
Δ_0	superconducting gap energy at zero temperature
λ	thermal conductivity
ρ	electrical resistivity

Reference for e, k_B and $\hbar$: 2002 CODATA recommended values

Introduction

A theory for high temperature superconductors is still lacking. A characteristic magnitude that is relatively easily accessible from both the experimental and theoretical side is the so-called superconducting gap. For conventional superconductors the BCS theory describes the experimentally confirmed relation between the gap and T_c.

In high temperature superconductors the temperature and doping dependence of the gap has been studied by different experimental techniques, like tunnelling or ARPES. The BCS theory and its d-wave generalisation are in obvious contradiction with these results. A theory for the high temperature superconductors has to be able to describe these experimental findings, thus the exact temperature and doping dependence of the gap can give a hint how to solve the mystery of high T_c superconductivity.

In our break junction technique the derivative of the current with respect to the voltage shows the well known peak-dip-hump structure. It is believed that the position of the peak is approximatively at two times the energy of the gap. In $Bi_2Sr_2Ca_{n-1}Cu_nO_{2(n+2)}$ we measured the temperature dependence of these spectra. The doping dependence was measured in samples where underdoping had been achieved by substituting calcium with praseodymium. We compared our results with the ones from literature.

After the publication of an article about heating effects in mesa structures by Zavaritsky [Phys. Rev. Lett. **92**, 259701 (2004)] it became clear that our data could also be explained principally in a completely alternative way, by a heating model. The independence of our spectra on the junction area seemed to be an argument against heating. Nevertheless we did some simple estimates of the junction temperature, and we realised soon that heating cannot a priori be excluded. For this reason we started to focus on the verification of the heating model.

As a first attempt we tried to measure very precisely the temperature dependence of the resistance of our junctions. The equality of the temperature and voltage dependence of the resistance could give a strong support for a heating picture. Due to problems of thermal dilatation of the sample holder, it is unfortunately not possible to perform these measurements precisely enough. We looked also for a theoretical expression to estimate the contact temperature. As an approach we took the Kohlrausch relation, and studied its applicability to our experiments. We had the possibility to test the predictions of the heating model and the Kohlrausch relation on data measured in a junction formed by a grain boundary in a thin layer of a cuprate. The stability of these junctions permit a good measurement of the temperature dependence of the resistance. Another attempt to detect heating effects was the realisation of pulsed measurements. The motivation was to try to record the $I(V)$ curves faster than the thermalisation of the junction.

Outline

In the first chapter I give an overview of some properties of high temperature superconductors. The aim of this chapter is to give the knowledge that is necessary to discuss the results and models of the following chapters.

Chapter 2 gives first a short description of the interpretation of the tunnelling curves with the semiconductor model. Then results of different tunnelling experiments are presented.

In Chapter 3 I show the results of our experiments in break junctions: we studied the temperature and doping dependence of the dI/dV curves. We performed pulsed measurements and studied hysteresis effects.

An alternative model for the interpretation of the non-linear current-voltage characteristics is given in Chapter 4. A heating model is described. An approach to find the temperature of the contact as a function of the voltage is given. We compare the predictions of the model with experimental findings. At the end of the chapter, the two models are opposed. We show arguments in favour and against both models.

In the last chapter I give a summary of the discussion about heating in tunnelling structures in the literature.

Chapter 1

High Temperature Superconductors

Superconductivity was discovered by Onnes in 1911 [1]. He found that the electrical resistivity in mercury disappears abruptly below a critical temperature T_c of 4.15 K. Similar behavior has been found in approximately 25 other chemical elements. T_c of all the elements is lower than 10 K. For almost 50 years after the discovery of superconductivity, there was no successful microscopic theory that could explain the phenomenon. Finally, in 1957, an apparently satisfactory theory [2] of superconductivity was presented by Bardeen, Cooper, and Schrieffer (BCS theory). This theory is based on the idea that under certain conditions, the electron-phonon interaction can lead to a net attraction. These coupled electrons can then take the character of a boson and condense into the BCS ground state. One of the most important pieces of experimental evidence which supports the BCS theory is the measurement of the gap, which is given by the BCS ratio. Tunnelling experiments played an essential role in the determination of the energy gap.

In 1986 Bednorz and Mueller [3] discovered superconductivity in the barium-lanthanum cuprate. At optimal doping, this compound has a critical temperature much higher than any other material known at that time. Already this discovery made clear that the BCS theory cannot explain this phenomenon, the so-called high-T_c superconductivity. Shortly afterwards many other compounds with similar structures were discovered. Among the most studied families are for example the yttrium-compounds or the BSCCO-family. To date, the highest T_c is attained in a mercury containing cuprate under pressure (Schilling *et al.*, Chu *et al.*) [4]. It lies around 160 K. It is clear that it would be difficult to explain superconductivity with a T_c of 100 K and more using electron-phonon coupling alone. Many different types of coupling mechanisms have been proposed. But a satisfactory theory explaining the high transition temperatures is still lacking, in spite of the over 100 000 articles on superconductivity that have been published after 1986.

1.1 Cuprates

The family of superconductors with the highest known T_c is the one of the cuprates. These materials have a complicated layered structure. Many physical properties, as

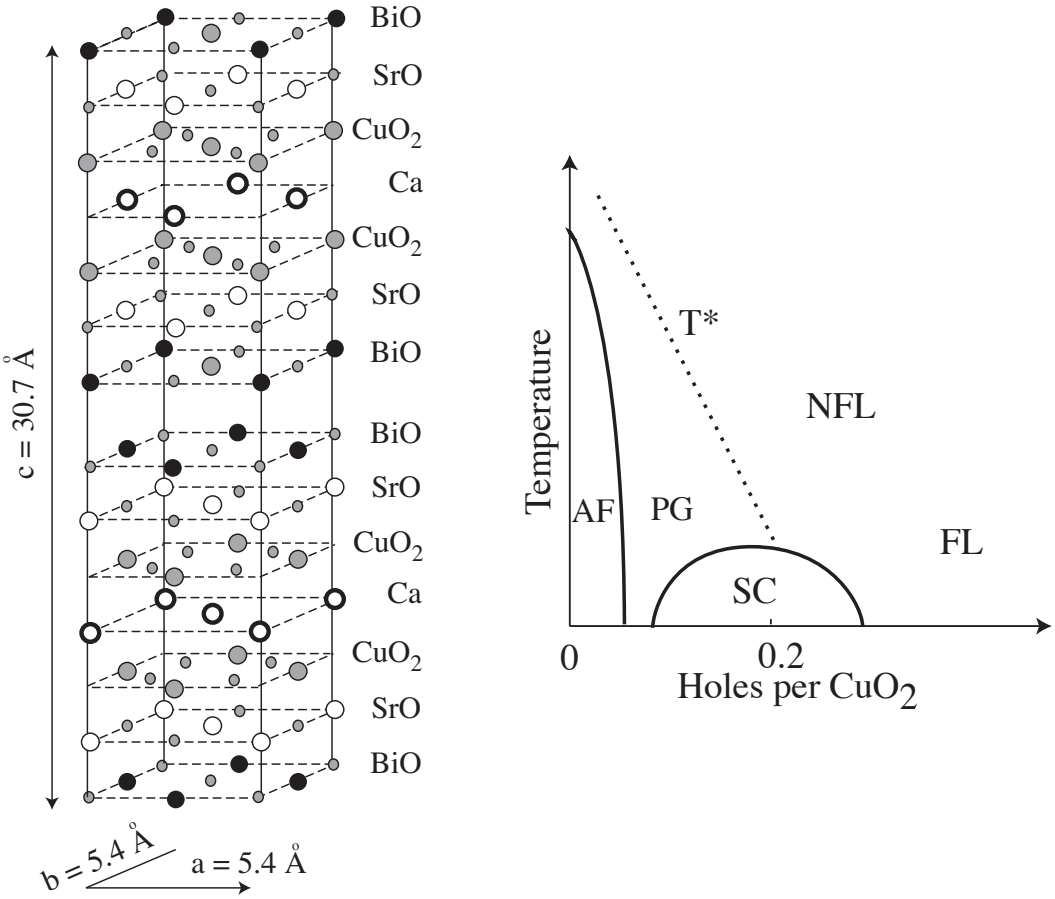

Figure 1.1: Left panel: The unit cell of the two layer BSCCO-2212 compound. Right panel: The phase diagram is strikingly similar for all the cuprates. The typical phases are the antiferromagnetic phase (AF), the superconducting phase (SC), the pseudogap phase (PG) in the non-Fermi liquid (NFL) phase and the Fermi liquid phase (FL).

for example the normal state conductivity, are significantly different when they are measured in the plane direction or perpendicular to the layers. Superconductivity is believed to occur in the CuO_2-planes, which are separated by various other layers.

The BSCCO-2212 compound is very suitable for break junction tunnelling experiments. As it cleaves easily, it it is simple to produce flakes. BSCCO exists in a one, two or three layer compound. The critical temperature, T_c, increases with the number of oxide layers between the CuO_2-planes. The general formula is $Bi_2Sr_2Ca_{n-1}Cu_nO_{2(n+2)}$, with $n = 1, 2$ or 3. The unit cell of BSCCO-2212 is shown in figure 1.1.

The physical properties of cuprates depend strongly on doping. All the cuprates have a generic phase diagram (see figure 1.1). Not only the superconducting region is a big mystery, but also many other regions of the phase diagram have properties that cannot be explained with the models of the actual solid state physics. A region of the phase diagram that is quite well understood is the undoped and strongly underdoped area: the material is an antiferromagnetically ordered insulator, with a Néel temperature of

several hundred Kelvins. With increasing doping, the Néel temperature falls quickly to zero, and we enter a spin-glass phase. This region of the phase diagram is followed by the so-called superconducting dome, which can empirically be approximated by a parabola with the formula (Tallon *et al.*) [5]

$$\frac{T_{\mathrm{c}}}{T_{\mathrm{c,max}}} = 1 - 82.6(p - 0.16)^2 \qquad , \tag{1.1}$$

where p is the doping level and $T_{\mathrm{c,max}}$ the critical temperature at optimal doping. At high doping levels we have a Fermi liquid. When we decrease the doping concentration, we enter into a non-Fermi liquid region. In the underdoped region, limited by the T^*-line, the cuprates are in a so-called pseudogap phase. This pseudogap has been a matter of particular interest and is also related to tunnelling experiments.

1.2 The superconducting energy gap

According to the BCS theory (Bardeen *et al.*) [2], the ground state of a superconductor is formed by condensed electron pairs. To remove a pair from the condensate, a certain energy is required. The lower bound is the double of the so called gap energy.

The gap is a fundamental quantity in the theory of superconductors. The BCS theory predicts a relation between the critical temperature and the gap at zero temperature:

$$\Delta_0 = 1.76\, k_{\mathrm{B}} T_{\mathrm{c}} \qquad . \tag{1.2}$$

When increasing the temperature, the magnitude of the gap decreases monotonically to zero at T_{c}. For temperatures near T_{c}, its temperature dependence can be approximated by $\Delta(T) = 1.74\Delta(0)[1 - \frac{T}{T_{\mathrm{c}}}]^{\frac{1}{2}}$. Experimental verification for this relation is one of the most important tests for the BCS theory.

Besides tunnelling measurements, many other techniques were used to determine the energy gap. In a short historical overview I list some of them:

An energy gap was implied, even before the BCS theory has been developed. Already in 1956, Corak *et al.* [6] measured the *specific heat* at low temperatures in tin. In order to find the electronic part of the specific heat C_{es} they subtracted the lattice contribution C_L from the measurements in the superconducting state. They assumed that $C_L = C_n - \gamma T$, where C_n is the total specific heat in the normal state and γ is the Sommerfeld constant. Between $0.3\,T_{\mathrm{c}} < T < 0.7\,T_{\mathrm{c}}$ they fitted the electronic part with an exponential of the form $C_{es}/\gamma T_{\mathrm{c}} = a \exp(-b\,T_{\mathrm{c}}/T)$ with the fitting parameters $a = 9.17$ and $b = 1.5$. These values are in accordance with the expression found in the original BCS paper (Bardeen *et al.*) [2] $C_{es}/\gamma\, T_{\mathrm{c}} \cong 8.5\, e^{-1.44\, T_{\mathrm{c}}/T}$. In the literature (see for example in the book of de Gennes [7]) one can often find an approximation of the BCS result, where C_{es} is proportional to $e^{-\beta\Delta_0}$, where $\beta = 1/k_{\mathrm{B}}T$.

Ginsberg and Tinkham (1960) [8] measured the *infrared transmission* through a few Å thick lead, tin, indium and mercury films. For the BCS ratio they deduced values close to $3.5\, k_B T_{\mathrm{c}}$.

Biondi *et al.* (1959) [9] measured the *absorption of microwaves* in aluminium. The amount of absorbed energy was calculated from the heating of the sample due to the absorption. The increase in absorption which takes place at energies above $3.2\,k_B T_c$ was attributed to the gap edge.

Ultrasonic absorption experiments imply that the ratio of the absorption coefficient of the superconducting α_s to the normal state α_n depends just on the energy gap according to the following expression: $\frac{\alpha_s}{\alpha n} = \frac{2}{1+\exp[\Delta(T)/(k_B T)]}$. Morse *et al.* (1959) [10] performed such measurements on single crystals of tin. Their fit to the theoretical curve is not perfect, but they find gap magnitudes not so far from the BCS prediction. Moreover they observe an orientation-dependence in the gap.

Yet one of the most convincing experimental confirmation of the BCS relation at the time was found by Giaever [11] (see section 2.2.1). In his *tunnelling* experiments he found surprisingly that the current through a planar junction sandwich is suppressed below the voltage which corresponds quite well to the one predicted by the BCS theory. Tunnelling is one of the most used techniques to determine experimentally the gap. At the same time, the most important experimental verification of the validity of the BCS theory is to measure the gap. From these two facts it gets evident where the importance of tunnelling measurements lies.

Later, many other techniques have been developed to measure the gap. With *ARPES* (angle resolved photoemission spectroscopy) one tries to measure the energy and momentum of the filled electronic energy states below the Fermi surface. A lot of measurements have been done on BSCCO, because by cleaving, one can easily obtain nice surfaces. ARPES has the advantage that an angle dependence is easy to measure. However a lot of other drawbacks are associated with this technique, for example that it is only surface-sensitive. Figure 1.2 shows a typical temperature dependence of an ARPES spectrum, measured in an underdoped BSCCO-2212 sample with a T_c of 79 K. A sharp peak at around 40 meV below the Fermi level and a dip appear. This peak is still visible above T_c. Usually one takes the midpoint of the leading edge to determine the gap. Striking is the fact that the leading edge gap does nearly not depend on temperature below T_c, and it does only close at significantly higher temperatures. This gap like structure, which is observable between T_c and T^*, was assigned to a pseudogap. The symmetry of this pseudogap feature is the same as the one for the gap feature. It is in agreement with $d_{x^2-y^2}$.

In high temperature superconductors, the measured gap value does not correspond anymore to the predicted value of the BCS relation. In optimally doped BSCCO-2212 for example the s-wave BCS relation in the weak coupling limit predicts a value of $\Delta_0 = 1.76\,k_B T_c \approx 14\,\text{meV}$. However the gap magnitude measured by tunnelling lies around 40 meV (see section 3.3).

1.2.1 The symmetry of the gap

It was proposed from the theoretical side that the gap has not a spherical s-wave symmetry like in conventional superconductors, but that it is rather d-wave like.

Won and Maki [13] studied the thermodynamics and the transport properties of

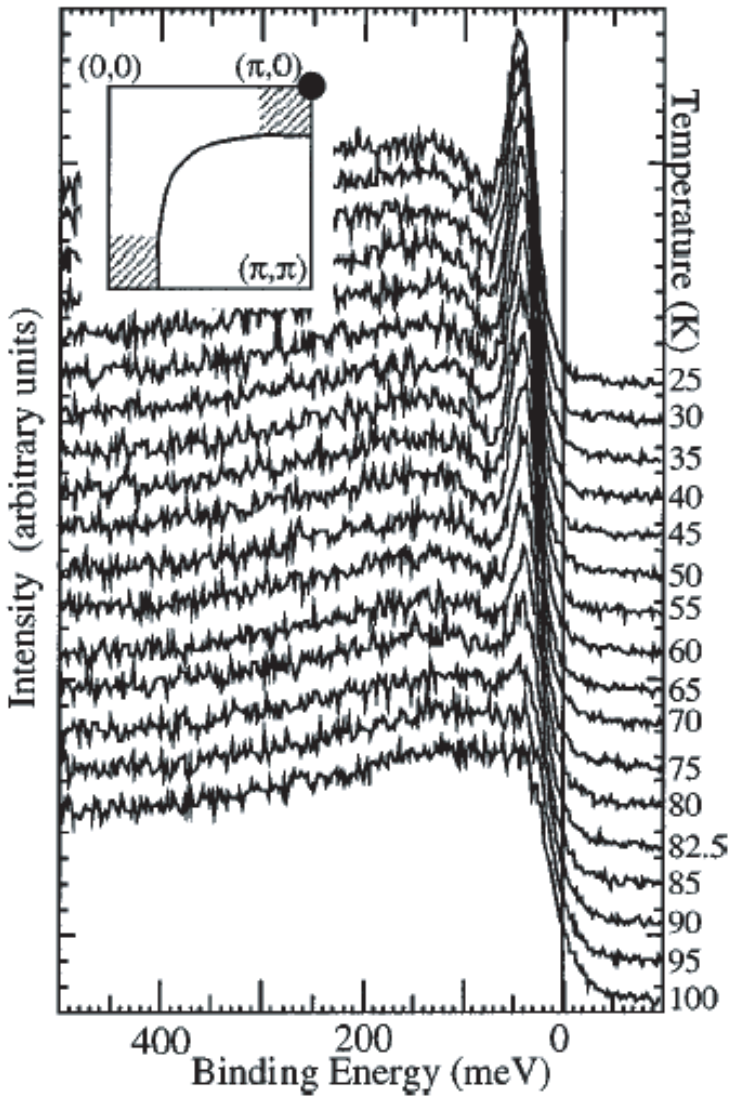

Figure 1.2: A temperature dependence of raw ARPES data in the direction in which a $d_{x^2-y^2}$ gap has its maximum (Loeser *et al.*) [12]. (BSCCO-2212, underdoped, T_c= 79 K).

d-wave superconductors, following the BCS theory. They found that the gap compared to T_c is 1.2 times bigger than in the s-wave case. The density of states is, in contrast to the s-wave case, different from zero below the gap. They found that the predictions of this d-wave model is qualitatively similar to the conductance observed with the same break junction technique we use in BSCCO-2212.

The intensity of the photoemission in ARPES is angle dependent. These and other experiments indicate that the gap has not a spherical symmetry. The symmetry of the gap was a controversial issue for a long time. Nowadays, it is generally agreed that cuprates have a gap with d-wave symmetry. One of the concluding experiments was that by Kirtley *et al.* [14]. They constructed a ring with three Josephson-junctions. When they oriented the crystalline axis of each segment in such a way that the total phase-shift in a $d_{x^2-y^2}$-wave picture was π, they could observe a spontaneous magnetisation with a half integer fluxquantum. That shows that the sign of the order parameter is in fact direction dependent.

The d-wave symmetry of the gap is more favourable for coupling than s-wave if the short range Coulomb repulsion between electrons is significant.

1.3 The pseudogap

A lot of the features that are observed in cuprates in a wide variety of experimental techniques and that, below T_c, are related to the superconducting gap, are still present at temperatures higher than T_c. This leads to the notion of the so-called normal state pseudogap that opens already above T_c at the temperature T^* (see figure 1.1).

To find an explanation of the experimentally observed pseudogap, various models were proposed. Some of them involve preformed pairs, which get formed below T^*, already before the phase coherence is established at T_c (Ranninger *et al.*; Emery *et al.*) [16]. Another approach is based on strong antiferromagnetic fluctuations that compete with superconductivity (Millis *et al.*) [15]. By investigating the pseudogap region, one hopes to understand the condition under which electrons can condense into the superconducting state, and thus get important information on the mechanism of high-T_c superconductivity.

The presence of a pseudogap was first suggested from NMR studies (see e.g. Alloul *et al.* [17], Warren *et al.* [18]). In other techniques like ARPES (see section 1.2), gap like features that are observed below T^* are assigned to a pseudogap. A good review on the pseudogap is given by Timusk *et al.* [19]. In the rest of this section I mention only resistivity and tunnelling measurements, since these are two techniques which we used in our BSCCO-crystals.

Measurements in $YBa_2Cu_4O_8$ (Bucher *et al.*) [20] (see figure 1.3) show that the resistivity in the CuO_2 planes is reduced below a temperature T^*, close to where NMR data indicate the opening of a pseudogap. This material is convenient for such measurements, as they write, because it is simultaneously stoichiometric, underdoped and genuinely untwinned. Resistivity as a function of temperature has been measured in other materials also. However one has to be very careful with such measurements. $La_{2-x}Sr_xCuO_4$ for

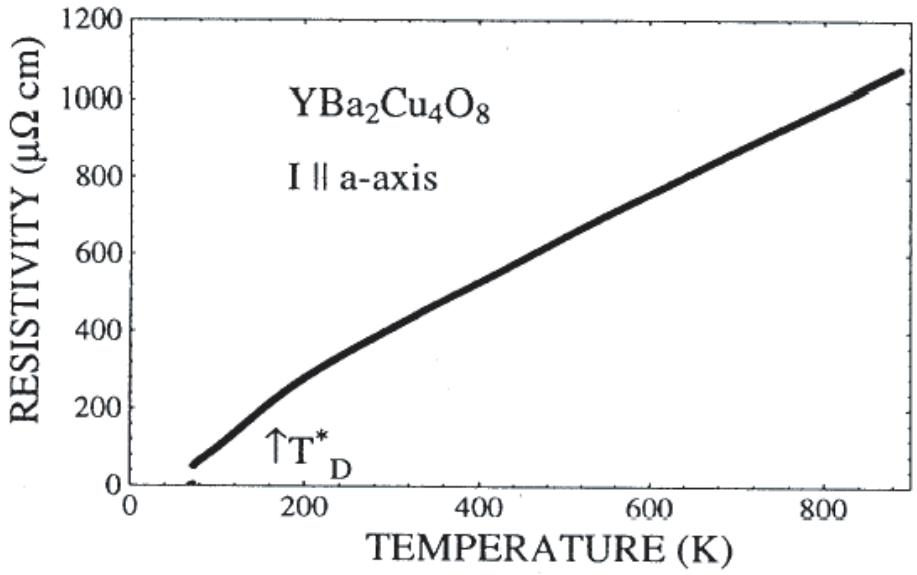

Figure 1.3: The in-plane resistivity of $YBa_2Cu_4O_8$ as a function of temperature as measured by Bucher *et al.* [20]. They compare it to NMR studies by Zimmermann *et al.* [21], from where they find the spin gap temperature (indicated as T_D^* in the figure).

example undergoes a tetragonal to orthorhombic transition (see Birgeneau *et al.* [22] and references therein) very close to the T^*-line found by Batlogg *et al.* [23]. From the resistivity curves we measured in underdoped BSCCO-2212 crystals, it was impossible to deduce a pseudogap temperature, since the variation from one sample to the other was too large.

In tunnelling experiments a depression in the differential conductivity can be observed above T_c. Figure 1.4 shows an example of an STM study. In our break junctions, the same features appear.

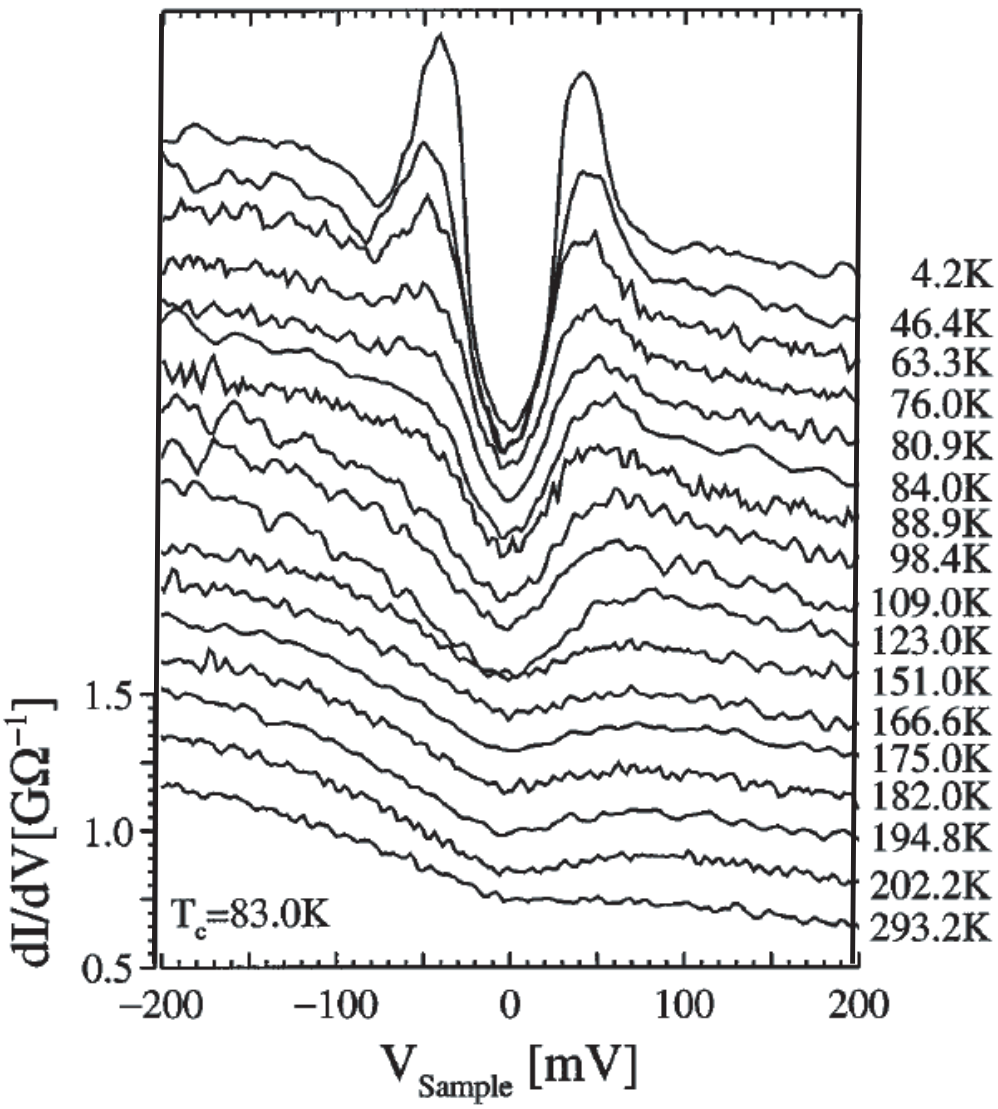

Figure 1.4: The evolution of the STM spectrum with temperature, as measured by Renner *et al.* [24]. The curves were taken on a underdoped BSCCO-2212 sample with $T_c = 83\,\mathrm{K}$. A gap like depression is observable up to room temperature.

Chapter 2

Electron tunnelling in the literature: Theory and experimental results

The so-called semiconductor model gives a widely accepted interpretation of the experimental results in tunnel structures. Experiments in low T_c superconductors give results that agree well with the predictions of the model. Many different types of structures have been designed to measure tunnelling in superconductors. In this chapter I give a description of the semiconductor model. Further, I describe briefly various techniques.

2.1 Theory of electron tunnelling

The ability of a particle to cross a barrier of an energy higher than its proper energy is called tunnelling. This process is classically forbidden and can only occur in quantum mechanics. When we couple two superconductors, a current can tunnel in two different ways. Either we have single electron tunnelling, or the electrons tunnel in Cooper pairs. The latter process is influenced by the phase between the two superconductors. The theory for this Cooper pair tunnelling was developed by Josephson [25]. In this work we focus on single particle tunnelling.

We can have three different types of strucures: superconductor-insulator-superconductor (SIS), superconductor-insulator-normal metal (SIN) or superconductor-normal metal-superconductor (SNS) junctions, where in each case the barrier is formed by the material in the middle.

To explain tunnelling results, Giaever [11] proposed a simple model, which is often called the semiconductor model (see figure 2.1). The idea is that by the application of a voltage, the two densities of states are shifted in energy with respect to each other and the current is always given by the probability for an electron to jump from an occupied to an unoccupied state. This model might appear as oversimplified, yet surprisingly, its application still gave a very accurate value for the BCS gap. For his work Giaever got the Nobel prize in 1973.

Written in formulas, this model needs the convolution of the densities of states $N(E)$:

$$I \propto \int |T|^2 \, N_{\mathrm{L}}(E) N_{\mathrm{R}}(E+eV)[f_{\mathrm{L}}(E) - f_{\mathrm{R}}(E+eV)]dE \qquad , \tag{2.1}$$

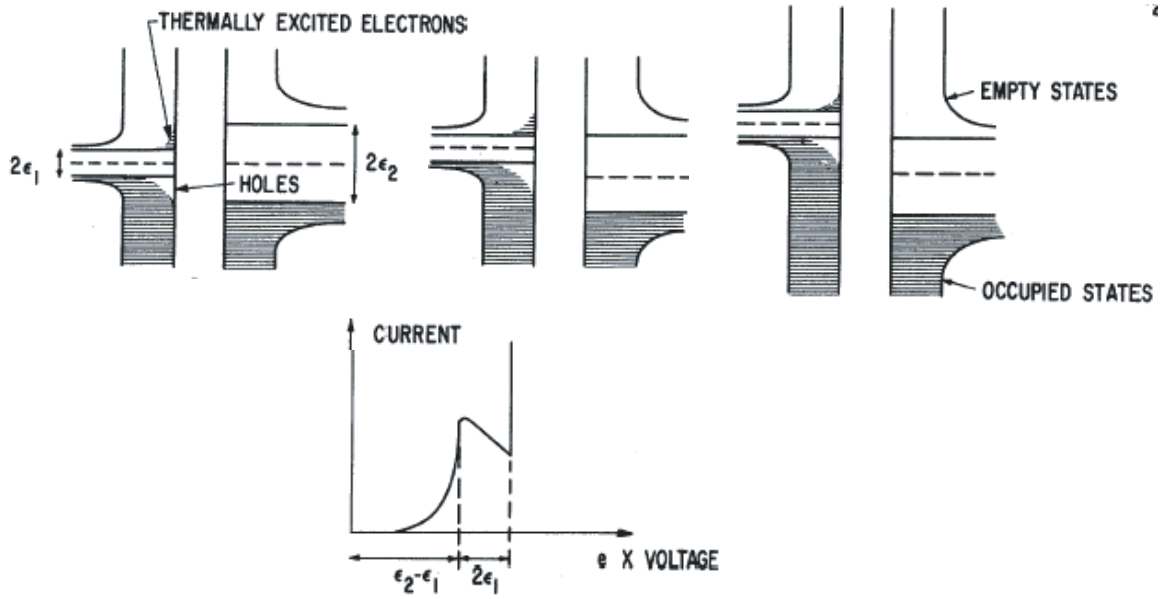

Figure 2.1: In the model of Giaever [11], the two densities of states shift with respect to each other due to the application of a voltage. When the voltage is higher than the gap energy, electrons can easily jump from one side to the other.

where $f(E)$ is the Fermi function, $|T|$ the matrix element between states of equal energy and the index L and R stay for the material on the left, respectively on the right side. The matrix element is usually assumed to be energy independent for voltages low enough (Wolf) [26], so that we can take it out of the integral. Bardeen [27] discusses tunnelling from a many-particle point of view and finds it plausible to treat $|T|$ as a constant. Furthermore $|T|$ has to be assumed to be unchanged when the metal goes from normal to superconducting.

The density of states can easily be extracted for SIN junctions (like it is ideally the case in STM). Here, as the density of states of the normal metal side is a constant, the derivative of the current is directly proportional to the density of states in the superconductor:

$$\frac{dI(V)}{dV} \propto \int_{-\infty}^{+\infty} N(E)\left(-\frac{\partial}{\partial eV} f(E+eV)\right) dE \cong N(eV) \quad . \tag{2.2}$$

The situation is somehow more difficult for SIS junctions. Here the density of states is not proportional to the derivative dI/dV. This derivative is very often shown in publications of SIS structures, even tough authors agree that this curve does not represent the density of states. It is a relatively difficult task to extract the density of states. Some sort of deconvolution process has to be done, but for that aim many hardly accessible elements like the k-dependence of the matrix elements or the conservation of momentum have to be known. The peak position of the dI/dV curve is usually associated with

twice the gap magnitude 2Δ. If we take however the dI/dV curve measured in STM and convolute it with itself we get a peak position that is only about 1.6 times (not 2 times) higher than that of the original peak. Respecting lifetime effects by using a Dynes Γ term (Dynes *et al.*) [28] may change this value. When we take the BCS density of states for the convolution we obtain, thanks to the singularities, a peak at 2Δ in the dI/dV curve. In the experimental part of this work (chapter 3) I will nevertheless show the dI/dV curves of our break junctions, with the aim to compare them to other results from the literature.

Even more complicated is the situation in SNS structures. Here, the barrier is not like usually a forbidden region for the particle. In the normal part, the electrons can form a Bloch state. The transition from normal to superconductor has however been discussed in terms of Andreev-reflection. The idea is here roughly that an electron is reflected as a hole at the SN interface, so that a pair that is formed in this way can propagate into the superconductor.

2.2 Tunnelling techniques

The idea of a tunnelling device is to couple two materials in such a way that they are separated by any type of a thin barrier.

Very different geometries have been conceived in which tunnelling phenomena are supposed to occur. The situation is well described in the book of Hansma [29]: "It should be understood that the closest classical analog of tunneling is cooking. Every chef has his own recipes and procedures based on experience and superstition. It is not practical to test every superstition in detail; when the chef finds a good recipe he follows it."
Among the different techniques are planar junctions, point contacts, STM, break junctions, mesa structures or grain boundary junctions. In this section I will outline some of the major results of these techniques.

2.2.1 Planar junctions

The history of tunnelling experiments dates back to 1960 when Giaever [30] measured an Al-Al_2O_3-Pb sandwich. An about 1000 Å thick aluminium strip was evaporated onto a glass slide. Before evaporating the Pb layer, they let the aluminium oxidise for some minutes at ambient pressure and temperature, so that a 15 to 20 Å thick Al_2O_3 layer was formed. He measured the current as a function of the voltage through this structure at 1.6 K, a temperature at which the aluminium is in the normal state. The derivative dI/dV (see figure 2.2) was interpreted qualitatively in terms of the change in the density of states in Pb around the Fermi level. From the peak position he estimated the gap to be of the order of $4.2\,k_{\mathrm{B}}T_{\mathrm{c}}$.

The measured $I(V)$ curves could be fitted nearly perfectly using the BCS density of states, for example by Nicol *et al.* [31] or Giaever *et al.* [32]. This is a very impressive result if one considers the possibility of experimental errors and that the fit is based on

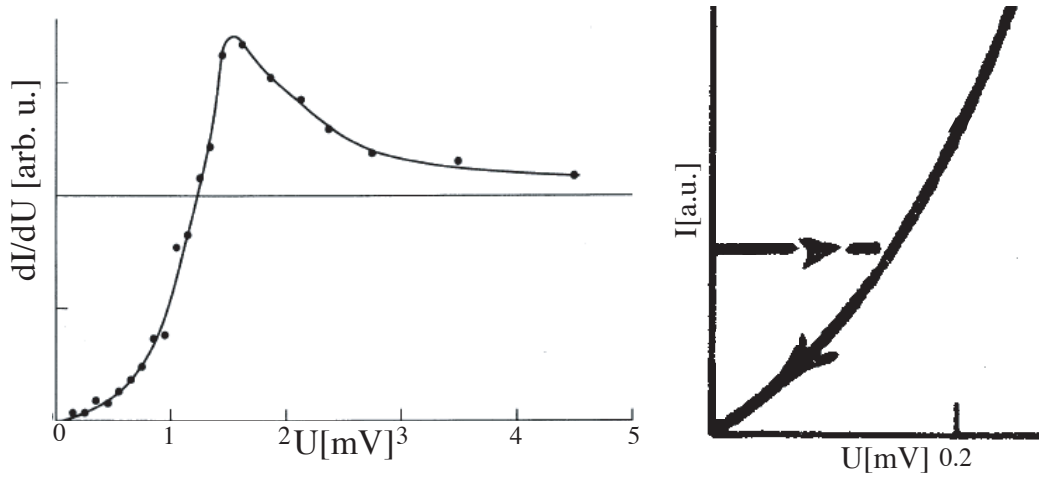

Figure 2.2: Left panel: The first tunnelling experiments in superconductors were performed by Giaever [30]. The gap magnitude was estimated from the peak in the derivative dI/dV. (Planar Al-Al_2O_3-Pb junction, 1.6 K). Right panel: The zero bias current measured in (Giaever) [11] was interpreted as a superconducting bridge over the oxide barrier going normal at nonzero voltages. (Planar Al-Al_2O_3-Al junction, 1.1 K).

models that are approximative or strongly simplified: BCS model and semiconductor model.

When the planar structure is made out of two metals with different transition temperatures the semiconductor model predicts a region where the current decreases with increasing voltage. This occurs when the bath temperature is below T_c of both materials, because the number of accessible unoccupied states decreases (see figure 2.1). This phenomenon, and its expected temperature dependence could be measured (see e.g. Giaever *et al.* [32] and figure 2.3).

Fisher and Giaever [33] observed that the resistance of the oxide films tends to increase exponentially with thickness. The decay length of 3.8 Å is in the order of magnitude of an Al_2O_3 cell. It was observed that samples with thinner barriers give better spectra (Giaever *et al.*) [34].

The barrier in planar structures is very thin. If one assumes that the oxidation occurs in a random way, the process can be described by a Poisson distribution. One event in the distribution is the formation of one Al_2O_3 cell. An average oxide thickness of 15 Å corresponds only to about 4 events. The probability to find unoxidised sites, where a superconducting bridge is formed is thus approximatively 2%. Giaever [11] actually describes such superconducting bridges. In an Al-Al_2O_3-In sandwich, with an approximately 20 Å thick aluminium oxide barrier he observed a zero bias current (see right panel of figure 2.2). His interpretation was that the oxide layer was pierced by a superconductive bridge. When the current is increased, the bridge goes normal. When the current is decreased, the bridge remains normal at a lower current due to Joule heating. In the same oxidation model a one unit thick layer is found with a probability of about 7%. When does the superconductor above this one cell thick layer go normal?

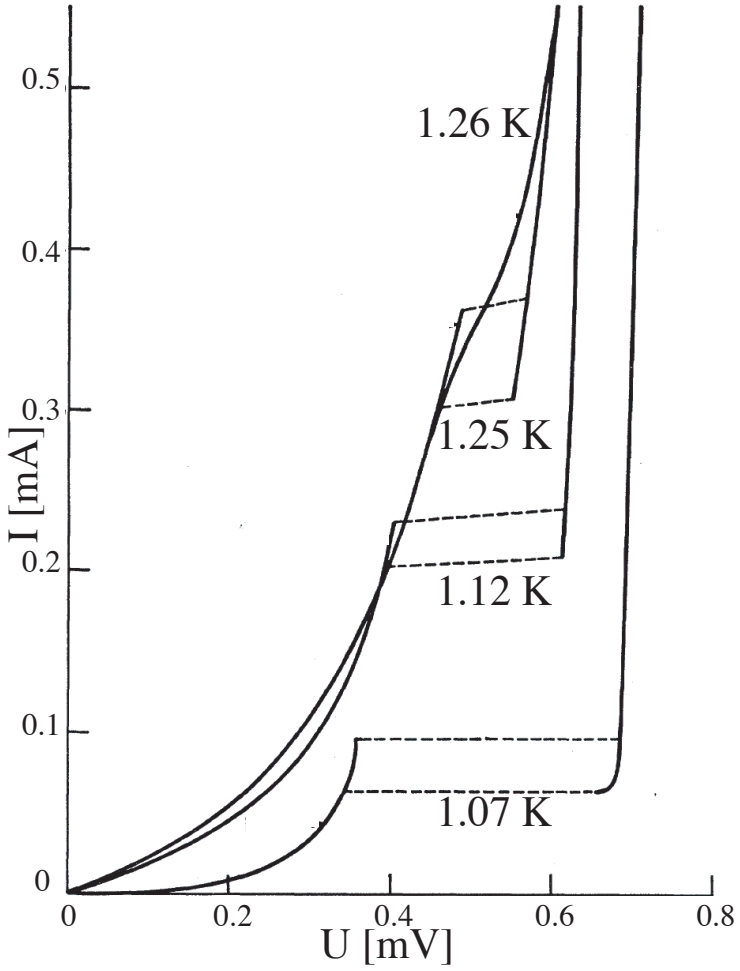

Figure 2.3: The region where the current decreases with increasing voltage was observed as a hysteretic loop in an Al-Al_2O_3-In planar junction (Giaever *et al.*) [32]. The curves were measured at the bath temperatures of 1.07 K, 1.12 K, 1.25 K and 1.26 K.

What is the smallest possible barrier thickness in the semiconductor model? What happens when the transfer matrix element in the semiconductor model approaches one?

Fisher and Giaever [33] write about this problem: "One difficulty with thin films is that small metal bridges often are responsible for conduction across them. This form of conduction is ruled out qualitatively for our films by the presence of non-linear current-voltage characteristics, rectifying properties, the slight increase of resistance with decreasing temperature, the observed sharp breakdown at high voltages, and the inverse proportionality of resistance to film area."

This so-called planar junctions were mainly used to investigate low temperature superconductors. The oxide layer can be replaced by any insulator. Planar structures with high T_c superconductors were fabricated to observe the Josephson effect. Bozovic *et al.* [35] produced high quality sandwich structures of BSCCO-2212, with an about 3 nm thick dysprosium doped BSCCO barrier. A Josephson like current was measured at zero voltage. Under microwave irradiation he observed Shapiro steps. In some samples, the $I(V)$ curve showed gap-like features.

Recently the same author produced junctions with a $La_2CuO_{4+\delta}$ barrier [36]. He varied the barrier thickness d between one unit cell and $d = 200$ Å. Even at temperatures above T_c of the barrier, he observed a supercurrent through all of these junctions. That is very surprising, since normally it is assumed that the critical current decreases exponentially with a decay length of the order of the coherence length of the superconductor. He calls this phenomenon giant proximity effect.

A one unit cell thick antiferromagnetic La_2CuO_4 barrier between the superconducting material $La_{1.85}Sr_{0.15}CuO_4$, however, blocks completely a supercurrent (Bozovic *et al.*) [37].

2.2.2 Point contacts

Point contacts have first been built with the intention to observe the Josephson effect (Zimmerman *et al.*) [38]. This type of junction is usually produced by pressing a sharp superconducting or normal metal tip against a flat superconductor. A problem of this technique is the uncertain geometry of the contact. In principle there are two different types of junctions envisaged. In one the barrier is formed by an oxide layer between the tip and the sample, and in the other, the junction is produced from the contact going normal due to a high current density. The contact area between the tip and the sample is usually bigger than 1000 Å in diameter.

Later, some authors (Zasadzinski *et al.*) [39] also claimed that the peak-dip-hump structure of the spectra obtained with point contacts in cuprates, represents the density of states of the superconductor. They even tried to explain the dip feature. In other experiments (Ekino *et al.*) [40] BSCCO crystals were brought in contact with a polished and oxidised aluminium sheet. The contact area was $0.1 - 1.0\,\mathrm{mm}^2$. Also in this experiment they observed peak-dip-hump like curves. Ozyuzer *et al.* made a point contact with a Au tip and reported on three different types of measurement in the same sample [41]: A SIN contact when the gold tip touches the sample, a SIS contact when

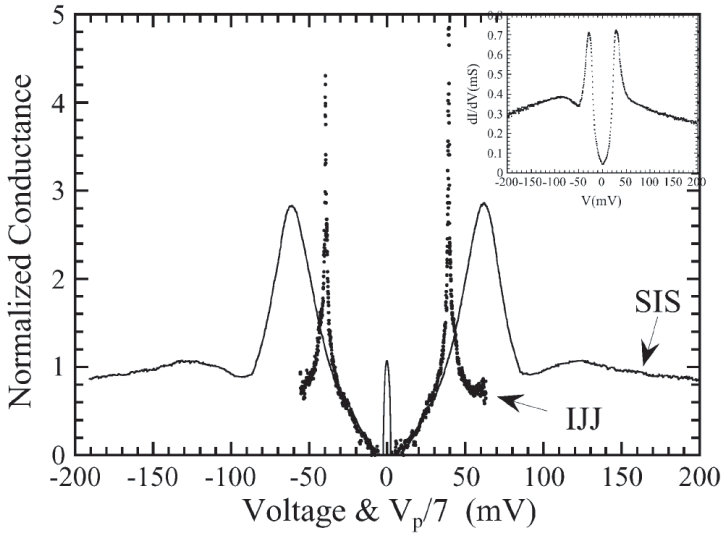

Figure 2.4: Three different types of spectra obtained with a point contact technique in the same sample: An SIN contact when the gold tip touches the sample (inset), an SIS when a crystallite breaks off and is stuck to the tip and an "intrinsic junction" contact when the spectra show hysteresis. The voltage scale is divided by the number of hysteretic branches (7) for the "intrinsic junction". BSCCO-2212 sample at 4.2 K (Ozyuzer *et al.*) [41].

a small crystallite breaks off, is stuck to the gold tip and touches the rest of the sample and an "intrinsic junction" contact if the sample breaks in such a way that hysteresis is formed (see figure 2.4). The SIN contact shows a peak around Δ, the SIS contact around 2Δ and the hysteretic contact at a significantly smaller value than Δ multiplied by the number of branches. They believe that heating effects are responsible for the low value of the peak in the intrinsic junction.

2.2.3 STM

One of the most sophisticated techniques among tunnelling spectroscopy experiments is STM. A very small tip of a normal metal is approached to the sample surface. The tip is so sharp that atomic resolution is attained. Thanks to this local resolution, a spatial map of the sample can be made. Vortex cores (Maggio-Aprile *et al.*) [42], for example, could be imaged. In the ideal case, when the tip forms a SIN junction over the vacuum into the superconductor, the dI/dV curve gives directly the density of states in the sample. The peaks of this spectrum are attributed to the gap. The position of the peaks does not depend significantly on the spacing between the tip and the sample (see figure 2.5). When the tip is brought even closer to the surface, a point contact is achieved. Even in this point contact configuration a superconducting gap was observed (Renner *et al.*) [43], but not systematically.

One of the most suitable materials for STM are the BSCCO-2212 compounds, because the sample cleaves easily between the BiO planes, and one obtains atomically

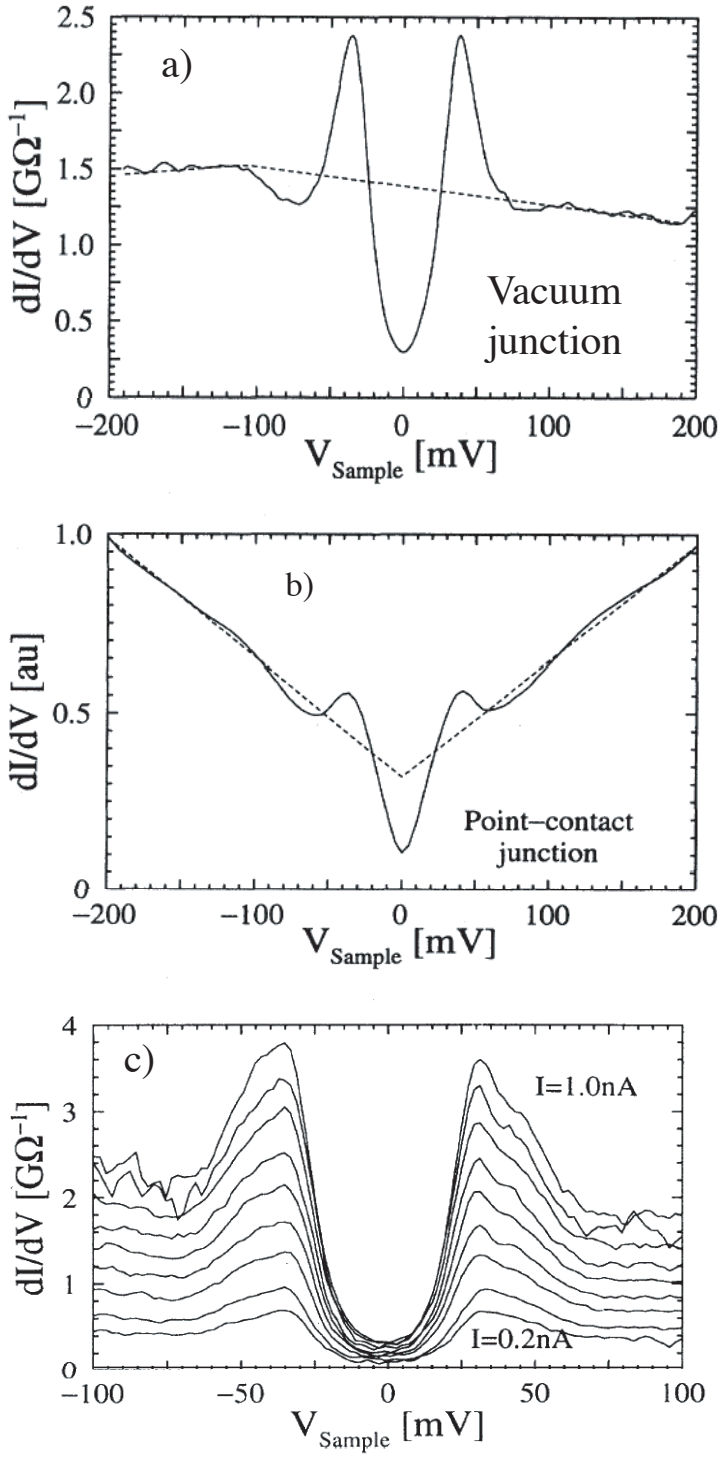

Figure 2.5: dI/dV curves measured in BSCCO-2212 with STM (Renner *et al.*) [43]. a) Vacuum junction ($R = 0.6\,\mathrm{G\Omega}$). b) Point contact junction ($R = 0.03\,\mathrm{G\Omega}$). c) Dependence of the spectra on the distance between tip and sample. The current is varied from 1.0 nA to 0.2 nA at constant $U = 0.4\,\mathrm{V}$. The spectra can be scaled onto each other by normalising the current at high biases.

flat surfaces. Renner *et al.* [24] obtained for the peak separation in optimally doped BSCCO-2212 a value of $2\Delta = 83\,\mathrm{meV}$. Furthermore they found that the gap magnitude decreases with increasing doping. They observed also a gap-like structure above T_c and attributed it to the opening of a pseudogap.

Recently the role of inhomogeneity and its possible importance for superconductivity has been intensely discussed. During the past few years, the group of Davis published several results, which attracted a major interest. I will shortly mention some of their measurements ([44] to [51]) in BSCCO-2212:

Pan *et al.* [44] observed an electronic inhomogeneity with a spatial correlation length of $\sim$14 Å. This correlation is reflected in both the local density of states and the superconducting energy gap.

Lang *et al.* [45] found a segregation into hole-rich superconducting domains that are $\sim$3 nm in size. In addition they did measurements in samples with Ni impurities. In the region with $\Delta > 50\,\mathrm{meV}$ they did not observe any Ni scattering resonances. From these results they propose a picture with purely superconducting regions with $\Delta < 35\,\mathrm{meV}$, an undefined second phase when $\Delta > 50\,\mathrm{meV}$, and a mixture of two different electronic orders in between.

In 1999 Hudson *et al.* [46] observed regions, about 3 nm in diameter, with elevated zero bias differential conductance. They relate these areas to quasi-particle scattering resonances. The spectra obtained in these regions, as well as the spatial dependence, are consistent with several theories of the effect of scattering at the atomic scale in d-wave superconductors. The scattering centres could not be identified in this study. However, in a later experiment (Pan *et al.*) [47], copper atoms were replaced by zinc impurities. At these zinc sites, a huge peak was observed in the differential conductance at low energies.

Hudson *et al.* [48] replaced some Cu atoms by Ni impurities. From the shape of the spectra they conclude that local superconductivity continues to exist in the region of the magnetic Ni atom. They propose that the mechanism of high-T_c might be of magnetic origin.

A four unit cell periodic pattern under magnetic field around vortex cores was observed by Hoffman *et al.* [49]. The origin of this modulation is unclear. Also outstanding is the similar, but 10 to 100 times less intense energy dependent spacial incommensurate modulation which is observed in a zero field experiment (Hoffman *et al.*) [50].

McElroy *et al.* [51] found signals in the Fourier-space images of the atomically resolved real space image taken at a constant voltage. Interpreted as the manifestation of quasiparticle interference, elements of the Fermi-surface can be found, in agreement with photoemission experiments. The experimental results are consistent with the modelled dispersion relation of the scattering vectors.

Spatially resolved data come also from Vershinin *et al.* [52]. They observed an energy independent incommensurate periodicity at low energy and at temperatures above T_c. Whether these types of ordering play any important role in the mechanism of superconductivity is still unclear.

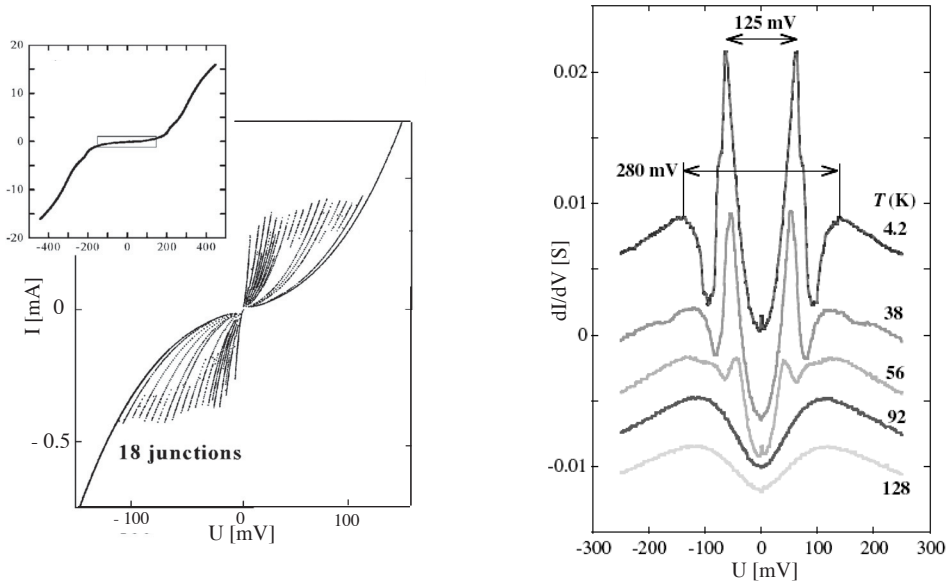

Figure 2.6: Left panel: The hysteretic branch structure in a $Bi_2Sr_{1.6}La_{0.4}CuO_{6+\delta}$ mesa. The rectangle in the inset denotes the region which is zoomed in the main panel (Yurgens *et al.*) [55]. Right panel: The typical Intrinsic tunnelling spectra for BSCCO-2212 at the bath temperatures 4.2 K, 38 K, 56 K, 92 K and 128 K. The voltage scale is per junction (Yurgens *et al.*) [55].

2.2.4 Mesa structures

Quite a fancy technique is the so called intrinsic tunnelling in BSCCO-2212 mesa structures. The basic idea is that superconductivity is located only in the CuO_2-planes, which are separated by insulating Bi_2O_3 and SrO layers. The phase coherence between the layers is realised by the Josephson effect, in such a way that each layer forms a Josephson junction (see Kleiner *et al.* [53] or Schlenga *et al.* [54]).

A mesa structure consists of a stack, fabricated of a highly anisotropic compound such as BSCCO-2212 or $Tl_2Ba_2Ca_2Cu_3O_{10+\delta}$. Usually, the stack is only a few layers thick and its sides are in the order of a few micrometers. When a voltage is applied in the c-direction, a supercurrent flows through the mesa. When the current is higher than the critical current I_c, the phase coherence between two layers break down, and a layer switches to its resistive state. By increasing the voltage continuously, more and more layers switch to the resistive state. This is seen as a multiple branch characteristic in the $I(V)$ curve (see figure 2.6). Each branch corresponds to one layer switching to the resistive state, as can be verified by counting the layers.

The idea is that superconductivity still exists in the CuO_2 planes of the resistive layers, so that tunnelling junctions are formed between them. It is believed that the critical current at which a voltage sets in is *not* the critical depairing current of the superconductor, where the superconductor goes normal. It is assumed that I_c is only the current where the phase coherence between the layers gets lost. However, the critical depairing current is certainly often reached, mainly when measurements are done slightly

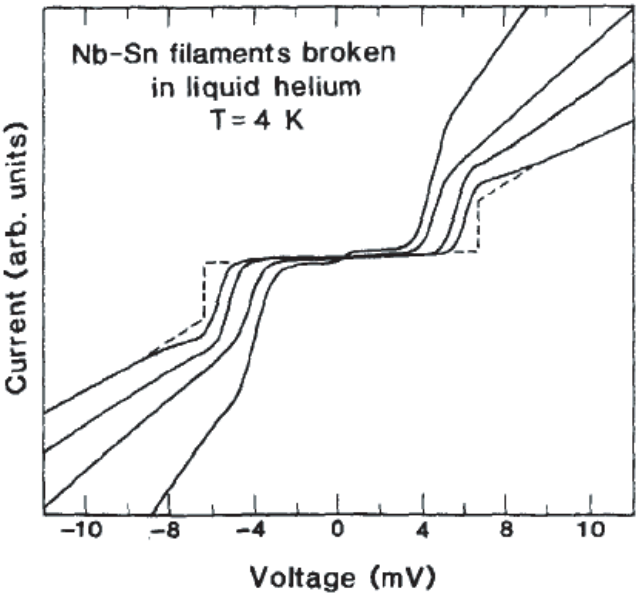

Figure 2.7: The $I(V)$ curve was measured in Nb-Sn with a break junction technique by Moreland and Ekin [57]. The different curves correspond to different samples. The dashed line is the predicted curve from the BCS theory, at $T = 0$.

below T_c. Why the exceeding of the critical current is not observable in the $I(V)$ curve is not obvious for me.

To prove the Josephson-junction nature of the coupling, one can irradiate the sample with microwaves. Shapiro steps should appear at the voltages $U_n = \frac{nh}{2e}\nu$, where n is an integer and ν the frequency of the applied radiation (see section 2.3). Such steps were observed in mesa structures (see e.g. Wang *et al.* [56]). The observation of Shapiro-steps does not imply that the measured $I(V)$ curve is a quasiparticle tunnelling spectrum. However, above the multiple branch structure, the dI/dV curve in small mesa structures shows a peak-dip-hump structure that is nearly identical to the one measured in other techniques like break junctions (see figure 2.6). That is the reason why it is often believed that the peak position of this spectrum corresponds to twice the gap magnitude.

2.2.5 Break junctions

The first break junction experiments were done by Moreland *et al.* [57]. They broke an Nb-Sn filament in a similar way as we do in our experiments (see section 3.1). By changing the applied force on the support, they were able to tune the spacing between the fracture elements. The $I(V)$ curve over this junction shows a clear gap-like structure (see figure 2.7). The result is close to the prediction of the BCS theory.

The main drawback of break junctions is that one has not a good control over the geometry of the junction. The advantages compared to other techniques are that the measurements are simple, not costly, stable up to relatively high temperatures, that the junction interfaces are not contaminated by oxidation or other impurities and that

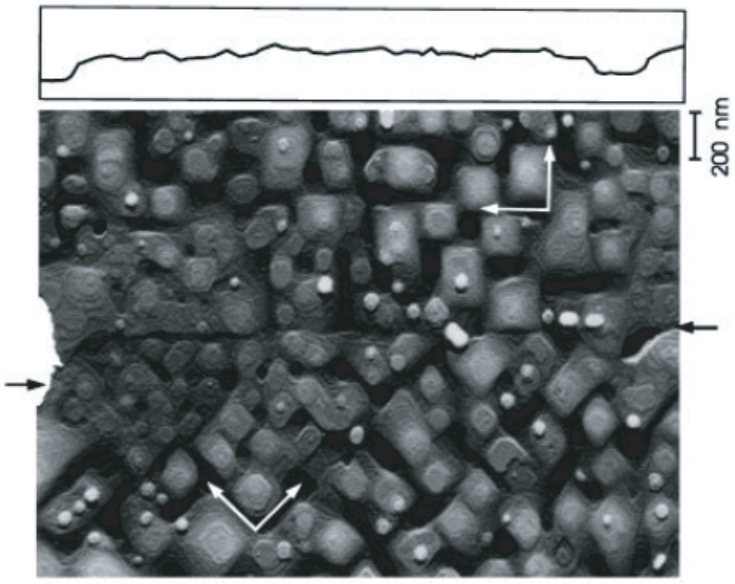

Figure 2.8: AFM image of the surface of an ∼150 nm thick $YBa_2Cu_3O_{7-x}$ film with an asymmetric 45° [001]-tilt boundary. The meandering boundary line has been replotted to the right (Mannhart *et al.*) [60].

the current density is not as high as for example in STM. Even direction dependent measurements can be done: Mandrus *et al.* [58] made junctions by re-approaching freshly cleaved BSCCO-2212 surfaces, in such a way that the contact is established in the *c*-direction. This type of spectra shows a V-shape in the dI/dV curve and not a peak-dip-hump structure like for the *ab*-plane. In the present work (see chapter 3) break junctions in the plane are investigated. In former studies (Hartge *et al.*) [59] the magnetic field dependence of the critical current was also measured.

2.2.6 Grain boundary junctions

Grain boundary junctions are formed during epitaxial growth of the material on a bicrystalline substrate. As can be seen by AFM, the junction is a zigzag interface (see figure 2.8).

In some materials, a current is observed at $U = 0\,\mathrm{V}$. Under the application of a magnetic field, the magnitude of this current shows a Frauenhofer pattern, like predicted for a Josephson junction. This was measured for example in $La_{1.85}Sr_{0.15}CuO_{4-\delta}$ over an 24° [001] tilt grain boundary (Beck *et al.*) [61].
Pronounced gap structures with peaks and dips can be observed in the dI/dV curves over grain boundaries in cuprates (see e.g. Alff *et al.* [62]).

The advantages of this technique are the stability of the junction under temperature changes and under the application of magnetic fields. Furthermore, the direction of the current-flow is well defined and lies in the *ab*-plane.

2.3 Josephson tunnelling

Weak link structures like Dayem bridges, proximity effect bridges or crossed wire weak links are normally designed to investigate the Josephson effect.

The phenomenon that electrons can tunnel in the form of Cooper pairs is called Josephson tunnelling (see e.g. Barone *et al.* [63]). For that aim two superconductors have to be brought together very closely, so that the phases of the two superconductors influence each other. A current can flow even if the voltage drop over the junction is zero. This so called d.c. Josephson effect is described by

$$I = I_c \sin \phi \qquad , \tag{2.3}$$

where ϕ is the phase difference between the two superconductors. When the current is increased above the critical current, I_c, a voltage drop over the junction sets in (a.c. Josephson effect). The phase changes after

$$\frac{\partial \phi}{\partial t} = \frac{2eU}{\hbar} \qquad . \tag{2.4}$$

For constant voltage, the result is an a.c. current with a frequency of approximatively 500 GHz/mV.

It is often difficult to identify the Josephson effect. For example a current was also observed at $U = 0\,\mathrm{V}$ in the first tunnelling experiment in planar junctions. But it was not clear, whether this supercurrent was caused by conduction through metallic shorts, or if it was due to Josephson tunnelling (Josephson) [64]. Mainly two methods are used nowadays to discuss the question about the nature of the current: First a Josephson junction should show the well known Frauenhofer like pattern (Barone *et al.*) [63] under the application of a magnetic field. Second, when the sample is irradiated with microwaves, Shapiro-steps (Shapiro) [65] should appear at $U_n = \frac{nh}{2e}\nu$, where n is an integer and ν is the frequency of the applied radiation.

Hysteresis effects were often observed in the current-voltage characteristics of Josephson junctions (see e.g. Barone *et al.* [63] page 13). Several models have been proposed to explain these observations. McCumber [66] for example proposed a model with a capacitance in parallel with the Josephson element. But such a hysteresis can also be provoked by simple heating. Attention was called to this fact in numerous publications (e.g. Wang *et al.* [67], Fulton *et al.* [68], Decker *et al.* [69]). Likharev even writes in section V. D. 5 of his review on weak links [70] about the "unending stream of publications in which the influence of heat on $I(V)$ curves of weak links is rediscovered".

Josephson junctions play also an important role in industrial applications. SQUIDs for example are essentially two Josephson junctions coupled in parallel.

An important point should be emphasised: The appearance of Josephson effects like Shapiro steps does not a priori require the presence of a tunnelling structure (see Katz *et al.* [71] or section II.A.3 of Likharev [70]). Shapiro steps have been observed even in Dayem bridges (Anderson *et al.*) [72] (superconducting bridge driven normal). It is important to discuss this point because for example the presence of Shapiro steps in mesa structures is often used to argue that the $I(V)$ curve in mesa structures represents the

convolution of the density of states, and that the curves represent an intrinsic tunnelling effect.

A big diversity of so called "weak link" structures has been designed with the purpose to measure the Josephson coupling. Among them are metal barrier junctions (proximity effect, S-N-S junctions, S-I-N-S structures), semiconducting barrier junctions, bridge type junctions, point contact weak links or junctions fabricated by nanolithography and ion implantation (Katz *et al.*) [71]. The most important property of such junctions is that the maximal dimension of the link is shorter than the coherence length of the superconductor. As one example of such structures I will just write some words about proximity effect structures. More references and details about other structures are given in chapter 7 of Barone *et al.* [63].

In a *proximity effect bridge* the middle part of the film is covered by a thin normal metal layer. Due to the proximity effect, the critical current through this covered part gets reduced. The result is a tunnelling barrier below the normal metal layer. The advantage of such a structure is that the coupling strength can be controlled very exactly by modifying the thickness of the covering normal layer. Notarys and Mercereau [73] measured such structures. Applying a magnetic field they found the expected Frauenhofer pattern in the intensity of the critical current. Under irradiation at radio frequency they observed Shapiro steps. These two phenomena are typical for Josephson effects.

In most of the structures that were designed to measure the Cooper pair tunnelling the authors do not speak about the high voltage part of the $I(V)$ curve.

In our experiments we observed also a current at $U = 0\,\mathrm{V}$. When the current is increased above the critical value I_c, the voltage switches to a finite value. The magnitude of the critical current depends a lot on the coupling strength. In the junctions where the two parts are very much approached, the critical current can easily reach the order of $10\,\mu\mathrm{A}$. Decreasing the voltage from high values, the current at which the junction switches back to its resistance-less state is smaller than the critical increasing-value. Under the application of a magnetic field, no Frauenhofer pattern was observed.

Chapter 3

Break junction tunnelling: Experimental results

3.1 Experimental setup

Flakes of single crystals of the material under study are produced by successive cleaving with an adhesive-tape. BSCCO-2212 compounds cleave easily between BiO-planes. In principle, with this technique, one can easily produce flakes thinner than a micrometer, even so thin that the sample gets transparent. As the results from transparent samples look like the ones from thicker flakes, we did not cleave our specimens till they got transparent. Usually in our experiments they had a thickness of a few micrometers, a width of about a tenth of a millimetre and a length of around one millimetre. Two or four electrical contacts were made with golden wires, glued with silver epoxy onto the surface of the sample. As the junction resistance is high compared to the contact resistance, the spectra measured in the four point configuration did not noticeably differ from the two point measurements. To get a more homogeneous oxygen distribution, the samples were annealed for at least 20 minutes at 600 °C in air at ambient pressure. After this heat treatment the samples were characterised by measuring the temperature dependence of the resistivity (see figure 3.1). From such curves T_c can be determined. Also the homogeneity and the quality of the sample can be checked with this measurement. Immediately afterwars the flake was glued with GE varnish on the support. In helium gas atmosphere, the specimen was cooled down. At liquid helium temperature we broke the sample by applying a force on the support (see figure 3.2). With a screw we could control the force on the bending support. By decreasing the force, the opening between the two parts can be reduced, and the two pieces can be re-approached. In this way we can tune very precisely the opening of the split, or correspondingly the area where the two parts touch each-other. However we have no absolute control of the spacing between the parts. We cannot even say with certainty, whether the two pieces touch each other or not.

The resistivity at high voltages of our junctions ranged from 500 Ω to 1 MΩ.

We studied the geometry of the break with an Atomic Force Microscope. The sample under study showed steps with a height of approximatively 50 nm when scanning

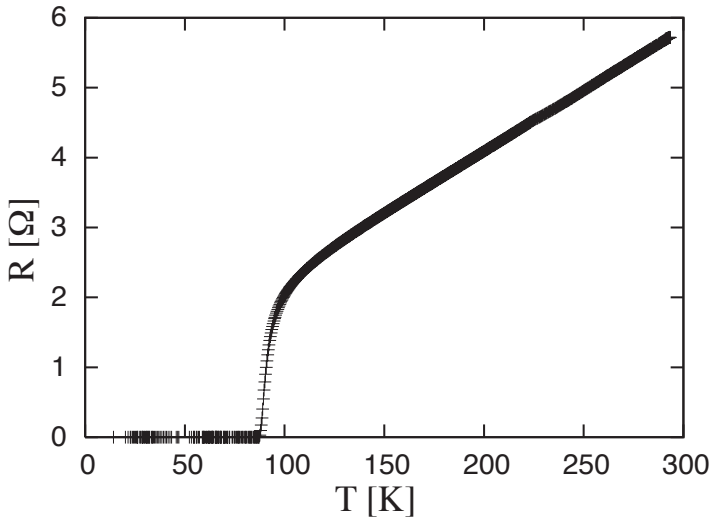

Figure 3.1: An example of a $R(T)$ curve measured in BSCCO-2212 with an approximate T_c of 90 K.

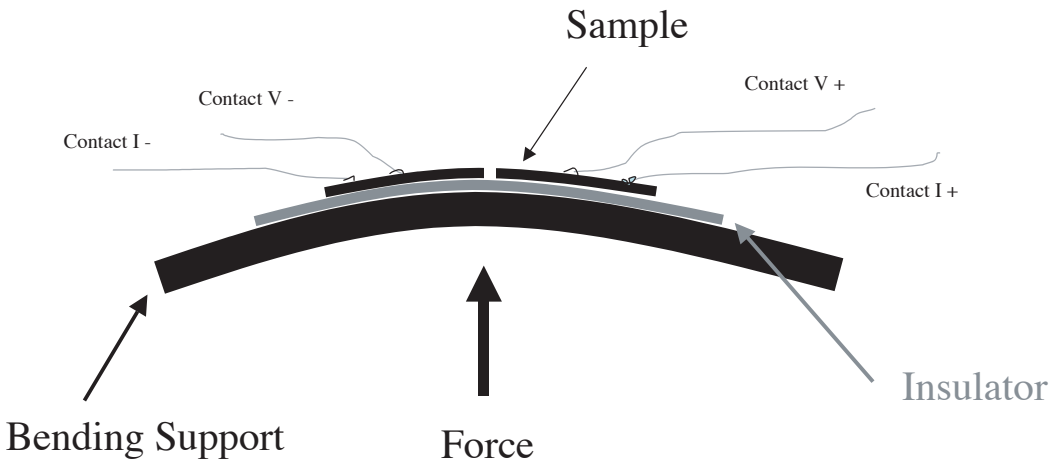

Figure 3.2: The experimental setup: the sample is broken by applying a force on the bending support.

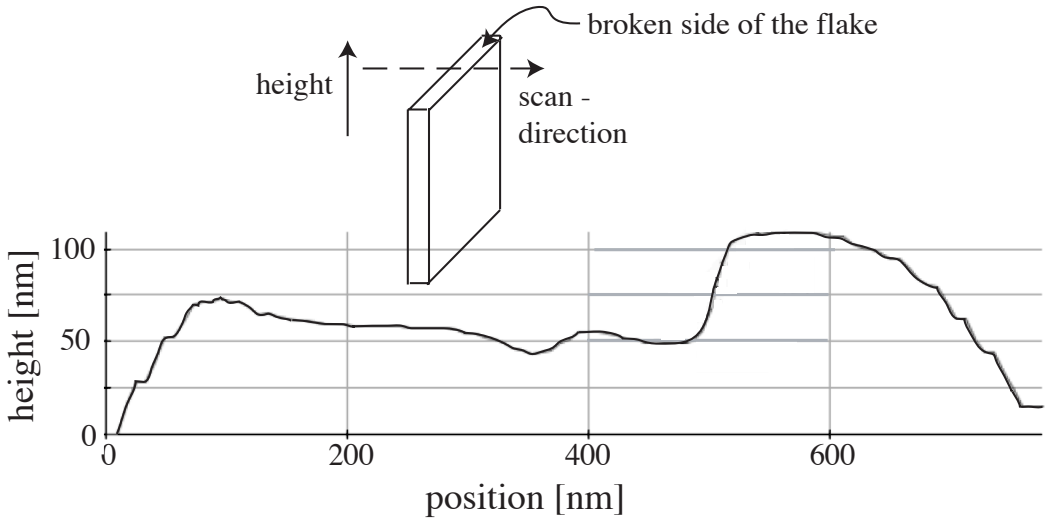

Figure 3.3: An AFM scan in the c-direction over the break of a BSCCO-2212 flake. Both, steps and relatively flat parts can be observed. We cannot say with certainty which direction of the current flow is dominant. Thanks to Kyumin Lee (EPFL, IPMC) for the images.

parallel to the *c*-direction (see figure 3.3). In some breaks, this step-height can reach hundreds of micrometers, as observed and estimated from other samples under the optical microscope. This leads to an overlapping region of the two broken parts of the flakes and favours transport in the c-direction. At a position between 100 nm and 500 nm in the AFM scan of the same break, we can see however that the break under study is flat enough to assume that in this region transport in the plane direction is more favourable. For our experiments it is thus not completely clear which direction of the current flow is dominant.

3.1.1 SIS or SNS?

There is an argument that speaks for an SNS geometry, that is that the two sides are touching each other and are only separated by a small part going normal:
If we release the force on the sample support, such that the two parts of the sample re-approach as much as possible, a supercurrent can flow through the junction. Only when the current is increased further, the junction switches to the resistive state. Even if we try to approach both parts completely, this switching to the resistive state is always possible. We just have to increase the current to a value high enough. The spectra we obtain in these low resistance junctions do not change. The best way to obtain a nice spectrum is actually to approach the two sample parts as much as possible. The only way in which one can think of an junction formed by a vacuum barrier is, when one supposes that it is not possible in our geometry to re-approach the two parts completely after breaking the sample. This assumption seems to be unlikely.

Curves that look very similar to ours are measured in the geometry Zasadzinski *et al.* [74] use. There it seems very probable that the two broken parts touch each other.

3.2 The materials under study

In this study we concentrate on BSCCO-compounds. When nothing else is mentioned, the measurements were done in the nearly optimally doped two layered compound BSCCO-2212. A few curves were taken also in BSCCO-2223. No qualitative difference between the spectra taken in these two materials could be observed, except that the typical features like the peak and the dip simply shift to higher voltages when an additional layer separates the CuO_2 planes. A BSCCO-2223 sample from Enrico Giannini (University of Geneva) with a T_c of 106 K, grown with a floating zone method showed its peak at around 70 meV. That means that $\frac{2\Delta_0}{k_B T_c} \approx 8$, if we assume that the peak position is at $2\Delta_0$. This magnitude is comparable to the one obtained in the optimally doped two layered compound.

The BSCCO-2212 crystals were grown with a flux melting method at our institute by Helmut Berger. Underdoping in this material can in principle be achieved by lowering the oxygen concentration. But this way of changing the doping concentration can provoke problems of disorder and inhomogeneity. Forro [75] measured the resistivity at various oxygen concentrations and came to the conclusion that oxygen inhomogeneity is the main source of disorder. Oxygen diffusion can be an important problem as well already at room temperature. To avoid these difficulties we produced praseodymium substituted samples. The idea is to realise underdoping by replacing Ca^{2+} ions by Pr^{3+}. The bulk resistance as a function of temperature for such samples was stable over several days.

3.3 The peak-dip-hump structure

When we measure the current as a function of the applied voltage, we observe that the resistance of the junction decreases significantly as the voltage is increased. This results in a strong non-linearity in this $I(V)$ curve (figure 3.4). At voltages higher than 0.1 V, the $I(V)$ curve goes nearer to a linear behaviour. When we approximate this part by a line, we notice that its intercept with the zero-voltage-axis differs from zero. This additional current was believed to be like an excess-current described by Blonder *et al.* [76]. A fit with a function of the type $U/(a + bU)$, with the fitting parameters a and b, is however much more appropriate for this region (see section 4.5).

The derived curve dI/dV shows the well known peak, dip and hump features (figure 3.4). The criteria for good spectra were a high resistance at low voltages and high peaks in the dI/dV curve, both with respect to the values at high voltages. Furthermore, they have to be symmetric.

The peak position in BSCCO-2212 samples with critical temperatures of 87 ± 2 K is at around 60 mV. This result is independent of the coupling strength between the two parts. The peak position of a junction with a resistance of 500 Ω was within error the same as the one with a resistance of 1 MΩ. After approaching the two pieces of the sample and thereby increasing the conductance by a factor of ten, the peak position stays the same within a error of ten percent. To get an impression about the distribution of the peak positions, a histogram is shown in figure 3.5. It has to be pointed out that a subjectivity can significantly change this histogram. In fact, in the majority of the

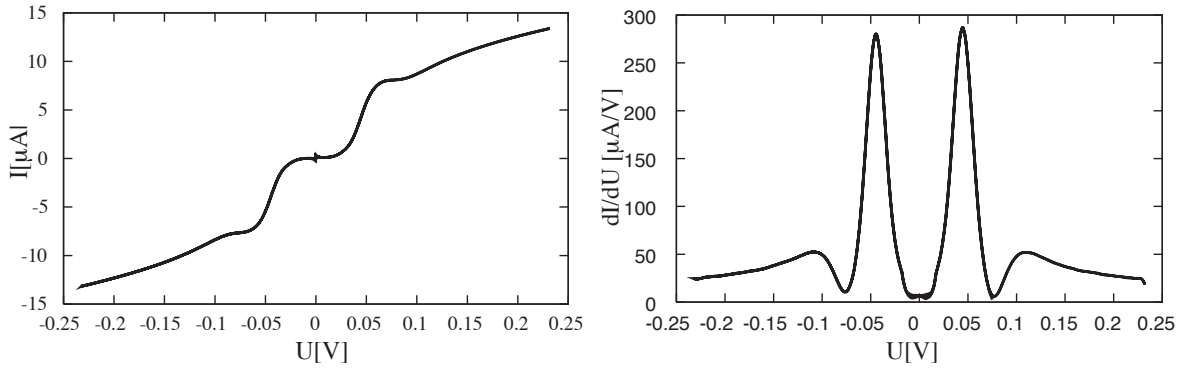

Figure 3.4: Left panel: A typical current versus voltage curve measured in BSCCO-2212. Right panel: The derivative shows the well known peak-dip-hump structure. (BSCCO-2212, 4.2 K).

cases, after approaching the two broken parts of the sample, the spectrum does not show any nice peaks. Usually the spectra are only recorded when they show peaks at the expected positions. Especially, peaks that appear from time to time at high voltages (see also section 3.8) are only rarely recorded. These high peak positions are not shown in the figure. Furthermore, the configuration was not changed between each measurement. Quite often, more than ten spectra were recorded without significantly changing the applied force on the support. That gives artificially an additional weight to the corresponding peak position. One sample with a relatively high T_c of 89 ± 1 K showed its peaks at 45 ± 5 mV. The spectra of this sample were among the nicest compared to the ones of the other samples (highest peaks with respect to the background).

The peak position is attributed to twice the gap magnitude 2Δ. In table 3.1 I compare different experimentally obtained values from the literature. These values are also plotted in figure 3.6. The results of the different techniques are more or less congruent. The result from Miyakawa, Suzuki and Anagawa represent the peak position of the dI/dV curve. As these are SIS junction, the peak position gives, as discussed in section 2.1, not directly the correct value for the gap. In early mesa structure measurements, much smaller values for the gap magnitude were proposed (12 meV for example in Yurgens *et al.* [77]).

We compare now these values from the literature with our break junction measurements. If we assume that our samples are optimally doped, what corresponds to a doping level of 0.16, then we observe that the measured peak position of 60 mV lies slightly below the literature value. Also for other doping levels, we obtain peak positions below the one from literature (see figure 3.10). We might get a higher gap value for our experiments if we determined the gap from the density of states, by de-convoluting the equation 2.1, which is ideally valid for SIS-junctions (see Mandrus *et al.* [78]). Including lifetime effects by using a Dynes Γ term (Dynes *et al.*) [28] gives also a gap magnitude different from the peak position.

One could think that the position of the peak should be dependent on the angle between the crystal axis and the main current flow. As the gap has a $d_{x^2-y^2}$-symmetry

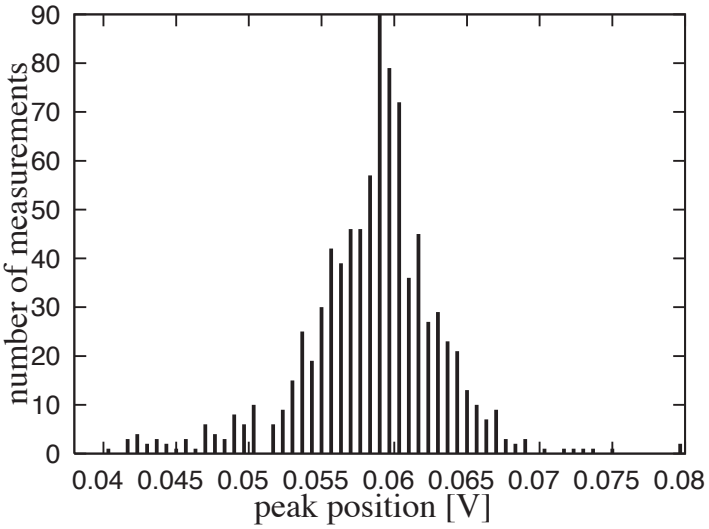

Figure 3.5: A histogram showing the peak position of the recorded spectra at $T = 4.2\,\mathrm{K}$ in 13 different BSCCO-2212 samples with T_c between 85 K and 88 K.

Table 3.1: The peak positions measured with different techniques in BSCCO-2212. The second column shows the T_c and whether the sample is underdoped (UD) or overdoped (OD) if it is specified in the publication.

Publication, Technique and Temperature	T_c / *Doping*	*Peak Position*
N. Miyakawa *et al.*, Phys. Rev. Lett. **80**, 157 (1998); Break Junction; 4.2 K.	95 K 83 K (UD) 82 K (OD)	$2\Delta = 75\,\mathrm{meV}$ $2\Delta = 90\,\mathrm{meV}$ $2\Delta = 52\,\mathrm{meV}$
Ch. Renner *et al.*, Phys. Rev. Lett. **80**, 149 (1998); STM; 4.2 K.	92.2 K 83 K (UD) 74.3 K (OD)	$\Delta = 41.5\,\mathrm{meV}$ $\Delta = 44\,\mathrm{meV}$ $\Delta = 34\,\mathrm{meV}$
B. W. Hoogenboom *et al.*, Physica C **391**, 376 (2003); STM; 4.2 K.	80.7 K (OD)	$\Delta = 36\,\mathrm{meV}$
K. M. Lang *et al.*, Nature **415**, 412 (2002); STM; 4.2 K.	79 K (UD)	$\Delta = 50\,\mathrm{meV}$
A. Matsuda *et al.*, Physica C **388-389**, 207 (2003); STM; 9 K.	89 K 67 K (UD)	$\Delta = 40\,\mathrm{meV}$ $\Delta = 55\,\mathrm{meV}$
M. Suzuki *et al.*, Phys. Rev. Lett. **82**, 5361 (1999); Mesa; 10 K.	87.1 K (OD)	$2\Delta = 50\,\mathrm{meV}$
K. Anagawa *et al.*, Appl. Phys.Lett. **83**, 2381(2003); Mesa; 10 K; Pulse Length $t = 60\,\mathrm{ns}$.	87 K (OD)	$2\Delta = 62\,\mathrm{meV}$

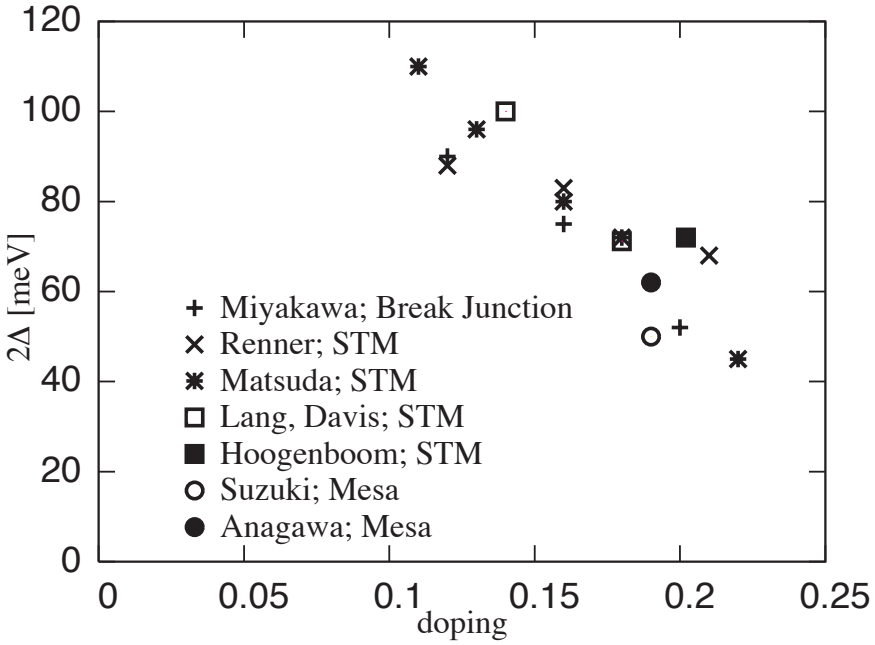

Figure 3.6: Twice the gap magnitude, measured with different techniques, is plotted as a function of doping. The references to the literature are given in table 3.1.

(see section 1.2.1), it goes to zero approaching the nodes. In our break junction technique we have no control about the direction of the break. The direction of the current flow is random. But we never measured peaks below 40 mV. No angular dependence could be observed. One could argue that the quantity we measure is an average over all directions. Why we should measure an average is however unclear.

3.4 The dip

As already mentioned, the derivative dI/dV shows a peak, a dip and a hump. The dips are sometimes very pronounced and the differential conductivity can even become negative at the dip position (see figure 3.7). Not only the peak, but also the appearance of the dip was believed to be caused by a physical property that might be important for the superconductivity (Norman *et al.*) [79]. Dips are also observed in other techniques like STM or ARPES (Ding *et al.*) [80].

A magnetic resonance peak was measured in inelastic neutron scattering in BSCCO-2212 (Fong *et al.*) [81]. This peak appears only below the critical temperature, indicating that it is strongly linked to superconductivity. In nearly optimally doped BSCCO-2212 its energy is at 43 meV. As this energy is similar to the energy difference between the peak and the dip of tunnelling and ARPES experiments, it was suggested that these two features are related. Zasadzinski *et al.* [39] proposed that the difference between the peak and the dip is a crucial magnitude in the dI/dV-spectrum. Such that the dip appears at a voltage of $2\Delta+\Omega$, where Ω is the energy of some type of collective excitation

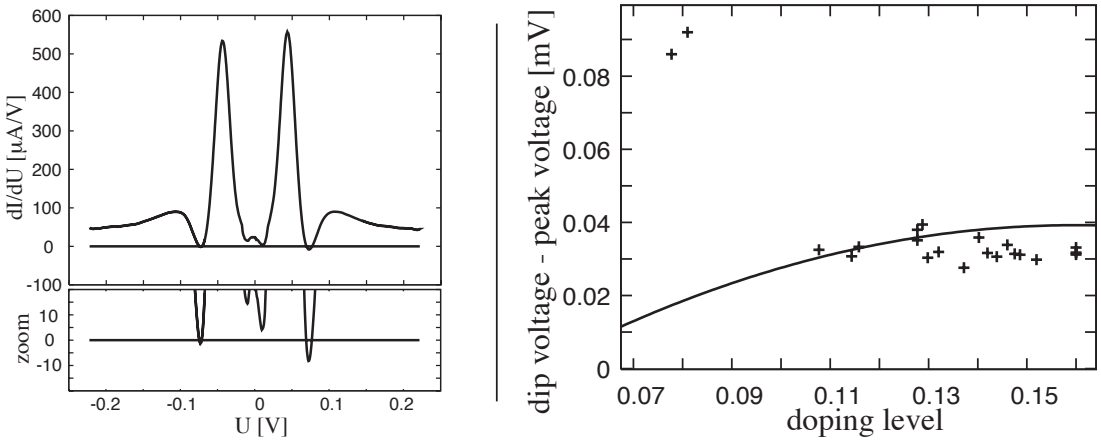

Figure 3.7: Left: We measure often highly pronounced dips. In some cases even negative differential conductance could be observed. Right: The line corresponds to the relation Zasadzinski *et al.* [39] proposed for the energy difference between the peak and the hump energy. With our measurements (+) we could not confirm this prediction. (BSCCO-2212, 4.2 K).

that is responsible for pairing in the cuprates. The similar energy levels implied that this collective mode is related to the magnetic resonance peak. He proposed that this energy Ω scales as $4.9\,k_B T_c$ with different doping levels. With our experiments we could not confirm this proportionality. In two underdoped samples a pronounced dip was observed at significantly higher energies than that proposed by Zasadzinski (see figure 3.7).

3.5 Temperature dependence and pseudogap

In the BCS theory, the gap closes when the temperature is increased. Its temperature dependence can be approximated with the formula $\Delta(T) = 1.74\Delta(0)[1 - \frac{T}{T_c}]^{\frac{1}{2}}$ for T close to T_c. If the peaks of our dI/dV curves represent the gap, one would expect that they approach when the temperature is increased and join at zero voltage when T_c is reached. In the experiment we observe that the peak voltage gets reduced with higher temperature, but it does not go to zero at T_c. The evolution of the spectra and the shift of the peak position with temperature are shown in figure 3.8. Around T_c the peaks decrease in height, and the dips disappear. The gap-like structure at $T > T_c$ was related to the pseudogap. Around 150 K the spectrum gets flat. This evolution of the spectrum with temperature looks very similar to that observed in STM (see section 1.3).

It is difficult to measure the temperature dependence of our break junctions due to thermal dilatation of the sample holder. But as the peak-dip-hump structure is nearly independent of the size of the juncion, the curves in figure 3.8 can be considered as correct. However, thermal dilatation makes it more difficult to know the temperature dependence of the absolute resisitvity. It would be interesting to measure the resistivity at low voltages, mainly if we want to discuss the effect of heating (see section 4.1). We measured the low voltage resistance in more than 10 temperature sweeps. As we

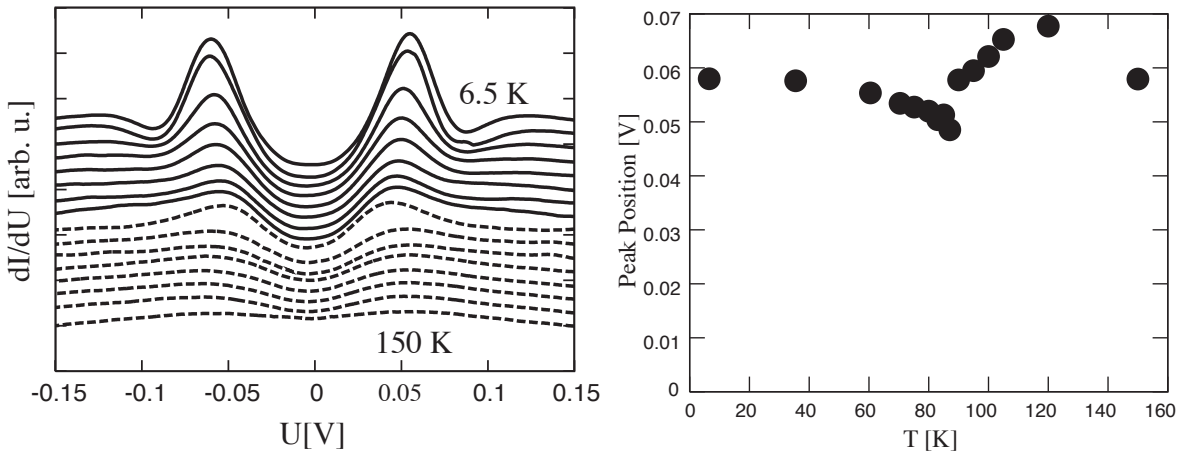

Figure 3.8: Left panel: The temperature dependence of the dI/dV curves is shown for a BSCCO-2212 sample. The spectra above T_c are drawn with a dashed line. The temperatures from the top to the bottom are: 6.5 K, 35.5 K, 60.5 K, 70.5 K, 75.2 K, 80 K, 83 K, 85 K (continuous lines), 87 K, 90 K, 95 K, 100 K,105 K, 110 K, 120 K, 150 K (dashed lines). The critical temperature of the sample is 85.5 K. The curves are vertically shifted for better visibility. Right panel: The position of the maximum of the dI/dV curve does not decrease to zero at T_c.

observed always a similar decrease of the resistance with the temperature we believe that a strong decrease in the resistivity, like the one shown in figure 3.9, is intrinsic.

3.6 Doping dependence of the gap and inhomogeneity

After the BCS theory, the ratio between the gap and the critical temperature is a universal constant. Hence one would expect that the gap magnitude decreases in a parabolic way while underdoping the sample. However many experiments like ARPES or Raman scattering (Hewitt *et al.*) [82] show that the magnitude of the gap increases with underdoping in BSCCO, similarly to the pseudogap temperature T^*.

We measured break junction spectra in our praseodymium substituted samples in order to verify this relation.

The dependence of the critical temperature T_c on the doping p can empirically be approximated with the formula $T_c/T_{c,\max} = 1 - 82.6(p - 0.16)^2$, where $T_{c,\max}$ is the critical temperature at optimal doping (Tallon *et al.*) [5]. From the measured T_c we could in this way estimate the doping level p. For $T_{c,\max}$ we took 93 K, the highest measured critical temperature in our samples.

For several reasons, the measurements with our underdoped samples are difficult to perform. As the praseodymium substituted samples are brittle, the risk to break them during the the preparation or characterisation is quite high. Furthermore, the measurements of the temperature dependence of the bulk resistance show often not a well defined transition temperature. And finally, the break junction measurements show only rarely reproducible spectra.

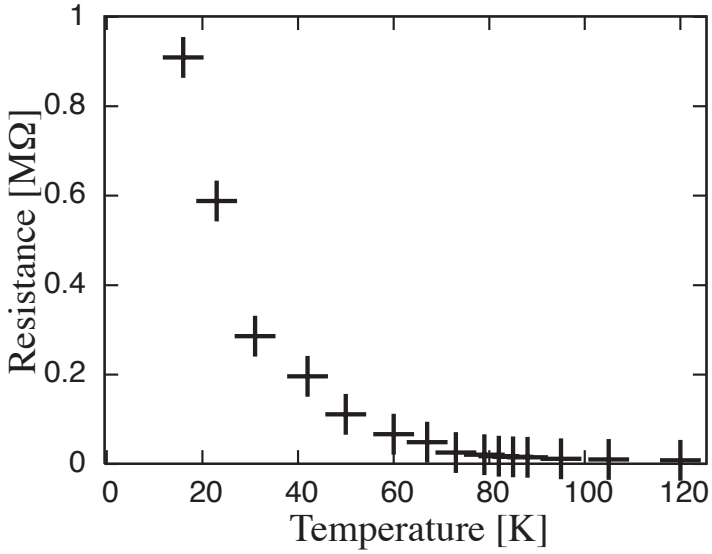

Figure 3.9: The resistance at 0.01 V decreases strongly when the temperature is increased (BSCCO-2212 sample). With this decrease the non-linearities in the $I(V)$ curves can be explained within a heating model (see section 4.1).

In figure 3.10 we plot the measured peak positions as a function of doping. Several features can be observed:

i) The variation of the measured values is large. This fact is not surprising. In view of recent STM results that showed that the peak position is significantly space dependent (see section 2.2.3 and Matsuda *et al.* [83]), we have to keep in mind that the underdoped samples are intrinsically very inhomogeneous. For this reason our measurements depend strongly on the location where the sample breaks. We should not forget either that we have a large variation of the peak position also in the optimally doped case (section 3.3).

ii) At low doping, only relatively high peak positions could be measured. This is consistent with the above-mentioned increase of the gap with lowering doping. For comparison, we added our points to figure 2 of (Hewitt *et al.*) [82] (see figure 3.10). In this figure Hewitt *et al.* collected data from tunnelling, ARPES and Raman spectroscopy. Our values lie lower than the ones mentioned in this article, but it can be supposed that the dependence on doping in our measurements is similar to the one that is proposed in this article. If one wants to obtain a more conclusive result for the doping dependence, more statistics should be done.

iii) Even near the optimal doping level very high peak positions (around 0.1 V) can be observed. This fact is discussed in section 3.8.

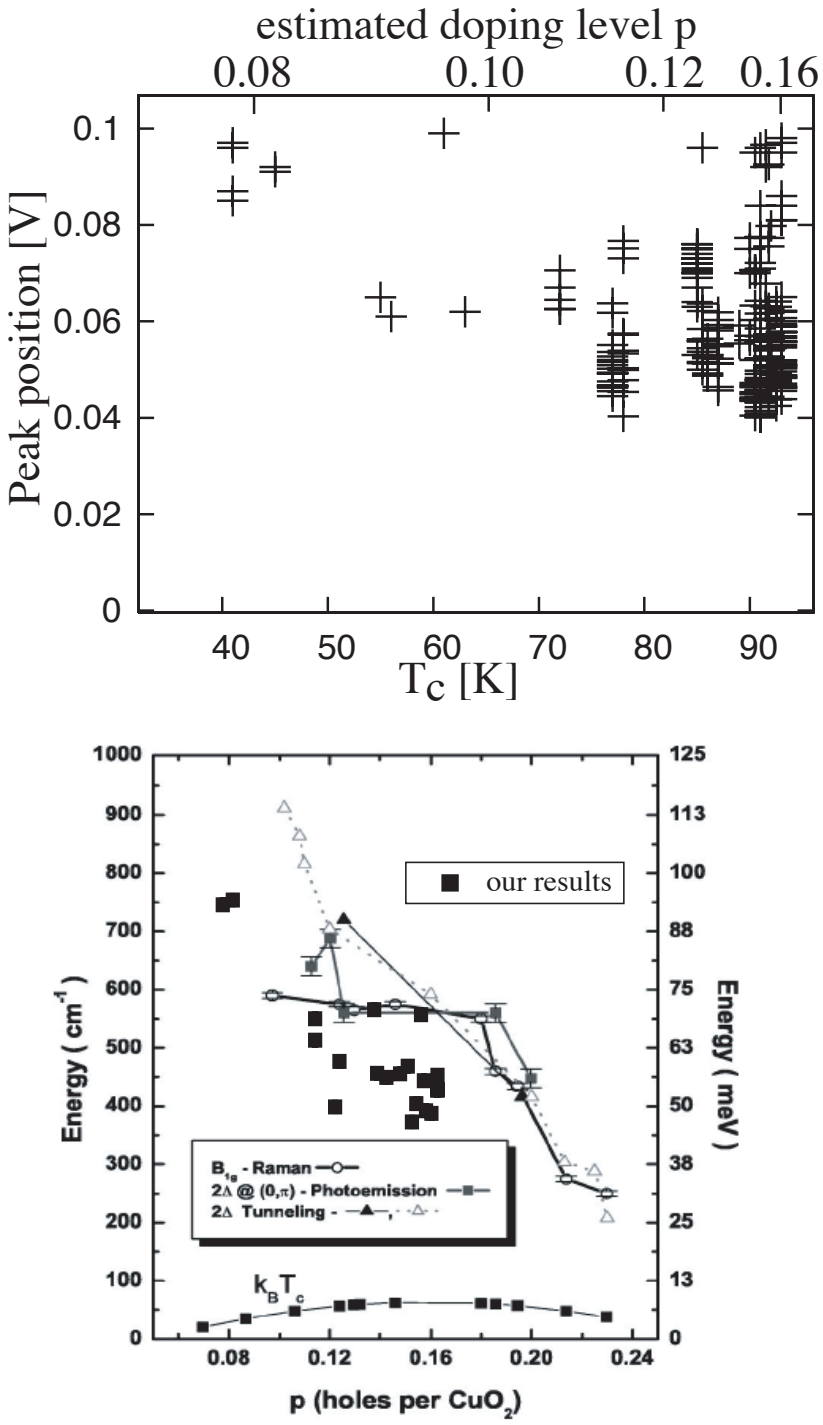

Figure 3.10: Upper panel: The peak position as a function of T_c and the estimated doping level in our experiments. The variation of the measured values is large. Each symbol corresponds to one spectrum. Lower panel: Our measurements (full squares) are included in a figure from Hewitt *et al.* [82] to compare them with the values from other techniques (Raman spectroscopy, photoemission and point contact tunnelling). Each square corresponds to one broken crystal and is the average over all nice spectra. (BSCCO-2212, 4.2 K).

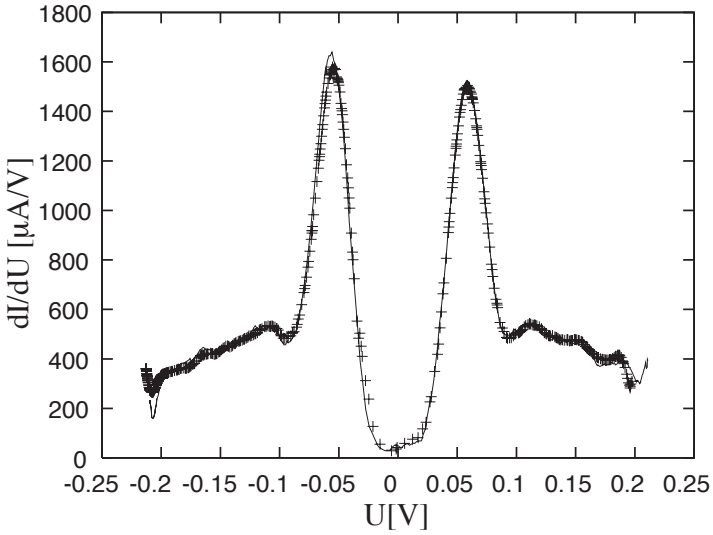

Figure 3.11: The spectrum measured at fast rates (line, $2.5 \cdot 10^5$ V/s) does not differ from the one measured slowly (+). In the fast measurement it takes 0.25 μs to increase the voltage from zero to the position of the peak. (BSCCO-2212, 4.2 K).

3.7 Pulsed measurements

The problem of self-heating in mesa structures has been known for a long time. Indications are given for example by $I(V)$ curves in a shape of an "S" (see section 3.9) or recently also directly by measurements of the temperature (see chapter 5). In order to overcome these problems, several groups (see section 5.1.1) tried to do pulsed measurements. They try to measure the $I(V)$ curve before the sample starts to heat up.

A time dependence of our spectra could give a strong indication for heating in our experiments as well. For this reason we measured with pulses. It is difficult to estimate the timescale that would be necessary to see an effect. The fastest measurements we could do, making sure that artefacts can be excluded, were at $2.5 \cdot 10^5$ V/s. That is, starting from zero voltage we reached the peak voltage after 250 ns. The curves do not change (see figure 3.11). Even big area junctions did not show any change at this speed.

Anagawa *et al.* [84] observed a change in the $I(V)$ curve at 300 ns in mesa structures (see section 5.1.1). This result can, however, not be compared directly with our data. The geometry of the heat and current flow is different. In addition, the volume of the mesa being of the order of $1.5\,(\mu\mathrm{m})^3$ seems to be bigger than the volume in which the energy is dissipated in our junctions. These results were thus not conclusive.

3.8 Hysteresis effects

After breaking a BSCCO-2212 or BSCCO-2223 flake and re-approaching the broken parts at temperatures below T_c we may obtain a nice spectrum with a well defined

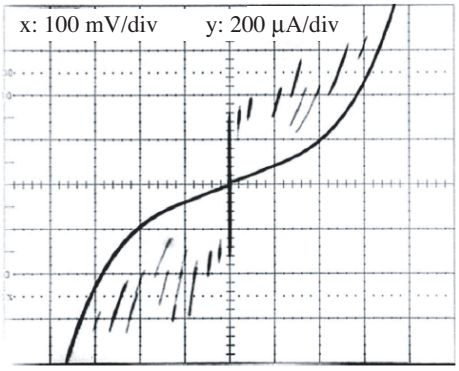

Figure 3.12: The $I(V)$ curve measured in a BSCCO-2223 mesa structure shows the multiple-branch characteristics (stack with 10 junctions, 7 K) (Yamada *et al.*) [85].

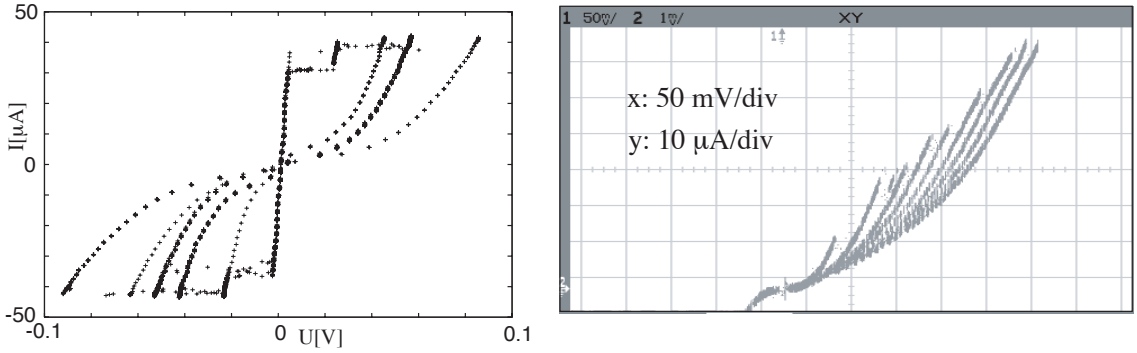

Figure 3.13: The $I(V)$ curves we measured in BSCCO with our break junction-technique often show hysteresis effects (4.2 K).

peak-dip-hump structure. In by far more than 50 % of the cases, however, we observe hysteresis-effects looking like those measured in the mesa structures (see figures 3.12 and 3.13) or point contacts (Ozyuzer *et al.*) [41]. In the same sample, hysteretic effects can appear and disappear consecutively after reassembling the two parts in a different way.

Increasing the voltage, we go up on a certain branch. When we increase the voltage over a certain threshold, we jump from one branch to the next higher resistive one. When we hold the voltage for some time at a constant value near to the top end of a branch, the voltage has a certain probability to jump to the next higher branch. This looks similar to effects which were observed in mesa structures (Mros *et al.*) [86]. While decreasing the voltage, we follow the chosen branch back, without jumping anymore. Each of these branches has a peak-dip-hump characteristic in its derivative (see figure 3.14). No hysteresis has been observed at bath-temperatures above T_c.

The jumps from one branch to the other explain also the huge gaps which are measured from time to time. In fact, in some samples with a customary peak value of 60 mV, peak positions much higher than 100 mV could sometimes be observed (see figure 3.15, left panel). The explanation of this phenomenon is, probably, that we measure on an

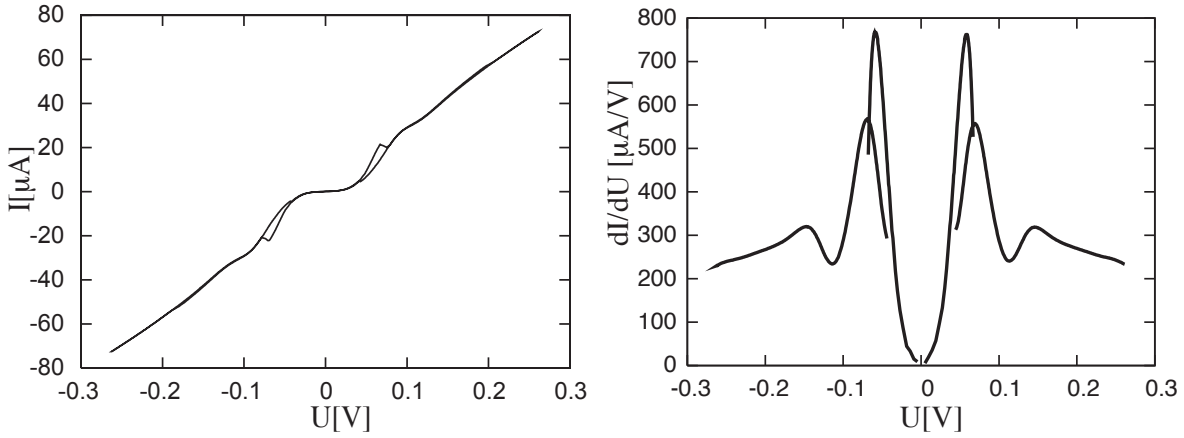

Figure 3.14: A hysteretic $I(V)$ curve (left) and its derivative dI/dV (right). Each hysteretic branch shows a peak-dip-hump structure in its derivative. (BSCCO-2212, 4.2 K).

outer branch. Often the jump to the outer branch is visible as a shoulder in the derived curve (see figure 3.15, right panel).

In the mesa structures, these hysteresis effects are usually explained as the successive transitions from the superconductive into the resistive mode of the junctions (see e.g. Kleiner *et al.* [53] or Schlenga *et al.* [54]). A jump from one branch to the other is interpreted as the switching of one complete layer from the normal into the resistive state. When the critical current of the junction is attained, the phase coherence between the CuO_2 planes gets lost, and we switch to the next branch. As our break junction curves look like the ones from the mesa structures, it is tempting to think that the same mechanism is responsible for the results of both techniques.

As the wires are contacted to the topmost layer and the junction is surely somewhere below, we can be sure that we have also some c-axis transport. However, as the surfaces of our flakes are of the order of one square millimetre, we have only a c-axis current density of roughly 0.01 A/cm^2 in the bulk, which is by order of magnitudes smaller than the typical current densities in a mesa experiments, which can reach 500 A/cm^2. The current density is too small to switch one entire plane into the resistive mode. Another way to keep the intrinsic junction model would be to assume that small crystallites in the order of a micrometer are formed during the break, and that they make in such a way a contact to the two other parts of the flake that we have a transport in c-direction through them. There are arguments against this hypothesis: Hysteretic effects are not a rare case but show up very often. We observed hysteresis in all the measured samples, even if the junction interface looks well defined. No complicated geometry was observed by electron microscopy (see figure 3.16). Another possibility to explain hysteresis effects might be that layers go partially normal around the contact. At each voltage jump a part of an additional layer goes normal.

Often, even if we measure a nice peak-dip-hump structure without any clearly visible hysteresis, we can discover one or more voltage jumps when we look more carefully with

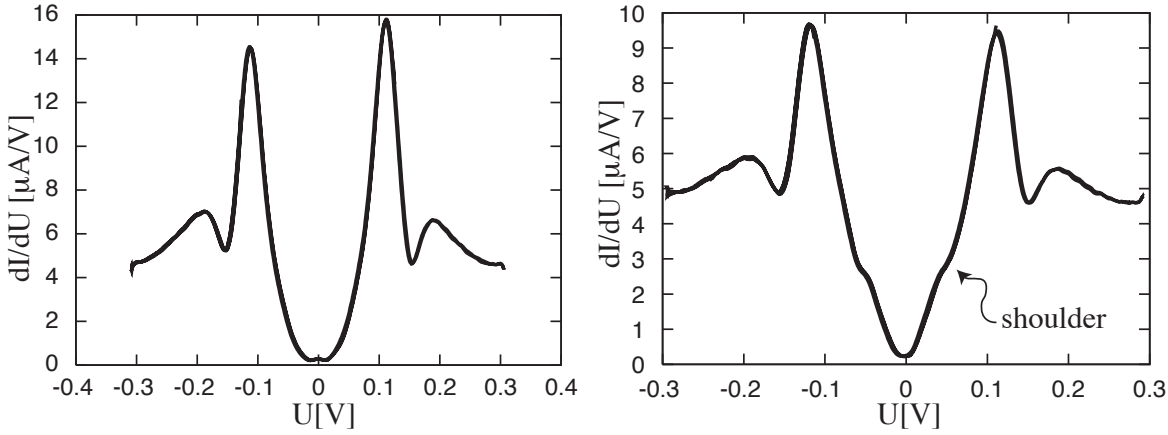

Figure 3.15: Left panel: Sometimes in BSCCO-2212 the peaks lie higher than 100 mV. Right panel: A shoulder is often visible in the spectra with the huge gaps. This shoulder corresponds to the voltage-jump from one hysteretic branch to the other. (BSCCO-2212, 4.2 K).

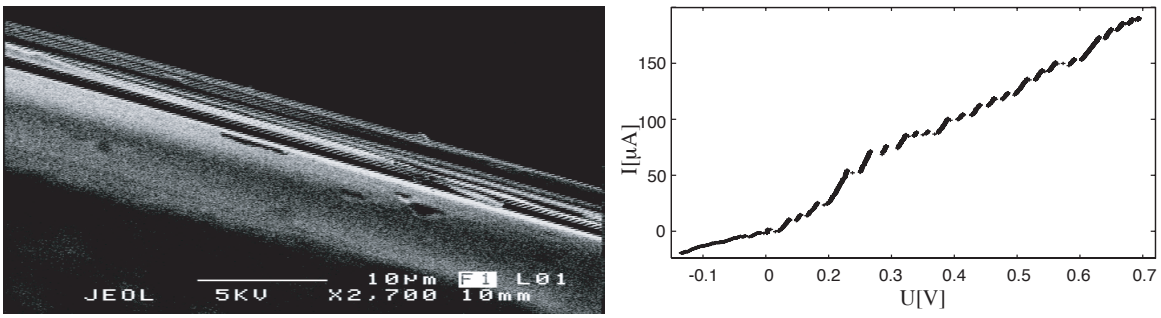

Figure 3.16: Top view on the junction interface of a BSCCO-2212 sample. (Electron microscopy, Mirko Milas, EPFL, IPMC). Even if it had a simple geometry, the $I(V)$ characteristic of this sample showed the hysteretic branches shown in the right panel.

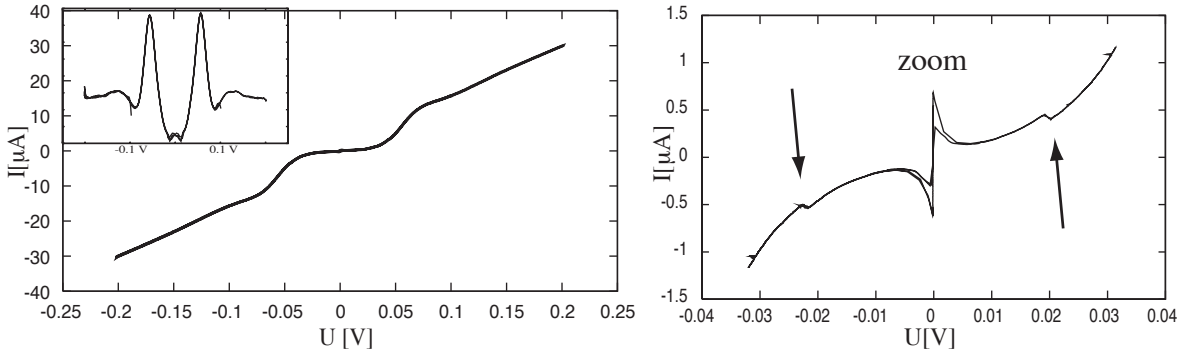

Figure 3.17: The left panel shows an $I(V)$ characteristic and its peak-dip-hump features. The peaks lie at 57 mV. When we zoom in (right panel) we observe voltage-jumps (arrows). The branch on which we measure the peak is thus at least the second one. (BSCCO-2212, 4.2 K).

a resolution high enough (see figure 3.17). Consequently, we have to ask ourselves which peak position corresponds to the real one. One could think that we have to choose simply the smallest peak positions, and the ones where no jump to the next branch is visible. In this way we could define the intrinsic curve as the branch with the lowest voltage. Unfortunately, we measured spectra with even three voltage jumps below a peak voltage of 55 mV. That means that we are measuring at least on the fourth branch. In most cases we move probably on a higher order branch from the very beginning. That is the reason why it is important to understand hysteresis effects and to know on which branch we are moving.

3.9 S-shape effects

Usually, when we lower the voltage over a sample, the current decreases. However, sometimes we observe the contrary: the current increases but simultaneously the voltage decreases (see figure 3.18). It is even possible to move back and forth on this backbent part without going to the normally inclined part, even at frequencies much lower than 1 Hz. This can be explained if we assume that the resistivity of the sample changes during the measurement. The change in the resistance as a function of the voltage is illustrated in figure 3.19. Most probably the resistance changes because the temperature of the sample changes. As the resistance is lower at higher temperatures, we can observe this backbending. In mesa structures this S-shape is observed very often. One can get rid of it by decreasing the size of the mesa structure and by using pulsed (fast) voltage sweeps. It is generally agreed that the increase in resistance in the backbent part of these experiments is due to heating. The increase in resistance that provokes the "gap" in the $I(V)$ curve however is interpreted as an effect of intrinsic tunnelling. See for example the work of Schlenga *et al.* [54] or Suzuki *et al.* [87] for literature about backbending in mesa structures.

Simple heating does not necessarily lead to an S-shape. As we can see in figure 3.19,

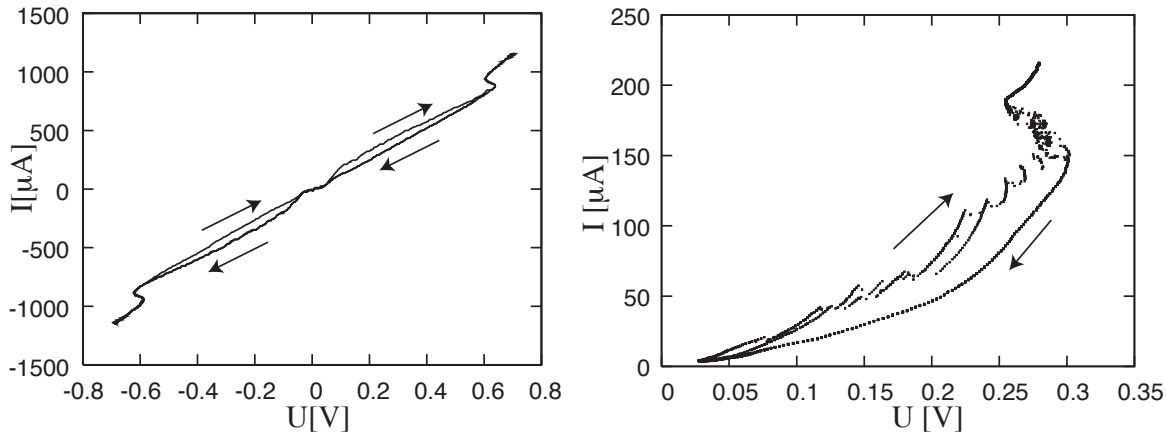

Figure 3.18: We measured backbending effects like those observed in mesa structures. The arrows indicate the direction of the recording of the curve. (BSCCO-2212, 4.2 K).

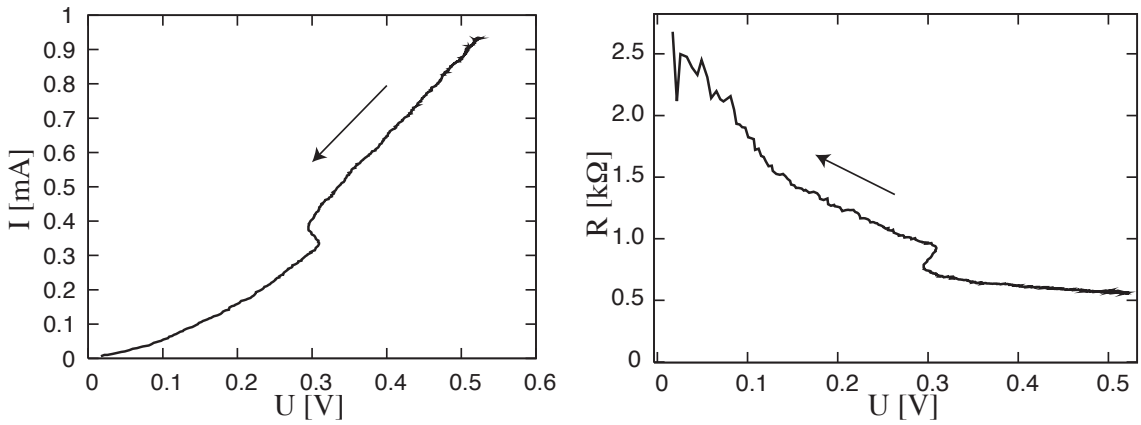

Figure 3.19: Left panel: An $I(V)$ curve showing an S-shape. Right panel: The same curve as in the left panel, but plotted as U/I (resistance) versus the voltage. The resistance increases suddenly, when the voltage reaches the position of the curvature of the "S". The arrows indicate the direction of the recording of the curve. (BSCCO-2212, 4.2 K).

the resistance drops suddenly in the backbent part. From that we can assume that the temperature increase has to be abrupt as well. The sudden rapid increase of the temperature in mesas may have something to do with the fact that the bottom part of the stack is still in the superconducting state while the upper part, where the electrical energy is dissipated, is in the resistive state. As the superconducting part has no more electrical but a high thermal resistivity, the heat is retained in the upper part and the temperature increases rapidly.

Chapter 4

An alternative interpretation of the dI/dV curve: A heating model

The peak-dip-hump features in the dI/dV curve are usually interpreted within the semiconductor model (see section 2.1). We realised however that alternatively these features can perfectly be explained in a heating model, which does not depend on the tunnelling effect.

For this model the resistance would be described by Ohms law, if we could keep the temperature constant. It needs the voltage dependence of the junction temperature and the temperature dependence of the junction resistance. These $T(U)$ and $R(T)$ relations are discussed in sections 4.2 and 4.3.

The experiments in which the confirmation of the heating model is the easiest for us are grain boundary junctions because they allow reliable $R(T)$ measurements due to their mechanical stability under a temperature change. For such a sample, one can reconstruct the dI/dV curve directly from the $R(T)$ relation (subsection 4.3.2). Even the temperature dependence of the dI/dV curves can be explained with this heating model (section 4.4).

This heating model has the same roots as the model that was the origin of many discussions about heating in mesa structures, and was proposed by Zavaritsky (see section 5.1).

In section 4.6 I discuss the influence of heating on a tunnelling model, assuming that the semiconductor model is valid.

4.1 The model

Let us start with a classical and very simple approach: we assume that all the non-linearities in the $I(V)$ curve are only caused by the temperature dependence of the resistance. For the moment we make the assumption that we are working in a SNS geometry (see section 3.1.1), where some part of the superconductor became normal due to the application of a current higher than the critical one. In principle there is no problem to include an insulating layer in this model.

The junction (the normal part in an SNS geometry) has a certain resistance that depends not on the voltage, at least not in a direct way. The power $P = UI$ that is dissipated in the junction is transformed into heat. The more we increase the voltage, the more the junction heats up. If the junction resistance depends on temperature, we will get a non-linear $I(V)$ curve.

If we want to obtain the exact $I(V)$ curve we first have to answer two questions:

1. How does the temperature of the junction depend on the applied voltage ($T(U)$ curve)?

2. How does the junction resistance or the normal state resistivity of our material depend on the temperature ($R(T)$ curve)?

The first question is difficult to answer. We will try to find an approach in section 4.2. Let us for simplicity assume for the moment that the temperature increases linearly with the voltage.

In section 4.3, I will try to give an answer to the second question. I will propose how to find $R(T)$ by means of different experiments. At this point, in order to explain the heating model, I take a curve that we already measured: the low voltage junction resistance of our experiments. It is the one shown in figure 3.9. At the moment we neglect the errors due to thermal dilatation or due to the change of the volume of the normal state material with temperature.

4.1.1 Reconstruction of the $I(V)$ curve from the $R(T)$ curve

From the $R(T)$ relation (figure 3.9) we are now able to reconstruct the $I(V)$ curve. For the moment, as we do not care for units, we ignore the proportionality factor between the junction temperature T and the applied voltage U. On the abscissa we simply plot the temperature instead of the voltage. In the same way, we plot on the ordinate the current $I = U/R(T) \propto T/R(T)$, where we replaced again the voltage by the temperature. The curve which we obtain in that way shows a gap-like structure (see figure 4.1).

It is clear that at this stage we cannot see exactly the same curve as the one which is usually interpreted as a tunnelling spectrum. Before we can get a better result we have to answer the above mentioned questions. But we realised already that with very few assumptions and a natural and simple model we can qualitatively reconstruct a gap-like structure from the $R(T)$ relation. The main hypothesis is that we measure the temperature-dependent (but voltage-independent) junction resistance.

4.1.2 Reconstruction of the $R(T)$ curve from the $I(V)$ curve

Alternatively we can tackle the problem from the other side. We can reproduce the resistance curve from the $I(V)$ characteristic by simply dividing the voltage by the current. If we plot this resistance as a function of the voltage we should obtain a similar $R(T)$ curve as the one in figure 3.9, assuming that the temperature increases linearly with the voltage. As expected, the curves that we obtain in this way show the strong decrease of the resistance at low temperature. They are shown in figure 4.2.

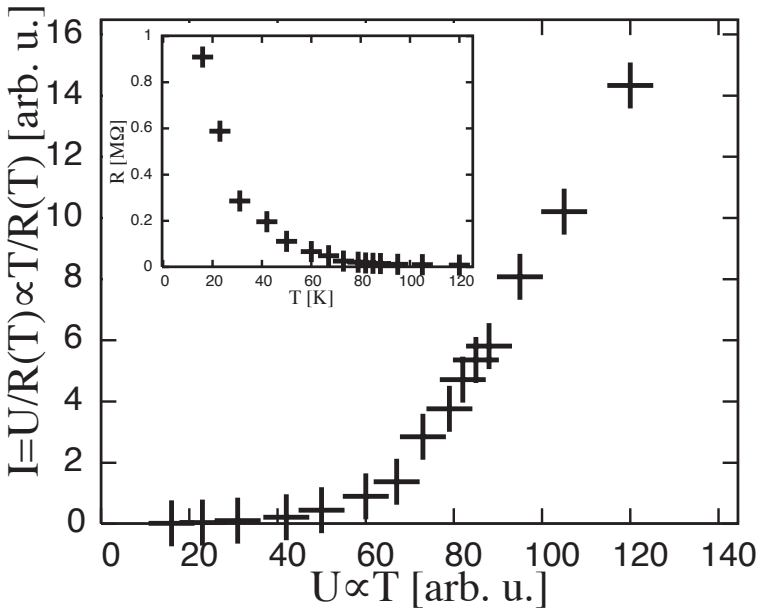

Figure 4.1: The reconstructed $I(V)$ curve shows a gap-like structure. The idea is simple: first, at low voltage we have little heating. And second, the junction resistance is high at low temperature as experimentally observed (see figure 3.9). For these two reasons the resistance at low voltages is big and consequently the current suppressed. Inset: The same $R(T)$ curve as in figure 3.9 is shown once more for direct comparison. (BSCCO-2212).

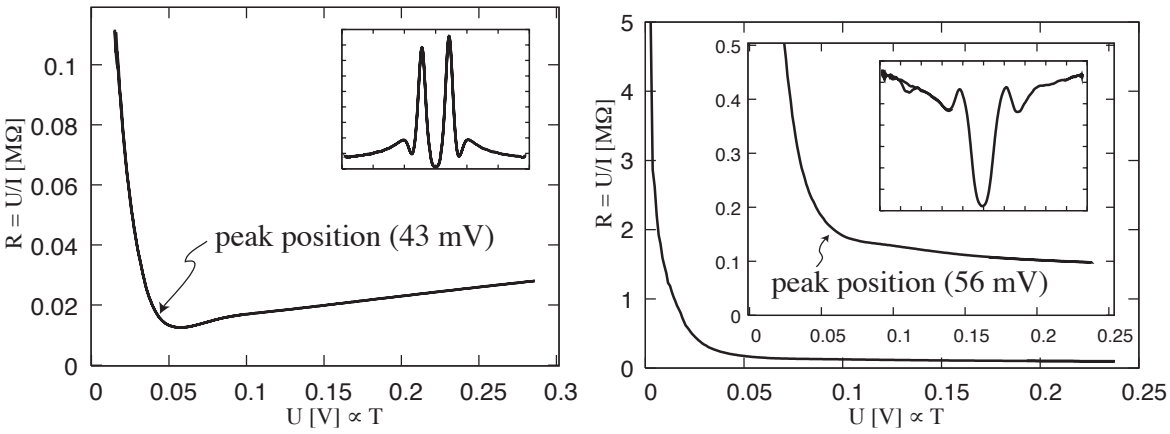

Figure 4.2: Left: The resistance calculated as U/I from the $I(V)$ measurement for a low resistance junction. The inset shows the corresponding dI/dV curve. Its peak position (43 mV) is indicated in the U/I curve. Right: The resistance of a high resistance junction has a dependence on the voltage that resembles the R(T) curve of figure 3.9. First inset: zoom in. Second inset: corresponding dI/dV curve. (BSCCO-2212, 4.2 K).

We notice that for the junctions that show a nice peak-dip-hump structure, the corresponding reconstructed resistance (U/I versus U curve) is nearly perfectly linear at high voltages. It shows a metallic-like behaviour. Mostly the low resistance, that is the big area junctions tend to be of this kind. The same is true for the junctions from good quality samples. For the high resistance junctions, the behaviour looks insulating-like until high voltages. These high resistance spectra look very similar to the ones observed in grain boundary junctions (see section 4.3.2). The reason of that behaviour might be that we have channels with metallic like and others with insulating like behaviour. In the big area junctions the probability to find a well conducting metallic channel is higher than in the low area junctions.

Notice also the fact that if we plot U/I versus U no special feature is visible at the position where the peaks appear in the dI/dV curve (see figure 4.2).

4.1.3 Recipes to reconstruct the $R(T)$ or the $I(V)$ curve

For a qualitative result it suffices to plot U/I versus U to reconstruct $R(T)$. Equivalently a plot with U/R on the ordinate and T on the abscissa gives a good qualitative reconstruction of the $I(V)$ curve. For a quantitative test a relation between the temperature T and the voltage U has to be found. An acceptable approximation for this $T(U)$ relation is in many cases given by the Kohlrausch relation $T^2 = T_0^2 + U^2/(4L)$, where $L \approx 2.4 \cdot 10^{-8}$ WΩ/K^2 is the Lorenz number. I dedicate the next section to discuss the validity of this relation. In the experiments described in the present work, a better result is generally attained when the factor four is replaced by a higher number.

Reconstruction of the $R(T)$ curve from the $I(V)$ curve:

- Take the $I(V)$ curve of a certain bath temperature T_0.
- Instead of T, plot $\sqrt{T_0^2 + U^2/(4L)}$ on the horizontal axis.
- Instead of R, plot U/I on the vertical axis.

Reconstruction of the $I(V)$ curve for a certain bath temperature T_0:

- Take the $R(T)$ data.
- Instead of U, plot $\sqrt{4L(T^2 - T_0^2)}$ on the horizontal axis.
- Instead of I, plot $\sqrt{4L(T^2 - T_0^2)}/R$ on the vertical axis.

4.2 The temperature as a function of voltage

When we first faced the problem of estimating the temperature of the junction as a function of the temperature and the voltage, it seemed to be hopeless to find a reasonable relation. First, it is difficult to know where in the junction the energy is dissipated.

Additionally, the thermal and electrical conductivity differ significantly or even dramatically from the superconducting to the normal state. The anisotropy of our material seemed to cause further problems. It was not clear, either, whether the heat flows away through the sample or if it is carried away by the surrounding helium gas.

The Kohlrausch relation however proved to give a good starting point.

4.2.1 The Kohlrausch relation

Finding the temperature $T(U)$ of an electric contact between two materials when a voltage U is applied, turned out to be an old problem. The interest came mainly from industrial applications. Investigations have been done on several types of electric contacts. For a concrete example I just mention the problem of sliding contacts like a graphite brush on a commutator in a motor. Soon it was clear that the contact temperature depends nearly exclusively on the voltage drop over the contact. More than hundred years ago Kohlrausch [88] found the so-called Kohlrausch- or $\phi\vartheta$-relation. It starts from the fact that the electrical and thermal currents flow in the same path. For a justification see §13 of Holm's book [89] or Greenwood *et al.* [90]. Its general form is

$$U^2 = 8 \int_{T_0}^{T_m} \lambda \rho dT \qquad , \tag{4.1}$$

where the integral is taken from the bath temperature T_0 to the contact temperature T_m. λ and ρ are the thermal conductivity and the electrical resistivity, respectively. Knowing the temperature dependencies $\lambda(T)$ and $\rho(T)$, one can calculate the contact temperature T_m as a function of the applied voltage U.

In metals, when the Wiedemann-Franz law is fulfilled, the relation $\rho\lambda = LT$ can be used to simplify the equation (4.1)

$$T_m^2 = T_0^2 + \frac{U^2}{4L} \qquad , \tag{4.2}$$

where $L = (\pi k_B)^2/(3e^2) \approx 2.4 \cdot 10^{-8}\,\mathrm{W\Omega/K^2}$ is the Lorenz number. It might be surprising that the contact temperature is a function of only two parameters: the bath temperature T_0 and the applied voltage U. When we measure at a given bath temperature, say room temperature, we are even able to define a softening, melting or boiling voltage, according to the corresponding temperatures. As these three points can bee seen in the contact resistance, the Kohlrausch relation (4.2) can easily be verified experimentally. That was successfully done for several metals (see §13 of Holm's book [89] or Timsit [91]). Also the ferromagnetic transition in gadolinium could be found (McLean) [92] in the differential resistivity curve at the expected voltage. Furthermore, the Kohlrausch relation was successfully applied for point contacts with ferromagnets (Verkin *et al.*) [93] or with UPd_2Al_3 (Naidyuk *et al.*) [94].

Timsit [95] studied the validity of the Kohlrausch relation with two aluminium cylinders separated by a fissured oxide film. He found that the equation (4.1) holds well for contacts with a size bigger than $0.1\,\mu$m. For junctions where the typical junction size is

smaller than the electronic mean free path, the Kohlrausch relation is inapplicable. In such small contacts we are in the ballistic regime and an additional, so-called Knudson resistance appears.

The book of Holm [89], the review of Timsit [91] or the article of Greenwood *et al.* [90] give a good starting point to get familiar with the Kohlrausch relation and its applicability.

4.2.2 Applicability of the Kohlrausch relation in our experiments

When we try to determine the temperature of our junction with the Kohlrausch relation (4.1) or (4.2), we encounter several problems.

First we have to check whether the use of the Wiedemann-Franz law is reasonable in a superconductor that turned into normal, either because the current exceeded the critical value or because the temperature is above T_c. Experiments that measure the electrical resistivity in the normal state at $T < T_c$ are rare and difficult to perform. The thermal conductivity in the normal state at $T < T_c$ is even more difficult to obtain. For $T > T_c$, the thermal and electrical resistivities have been measured. Crommie *et al.* [96] estimated the ab-plane Lorenz ratio for BSCCO-2212 to be around $8 \cdot 10^{-8}\,\mathrm{W/\Omega K^2}$, that is around three times higher than the Lorenz ratio of an ideal metal. In the c-axis direction however, the material does not behave like a metal anymore. Whereas the ratio of the electrical conductivities σ_{ab}/σ_c is in the order of 10^4, the ratio of the thermal conductivities $\lambda_{ab}/\lambda_c \approx 6$ is much smaller (Crommie *et al.*) [97]. One has to suppose that phonons carry a non negligible part of the heat away in the c-direction. This deviation from the Wiedemann Franz law, the anisotropy and the fact that we do not know exactly in which direction the electrical current and the heat flow, can produce problems in the application of the Kohlrausch relation.

Despite these uncertainties, the Kohlrausch relation should give quite a good value for a first approximation of the temperature in the normal state part of our junction. More difficult is the situation if we consider the superconducting region, where the electrical current flows without resistance and where at the same time the thermal resistivity is high. If we suppose that our junctions have a SNS-geometry, we have to consider that the heat might have difficulties to flow out of the normal region which is surrounded by a superconducting region. On account of this, the contact temperature might be higher than expected.

Furthermore, without knowing the dissipation mechanism, the decisive mean free paths and the contact area, it is difficult to estimate the validity of the Kohlrausch relation.

In conclusion, if we want to use the Kohlrausch relation to calculate a reliable value for the contact temperature in our experiments, we have to be careful. When I use this relation in what follows, it is mainly to simplify matters. A linear dependence $U \propto T$ does not in most cases change the results significantly.

4.2.3 What can we learn from the Kohlrausch relation?

Even if the application of the Kohlrausch relation in our experiments is delicate, we can nevertheless get important insights from it into the heating problem.

- It is not surprising that the temperature is only a function of the voltage and not of the junction size and geometry.

- A linear dependence of the temperature on the voltage at high voltages seems to be reasonable.

- For low bath temperatures, the Kohlrausch relation in a metal (4.2) approaches $eU = 3.6\,k_{\mathrm{B}}T$. This result resembles the BCS relation: $2\Delta = 3.52\,k_{\mathrm{B}}T_{\mathrm{c}}$. Very much care has to be taken in experiments not to confound these two relations.

- In mesa structures, as we will see in section 4.3.1 (figure 4.4), the temperature at which the reconstructed dI/dV curve shows a peak is at around 80 K. The peak voltage that is usually assigned to the gap was found to be 53 mV in the corresponding pulication (Suzuki *et al.*) [98]. This indicates that $T(53\,\mathrm{mV}) = 80\,\mathrm{K}$. The Kohlrausch relation (4.2), assuming that the Wiedemann-Franz law holds, gives $T(53\,\mathrm{mV}) = 170\,\mathrm{K}$, a value that differs only by a factor of 2.

- In our experiments, as we have problems of thermal dilatation when we measure the resistance as a function of the temperature, it is difficult to compare quantitatively the reconstructed curve with the original one. If we compare the reproduced $I(V)$ curve (figure 4.1) with the "normal" $I(V)$ curve, we can do the risky estimation that the factor 4 in front of the Lorenz number (in the Kohlrausch relation) has to be replaced by 15. That corresponds to $dT/dU \approx 1.6 \cdot 10^3\,\mathrm{K/V}$ for $U/\sqrt{4L} >> T_0$.

- When we apply a voltage of 0.5 V over our junction, we can damage it in such a way that irreversible changes in the low bias resistivity appear. With the same factor 15 (instead of 4) replaced in the Kohlrausch relation, we obtain a contact temperature of about 800 K. That is a reasonable value.

- In the grain boundary structures described in section 4.3.2, the $I(V)$ curve can surprisingly well be reconstructed from the $R(T)$ curve (see figure 4.7) with a slightly adjusted form of the Kohlrausch relation.

- In conventional superconductors, where the material is homogeneous, we do not have the difficulty of anisotropy. The question about the thermal and electrical conductivity in the normal state, as well as the problem for the heat to flow away through the superconducting part still exist. The Kohlrausch relation suggests that the planar junctions, measured by Giaever [11], are already heated to T_{c} by the application of a voltage near to twice the value of the gap.

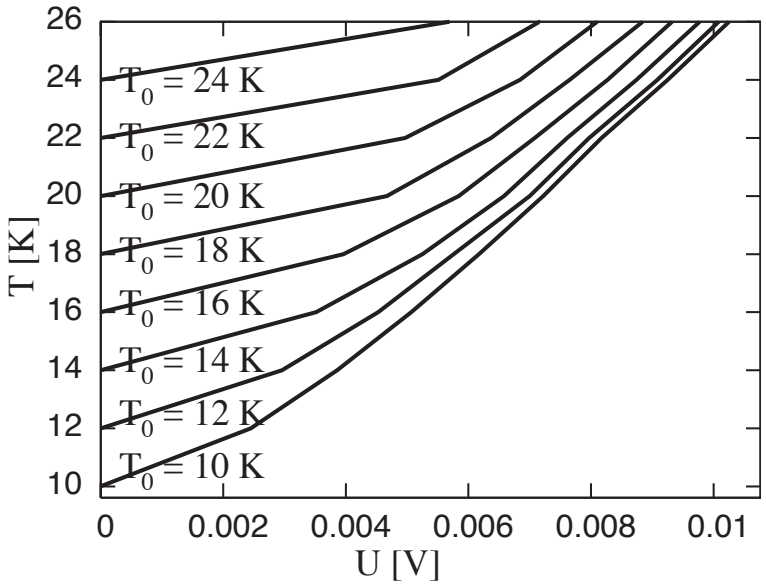

Figure 4.3: The temperature as a function of the applied voltage for different bath temperatures T_0, deduced from the heating model, by equating $R(U) = R(T)$. The estimate is done for data from a $La_{2-x}Ce_xCuO_4$ grain boundary junction with $x = 0.12$, with a T_c of about 28.8 K.

4.2.4 The temperature as a function of the voltage in the heating model

We can estimate the temperature of our junction directly with our heating model, by simply comparing the resistance at a certain voltage with the resistance at a certain temperature. That is, for a given voltage U we can find the temperature T by equating $R(U)=R(T)$. Inaccuracies arise from the change of the volume of the resistive part with the temperature and the voltage. The result for different bath temperatures is shown in figure 4.3. The data were taken in a grain boundary junction by Bettina Welter (WMI Muenchen, Germany). For such measurements, grain boundary junctions have the advantage to be much more stable against temperature changes than our break junctions. These results are close to the prediction of a modified Kohlrausch relation with $T^2 = T_0^2 + U^2/(8L)$.

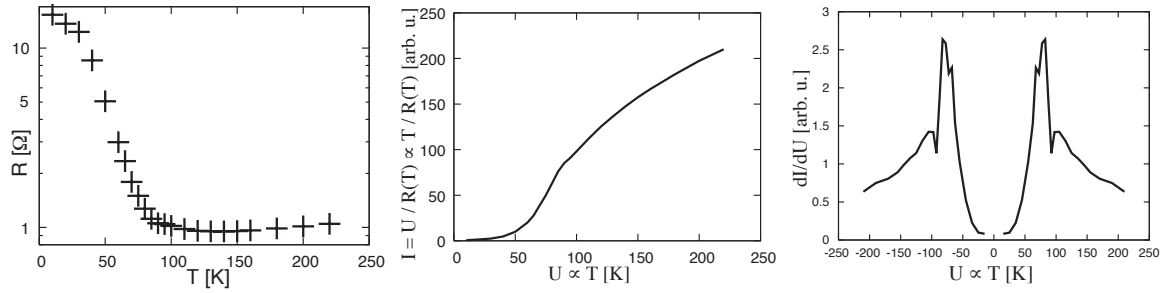

Figure 4.4: Left: The resistance versus temperature measured in a mesa sturcture (Suzuki *et al.*) [98] looks similar to the one observed in our break junctions. Middle: From the left figure we can reconstruct the $I(V)$ curve. At low voltages, where the temperature is low, the resistivity is high. Right: The derivative shows clearly a gap-like structure and a peak. Even a dip and a hump appear. (The curve is mirrored to negative values.)

4.3 From the temperature dependence of the normal state resistance $R(T)$ to the reconstructed $I(V)$ curve

4.3.1 $R(T)$ in mesa structures

In mesa structures, it is relatively easy to measure the temperature dependence of the low voltage resistance $R_{V\to 0}$. A problem of such measurements is that the fraction of the material that got normal changes with the bath temperature. For example, the bulk material below the stack adds a supplementary resistance when $T > T_c$. In fact, already below T_c, a part of the bulk near to the stack goes normal and gives an additional contribution to the resisitvity. This can be observed in figure 3 of Krasnov *et al.* [99]. There the resistance re-increases already at a temperature slightly above 50 K. For that reason we have to be careful with values between 50 K and T_c.

Now we do the same procedure as in section 4.1. First we measure the resistance of the stack at different temperatures. Here again that has to be done at low voltages, such that the stack temperature is close to the bath temperature. As we do not have the original data, we take the values from the article of Suzuki *et al.* [98]. The resistance can be read out in two ways, which give nearly the same values. Either we divide 0.01 V by the current at that voltage from the $I(V)$ curve (figure 1 of Suzuki *et al.* [98]) or alternatively we take $R = [dI/dV(V = 0)]^{-1}$ from the derived curve (figure 2 of Suzuki *et al.* [98]). The result is shown in figure 4.4. It is similar to the one of our break junction experiment. In the same figure (panel in the center) we show the $I(V)$ curve, which we reconstructed in the same way as in section 4.1. This curve looks obviously much nicer than the one from break junction experiments, and resembles very much the $I(V)$ characteristic that is usually interpreted as a tunnelling spectrum. Its derivative is shown in the right panel of the same figure. A clear peak appears in the dI/dV curve. Even a dip and a hump is present. But of course, we do not have enough

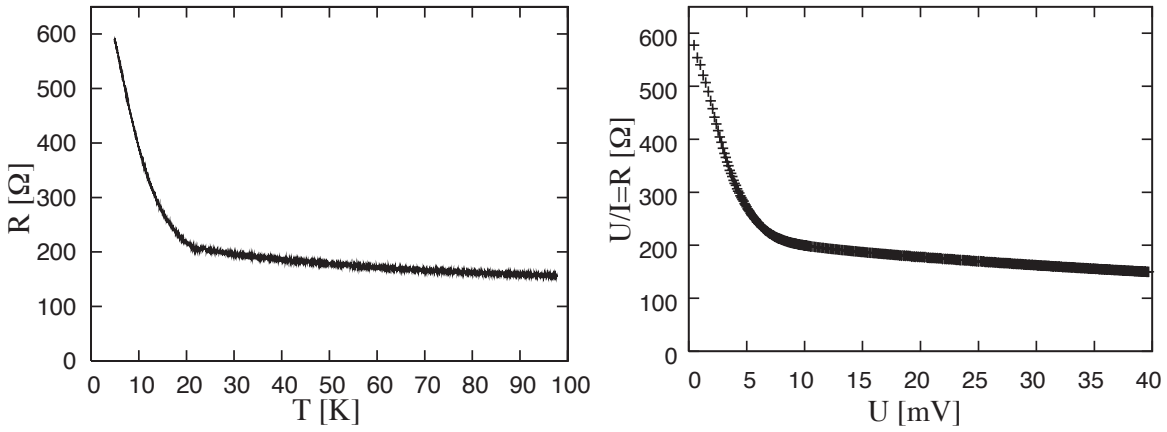

Figure 4.5: The $R(T)$ curve (left) looks amazingly similar to the $I(V)$ curve (right, $T = 6\,\mathrm{K}$), if the latter is plotted as U/I versus U. Grain boundary data (see text).

points to confirm that the appearance of the dip and the hump is reproducible. The fact that the peak is doubled can be explained by the above mentioned uncertainty of the measurement between 50 K and T_c. From this curve, we can now see that for this model we have to assume that T_c is attained at a voltage slightly above the position of the peak.

The application of the Kohlrausch relation is somehow more difficult in this geometry. An additional problem arises with thick mesa structures, when the stack switches into the resistive state starting at the topmost layer. This heat produced in the top layers has to flow first through a part that is in the resistive state, but afterwards also through a superconducting part, where the electrons, bound into Cooper-pairs, do not carry heat.

4.3.2 $R(T)$ in grain boundary junctions

Grain boundary junctions are like mesa structures: stable under temperature changes. This makes them a good candidate to check the heating model with. Bettina Welter (WMI Muenchen Germany) kindly provided us with original grain boundary data, giving us the opportunity to check the heating model.

Curves were taken in a 36.9° grain boundary structure of the electron doped cuprate $Pr_{2-x}Ce_xCuO_4$ with a doping concentration of $x = 0.15$ and a T_c of 22.9 K. The film's thickness was 200 nm and the width 10 mm. First the resistance of this junction was measured as a function of the temperature, at a low voltage where the heating effects should be negligible. Then an $I(V)$ curve at 6 K was recorded. Both curves are shown in figure 4.5. The $I(V)$ data are plotted as $R = U/I$ versus U for comparison. The similarity is amazing. If one uses a slightly modified Kohlrausch relation and plots U/I versus $T = \sqrt{T_0^2 + U^2/(5.5L)}$ together with $R(T)$ in the same figure, the good congruence of the two curves becomes evident (figure 4.6). Note also the fact that the resistance at low temperatures and high voltages is the same as the one at low voltage and high temperature.

The other way round we also get a convincing result. With the same slightly modified

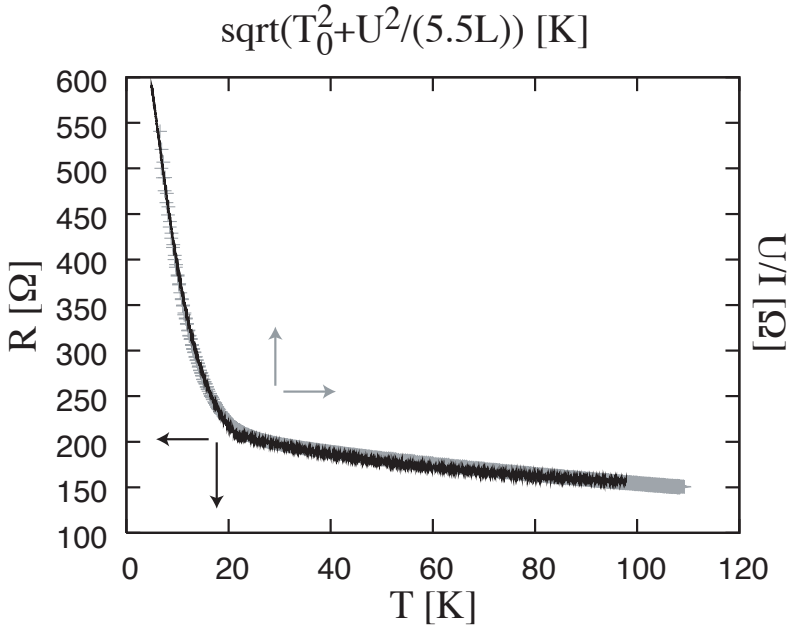

Figure 4.6: The $R(T)$ curve (black line) and the data from the $I(V)$ (grey +) measurements are plotted in the same figure. For direct comparison the latter is plotted as U/I versus $T = \sqrt{T_0^2 + U^2/(5.5L)}$. Same data as in figure 4.5.

Kohlrausch relation $U = \sqrt{5.5L \cdot (T^2 - T_0^2)}$ we estimate again the voltage that is needed to attain a certain temperature. Then we can plot the data from the $R(T)$ curve in a $I(V)$ form, by taking $U = \sqrt{5.5L \cdot (T^2 - T_0^2)}$ on the abscissa and $I = U/R = \sqrt{5.5L \cdot (T^2 - T_0^2)}/R$ on the ordinate. The derivative of this curve is shown in figure 4.7. The similarity between the two curves is again evident. The sharp dip after the peak below 10 mV in the reconstructed curve is caused by the fact that at T_c all the sample goes normal, and consequently an additional resistance is added.

In the same sample, measurements under magnetic field were also done. The original dI/dV curve coincides again well with the reconstructed curve, as it is shown in figure 4.8 for an applied field of 15 T perpendicular to the film (parallel to the c-axis). For this case the Kohlrausch relation was modified as follows: $T = \sqrt{T_0^2 + U^2/(8L)}$. I believe that this change is not astonishing. It indicates that the temperature-voltage relation is not the same in the field free case and in the case where the superconductivity is destroyed by a magnetic field, modifying the electronic and heat current paths in the sample.

In section 4.3.5 we will see that the $R(T)$ relation in the c-direction of BSCCO mesas is unchanged under the application of a magnetic field. This is apparently not the case for the grain boundary structures under study.

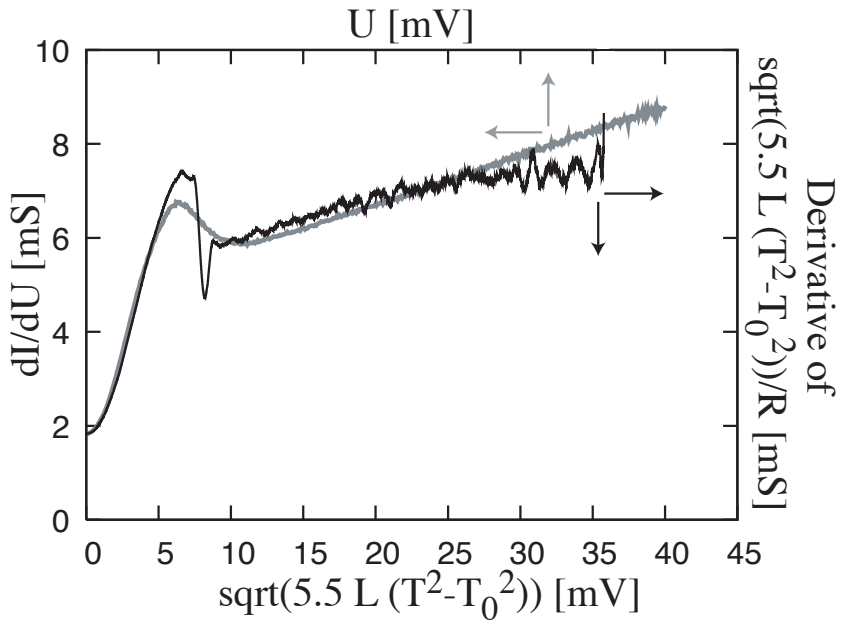

Figure 4.7: The reconstructed curve (black) overlaps well with the original dI/dV curve (grey). The former one is nothing else than the $R(T)$ curve plotted differently (see text). The measurements are the same as in figure 4.5.

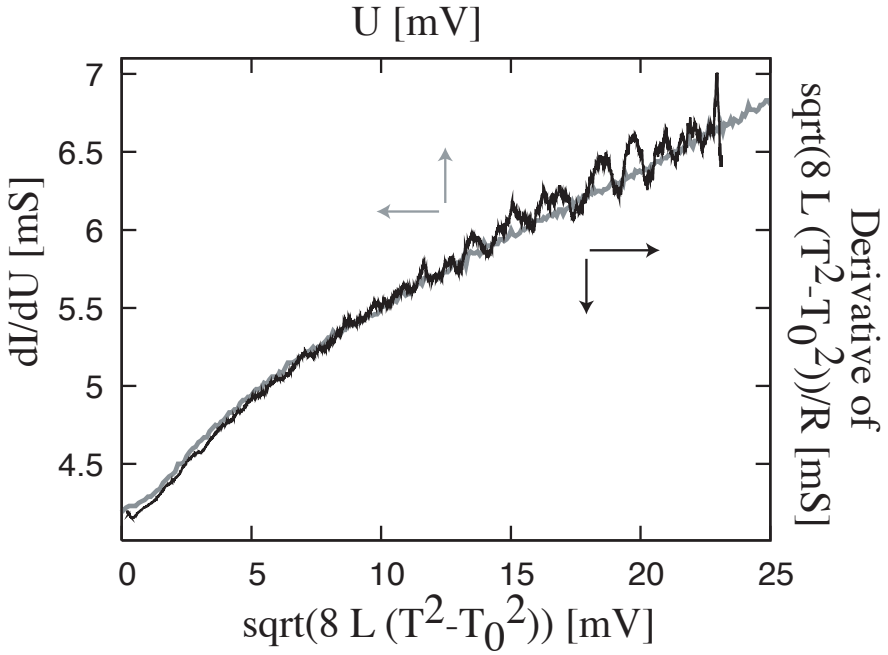

Figure 4.8: The original dI/dV curve (grey, $T = 6\,\mathrm{K}$) coincides with the differently plotted $R(T)$ curve (black). The measurements were done under the application of a magnetic field of 15 T in the same grain boundary sample as the ones in figure 4.5. These results are striking, already independent of any further interpretation.

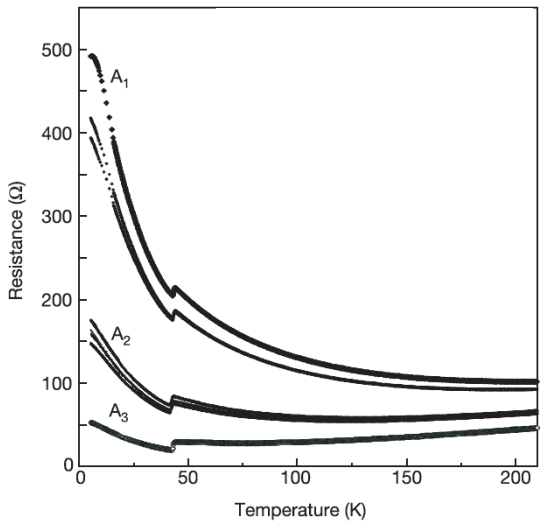

Figure 4.9: The $R(T)$ curve in a planar junction formed by a one unit cell thick antiferromagnetic La_2CuO_4 barrier between the superconducting material $La_{1.85}Sr_{0.15}CuO_4$ (Bozovic *et al.*) [37].

4.3.3 $R(T)$ in planar junctions

Bozovic *et al.* [37] formed planar junctions with a one unit cell thick antiferromagnetic La_2CuO_4 barrier between the superconducting material $La_{1.85}Sr_{0.15}CuO_4$. This layer blocks completely a supercurrent. At $T < T_c$, the resistance as a function of temperature of such a structure decreases with increasing temperature (figure 4.9). The authors do not write about the $I(V)$ curve measured in these structures. Bozovic communicated to me that most curves are linear, but many were non-linear, curving upwards. Until now we could not directly compare this $R(T)$ curve with the $I(V)$ relation measured in the same sample. As these junctions are stable under a temperature change, it would be interesting to do this comparison.

From planar junctions in low T_c superconductors we have no data of the low voltage resistance. The fact that Giaever *et al.* [32] are able to fit the measured low voltage resistance with the predictions of the semiconductor model shows however, that below T_c the resistance also decreases strongly with increasing temperature. (See section 4.3.6 for the predictions of the semiconductor model).

4.3.4 $R(T)$ in STM

Similarly to our break junctions, it is difficult to get a good temperature dependence of the resistivity in STM. The resistance depends strongly on the tip to sample distance, which is difficult to control during a temperature change. From the temperature dependence of the dI/dV curve in the article of Renner *et al.* [24] (see figure 1.4) we can estimate the $R(T)$ function. The inverse of dI/dV at $V = 0$ is plotted in figure 4.10. From this plot it is clear that the resistance drop is similar to the one in mesa structures, grain boundary or break junctions.

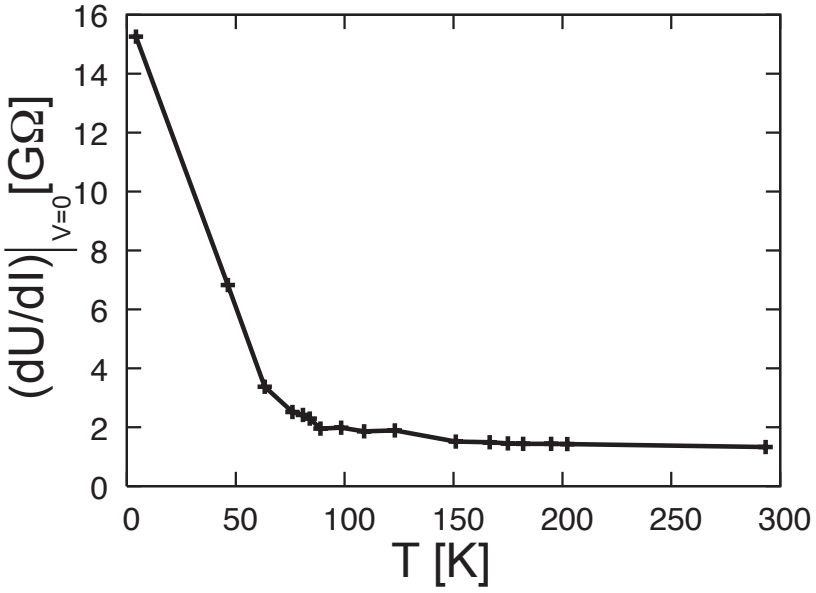

Figure 4.10: The low voltage resistance in STM shows also a strong decrease at low temperatures. The data points are taken from figure 2 of the article of Renner *et al.* [24].

4.3.5 The $R(T)$ in the bulk, from experiments where the superconductivity is destroyed by a high magnetic field

Not only a high current can destroy the superconductivity, but also a magnetic field. In the c-direction of a mesa structure it was observed (Yurgens *et al.*) [77] that the low voltage resistance $R_{V\to 0}$ can be correlated with the c-axis resistivity of the stack when the superconductivity is destroyed by a magnetic field perpendicular to the planes. In fact, $R_{V\to 0}$ in the c-direction of BSCCO-2212 is almost magnetic field independent. So it is worth having a look into the resistivity data from measurements under high magnetic fields. When the magnetic field is applied perpendicular to the c-direction, no dramatic magnetoresistance is observed below T_c (Briceño *et al.*) [100], thus the relation $R_{V\to 0} \approx R(H > H_{c2})$ does not hold. For the rest of the publications that I will cite in this section, the field was applied perpendicularly to the planes.

In optimally doped samples it is difficult to make measurements under magnetic fields. The values of the required magnetic field to suppress the superconducting state exceed the available stationary fields by far. In pulsed measurements, problems like heating by Eddy-Currents may arise.

In BSCCO-2212 the normal state resistance (Zavaritsky) [101] under pulsed magnetic field in the out-of-plane direction is huge at low temperatures and decreases to a nearly constant value when the temperature is increased over T_c (see figure 4.11, left). This temperature dependence resembles the low voltage $R(T)$ curve of our measurements shown in figure 3.9, the one measured at low voltage in mesa structures (figure 4.4), the one from grain boundary junctions (figure 4.5) and the one from STM (figure 4.10).

We are not aware of in plane $R(T)$-curves measured under magnetic fields in BSCCO-

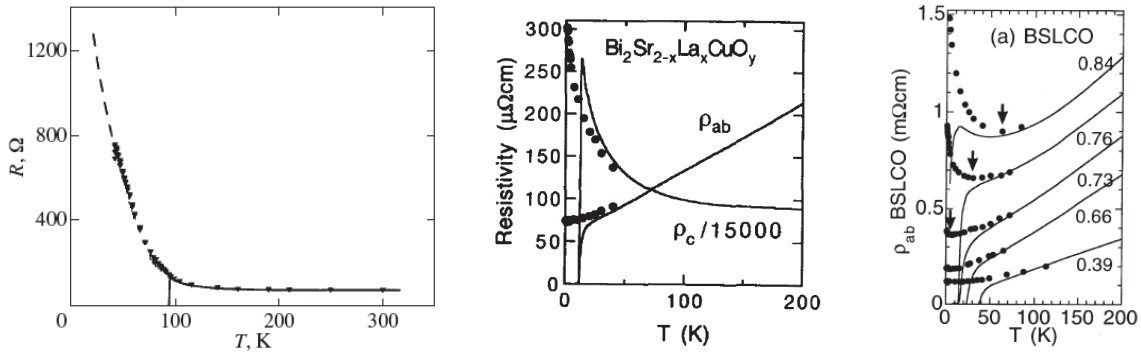

Figure 4.11: Left: The c-axis resistance of BSCCO-2212 in the absence of superconductivity, estimated from measurements under high magnetic field (Zavaritsky) [101]. Middle: Optimally doped $Bi_2Sr_{2-x}La_xCuO_y$ shows metallic behaviour down to 0.66 K in the plane direction under magnetic field (Ando *et al.*) [102]. Right: The in plane resistance in underdoped $Bi_2Sr_{2-x}La_xCuO_y$ is insulator like under magnetic fields of 60 T (Ono *et al.*) [103].

2212 where superconductivity is suppressed. For the similar material $Bi_2Sr_{2-x}La_xCuO_y$, the in plane resistance under a field of 50 T stays metallic (Ando *et al.*) [102] down to 0.66 K (see figure 4.11, middle) if the material is clean. If the sample is disordered, insulating behaviour could be observed even if it has the same composition as the clean one. In underdoped samples (Ono *et al.*) [103], the resistivity shows insulating behaviour (see figure 4.11, right). The temperature corresponding to the minimal resistance increases similarly to the pseudogap temperature when the doping level is lowered.

In other structures, like in grain boundary junctions, the approximation $R_{V\to 0} \approx R(H > H_{c2})$ is not valid anymore. The low voltage resistance $R_{V\to 0}$ is strongly magnetic field dependent at low temperatures.

4.3.6 $R(T)$ in the semiconductor model

The semiconductor model predicts, like the heating model, a high resistivity at low temperature and a decrease when the temperature is increased. We calculated the low voltage resistance in the semiconductor model for SIS and SIN contacts. For the density of states functions we used the s-wave or d-wave function from the BCS theory. Below T_c, the low voltage resistance shows a strong decrease with increasing temperature in all cases. The SIN case with an s-wave density of states is shown in figure 4.12. In the semiconductor model the increase of the resistivity with decreasing temperature is explained as the closing of the gap.

This R(T) behaviour looks similar to the one measured in break junctions (figure 3.9), grain boundary junctions (figure 4.5) or STM (figure 4.10). A simple similarity between the original $R(T)$ curve and the one that is reconstructed from U/I is consistent with the semiconductor model and is not an argument against it. From an approximative measurement of $R(T)$ we can only state that the curve is consistent with a heating model, but not that it is inconsistent with the semiconductor model.

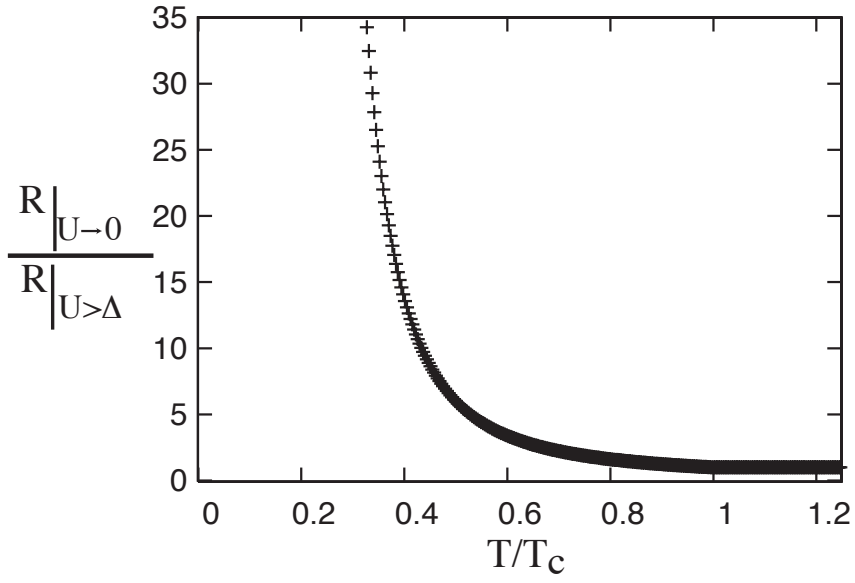

Figure 4.12: The decrease of the low voltage resistance, normalised with the resistance at high temperature versus the temperature in units of T_c as predicted from the semiconductor model (SIN junction, s-wave density of states). A strong decrease with increasing temperature below T_c is predicted not only by the heating model, but also by the semiconductor model.

4.4 Reconstruction of the temperature dependence of the dI/dV curve

If the change in the resistivity of a junction depends only on the temperature, then it should be possible to reconstruct the dI/dV curves at all temperatures by using only the $I(V)$ curve that is measured at the lowest temperature and additionally a relation between the temperature and the voltage.

As the best data we have come from grain boundary junctions, we choose again the same data as in section 4.2.4 to do this reconstruction [$La_{2-x}Ce_xCuO_4$ grain boundary junction with $x = 0.12$; T_c of about 28.8 K; from Bettina Welter (WMI München, Germany)]. The way to reconstruct the temperature dependence is as follows:

As the relation between the voltage and the temperature we take $T^2 = T_0^2 + U^2/(8L)$, with the Lorenz number L. We make this choice, because with this formula the corresponding $R(T)$ curve can be well approximated (see section 4.2.4). Furthermore, with this choice, the reconstructed dI/dV curves join the measured ones at high voltages. The main error in the reconstruction comes from this rude approximation.

From the $I(V)$ curve at a bath temperature of 10 K we reconstruct first the $R(T)$ curve by setting $R = U/I$ and $T^2 = 10^2 + U^2/(8L)$.

From this $R(T)$ curve we can now reconstruct the $I(V)$ and dI/dV curves at different bath temperatures T_0 by recalculating $I = U/R$ and $U^2 = (T^2 - T_0^2) \cdot 8L$.

This reconstruction process gives a good result in grain boundary junctions (see

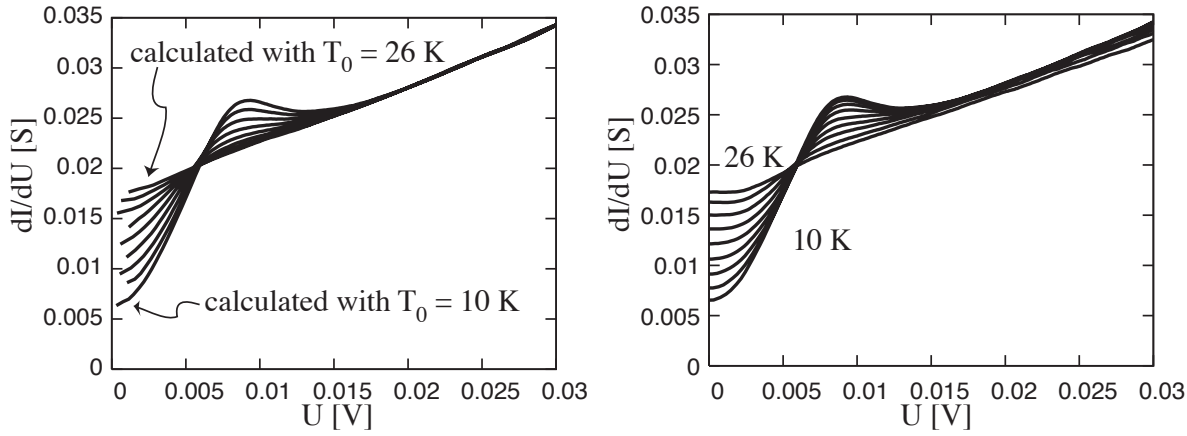

Figure 4.13: The reconstructed temperature dependence of the dI/dV curve (left panel) looks very similar to the measured temperature dependence (right panel). The only two pieces of information that the left figure contains is the dI/dV curve at a bath temperature of $10\,K$ and the formula $T^2 = T_0^2 + U^2/(8L)$ for the relation between the temperature and the voltage, where T_0 are the bath temperatures (10, 12, 14, 16, 18, 20, 22, 24 and 26 K) and L is the Lorenz number. The right panel shows the measured dI/dV curves at these bath temperatures. See text for more details.

figure 4.13).

In break junctions the same procedure can be used. Due to mechanical instabilities under temperature changes, it is difficult to measure $R(T)$, and therefore it is not easy to find the correct voltage dependence of the temperature. If we take again the same relation as for the grain boundary junctions, the curves below T_c can well be reconstructed. At bath temperatures above T_c the dip disappears in the dI/dV curve. The reconstructed curves however still show the dip. This inconsistency might give some hint about the origin of the dip, like for example an expansion of the normal state volume.

4.5 The concave $I(V)$-characteristics: can it be explained by heating?

For measurements that show a clear peak-dip-hump feature, the corresponding $I(V)$ curve is concave for voltages above the hump, that is above approximately 0.1 V. That is equivalent to the statement that the dI/dV curve decreases after the hump, or, that the resistance of the junction increases with the voltage.

In the heating model, we can assume that the non-linearity in the $I(V)$ curve are caused by the normal state resistivity of the material. At high temperatures, the normal state resistivity increases linearly with temperature, so the only outstanding question is: Can this linear dependence explain the way in which the $I(V)$ characteristic is curved?

In order to answer this question we make the assumption that the temperature increases linearly with the voltage for $U >> T_0\sqrt{4L}$. This assumption is consistent with

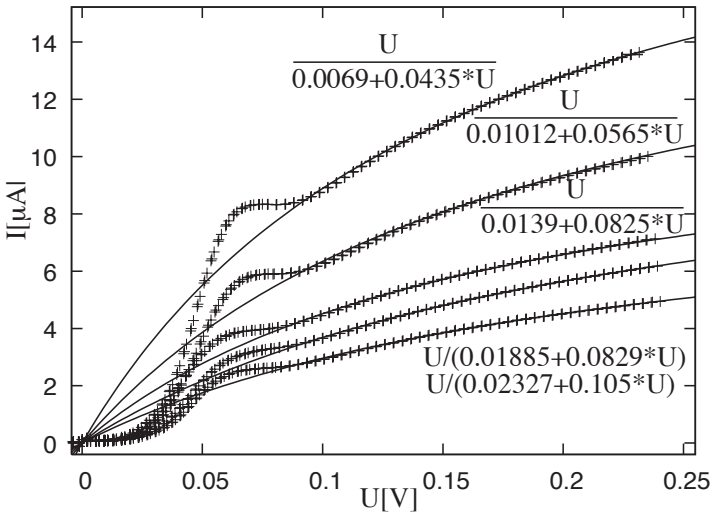

Figure 4.14: Under the assumption that the temperature increases linearly with the voltage, the measured $I(V)$ curves (+) can be fitted for $U > 0.1\,\mathrm{V}$ (line) in a heating model. (BSCCO-2212, 4.2 K).

the Kohlrausch relation [see equation (4.2)], that is $T^2 = T_0^2 + U^2/(4L)$. Furthermore, from the normal state resistivity we can take a linear relation of the form $R = p + qT$, with the fitting parameters p and q. We can now fit the $I(V)$ curve with the function

$$I = \frac{U}{R} = \frac{U}{p + qT} = \frac{U}{p + q\frac{dT}{dU}U} \quad . \tag{4.3}$$

With this function we can fit the concave high voltage part of our $I(V)$ curves (see figure 4.14).

The concave curvature of the $I(V)$-curve is equivalent to the fact that the U/I spectrum (see section 4.1.2) is in a very good approximation linear at high voltages for good junctions.

With the heating model the concave $I(V)$ curve can be explained.

4.6 A semiconductor model with heating effects

One might assume that the analogousness between the temperature and the voltage dependence of the resistance is accidental. Then a tunnelling picture (semiconductor model) can still be regarded as valid. But even in this case, heating has to be studied. We discuss a tunnelling picture, where the semiconductor model (section 2.1) is still valid, but it has to be modified due to a junction temperature higher than the bath temperature.

We assume a heated tunnelling picture, where the peaks of the dI/dV curve are still related to the superconducting gap. Further we assume that the gap magnitude is smaller at higher temperatures and that the junction gets heated by the voltage to a higher temperature than the bath temperature. From these assumptiona it gets clear

that the real gap value is bigger than the one which is estimated under the assumption that the junction temperature is equal to the bath temperature.

A temperature corrected value for the gap is bigger than the uncorrected one. Therefore the exact temperature dependence of the junction has to be studied, if one wants to measure the real value of the gap.

An attempt to deduce a "heating free" tunnelling spectrum by taking points at a fixed, estimated junction temperature and different bath temperatures and voltages was made by Yurgens *et al.* [104].

In most of the techniques which are used to determine the gap magnitude (for example ARPES or infrared spectroscopy), energy is dissipated in the sample. Two questions arise from this consideration: With which technique, other than tunnelling, can the gap magnitude be measured, excluding heating effects with certainty? What is the real magnitude of the gap?

4.7 Arguments in favour of the heating picture and its problems

Arguments in favour of the heating picture

- The resistance of the junction changes in the same way when the sample is heated from the surrounding bath as when a voltage is applied. In grain boundary structrues the dI/dV curve can perfectly be reconstructed from the $R(T)$ curve (see figure 4.7).

- The magnetic field (figure 4.8) and temperature (figure 4.13) dependence of the "gap" can be described by the heating model.

- The temperatures that are predicted from the Kohlrausch relation are consistent with the ones that are predicted from the heating model.

- The temperature measured with a thermocouple in mesa structures (see figure 5.2) is close to the one predicted in the heating model.

- The concave curvature of the $I(V)$ curve at high voltages (see section 4.5) can be explained in the heating model.

- The doping dependence of 2Δ is closely related to the doping dependence of the "pseudogap temperature" (T^*-line). That is consistent with the heating picture, noticing that at low doping levels a higher voltage has to be applied to reach the peak position, meanwhile a higher temperature is needed to attain T^*.

- The heating model, as it is essentially only based on a temperature dependent resistance, is simple and natural.

Problems of the heating picture

- It stays in contrast to the highly examined semiconductor model.
- The independence of the peak position in the dI/dV curve on the tip-to-sample distance in STM speaks intuitively against heating (see section 5.2).
- The direct application to STM experiments is difficult. The Kohlrausch relation does not hold and at that small scale it might be even difficult to define a temperature.
- The heating picture is not a microscopic picture. Many questions about the microscopic origin of the results stay unanswered.
- The temperature dependence of the hysteresis in low T_c planar junctions (see figure 2.3) are not directly described in a heating model. It is not evident why the beginning of the hysteresis loop shifts to higher voltage and higher current when the temperature is increased. It has to be verified if that can be explained by heating.
- The possibilities of the verification of the model are at the moment limited.

4.8 Arguments in favour of the semiconductor model and its problems

Arguments in favour of the semiconductor model

- The experimental results correspond very well to the BCS theory in low T_c superconductors.
- Many techniques (like ARPES) that claim to measure the same quantities show very similar results. They are consistent with the different tunnelling techniques, which are also consistent among each other.
- The semiconductor model predicts an $R(T)$ curve that is similar to the one with which the application of the heating model is justified. An approximatively measured $R(T)$ curve, like the one from STM for example, is consistent with both, the semiconductor and the heating model (see section 4.3.6).

Problems of the semiconductor model

- In the semiconductor model it is supposed that the temperature is a voltage independent magnitude. The estimations of the junction temperature presented in this work predict however a non-negligible dependence.
- No angle dependence of the gap could be observed with break junction or grain boundary experiments.

- Currents that are clearly higher than the critical (depairing) current are often applied over the junctions. Especially when T_c is approached, where the critical current goes to zero.

- At least when a very high power is dissipated in the junction, one has to suppose that a part of the material goes normal. In the $I(V)$ curve however no more special features indicating this transition are evident at high voltages.

- The semiconductor model simplifies the reality significantly. One might think for example, that the dissipation of the energy causes a certain resistivity. The semiconductor model does not describe the dissipation mechanism. The unimportance of such lacks is only justified by the good experimental results.

- The dI/dV curve does not represent the density of states in an SIS junction (see section 2.1). SNS structures do not even form a real barrier for quasiparticles.

- The measured gap does not close when the temperature is increased to T_c.

Chapter 5

Heating effects in the literature

In tunnelling structures a certain amount of energy is dissipated, which is transformed into heat. Heating effects have been discussed in weak link structures (Likharev) [70]. Currently many groups study heating effects in mesa structures (section 5.1). Pulsed measurements are performed in these structures with the aim to reduce the heating (section 5.1.1). Also in STM this problem has been addressed (section 5.2).

5.1 Heating effects in mesa structures

For a long time, it is clear that heating is a severe problem in mesa structures. To overcome these problems, authors strive for smaller stack sizes and for faster measurements. Currently many groups try to measure the temperature of the stack with different techniques.

Zavaritsky [105] published a high impact Physical Review Letters comment on an article by Yurgens *et al.* [55]. He called attention to the fact that simple Joule heating can explain $I(V)$ curves similar to those Yurgens interpreted as tunnelling curves. He believes that the peaks in the dI/dV curve are not related to the pseudogap but are only caused by heating (see figure 5.1). See also the other articles that were published on this topic by Zavaritsky [106]. This model explains in a straightforward way why the temperature at which the pseudogap features disappear (T^*) corresponds to the temperature at which $R_c(T)$ is minimal.

As an assumption for the voltage dependence of the temperature, he refers to Newton's Law of Cooling: $T = T_0 + IV/(Ah)$, where T_0 is the bath temperature, A the area of the mesa and h the heat transfer coefficient. He found $(hA)^{-1} \approx 60\,\mathrm{K/mW}$ for the inverse heat transfer coefficient by comparing the reconstructed dI/dV curves with the original curves. The problem of this temperature calculation is that the heat transfer coefficient is not easy to estimate from the theoretical side. Additionally it is not a constant when the temperature changes. For a qualitative analysis however, Newton's Law of Cooling is sufficient because the exact temperature-voltage relation is not needed to qualitatively reproduce the dI/dV curves.

He mentions also the correlation between the "subgap resistance" ($R_{V\to 0}$) and the resistance of the stack when superconductivity is destroyed by high magnetic fields. This

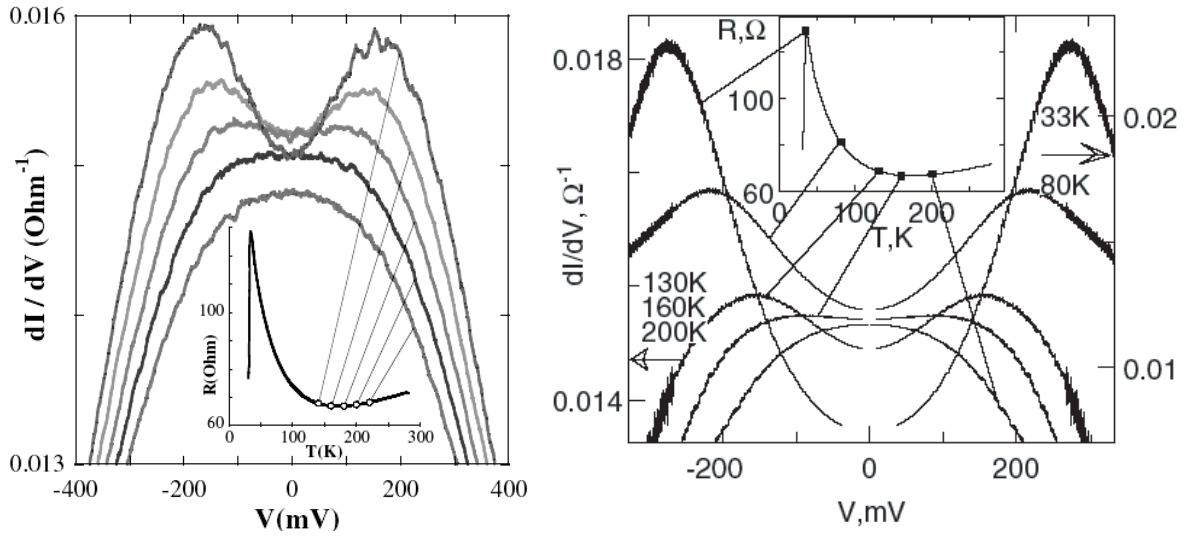

Figure 5.1: The original and the reconstructed curves: Left panel: The dI/dV curves measured at different temperatures in a mesa structure (Yurgens *et al.*) [55]. The inset shows the *c*-axis resistivity of the stack. Right panel: The dI/dV curves reproduced from $R_c(T)$ assuming that Joule heating is the only reason for non-linearity (Zavaritsky) [105].

is the resemblance that I described in section 4.3.5.

In consequence of this comment, Yurgens *et al.* tried to measure the temperature of their mesa structures [104, 107] with a thermocouple very close to the stack. They realised that the stacks are in fact strongly overheated. Temperatures as high as T_c were observed already at the voltage of the dip position. The temperatures he measured in his stacks are shown in figure 5.2. From these results he concluded that the pseudogap like humps are indeed an artefact of Joule heating. He believes however that it should be possible to observe the gap by intrinsic tunnelling in small sized mesa structures.

5.1.1 Pulsed measurements

Many groups tried to decrease heating by performing pulsed measurements. The idea is to measure before the sample heats up. Thus with faster pulses, we measure at lower temperature. To check qualitatively how the $I(V)$ curve should change in a pulsed measurement with our heating model, we assume a case in which the temperature in the pulsed measurement changes 1.2 times slower than in the measurement at equilibrium, that is $1.2 \cdot (dT/dU)_{\text{pulse}} = (dT/dU)_{\text{equ}}$. For simplicity we assume that the temperature increases linearly with the voltage. Then we get for the voltage $U_{\text{pulse}} = (dU/dT)_{\text{pulse}} T = 1.2 \cdot (dU/dT)_{\text{equ}} T = 1.2 \cdot U_{\text{equ}}$, and for the current $I_{\text{pulse}} = U_{\text{pulse}}/R = 1.2 \cdot U_{\text{equ}}/R = 1.2 \cdot I_{\text{equ}}$. The expected pulsed $I(V)$ curve is plotted in the left panel of figure 5.3.

Anagawa *et al.* [84] did pulsed measurements in a stack of about $100\,(\mu\text{m})^2$ in area and 10 junctions in height. With a pulse length as short as 60 ns, they observed a change in the spectra, but only at voltages higher than 50 mV per junction (see figure 5.3). The authors concluded that heating is negligible, at least for voltages lower than 50 mV.

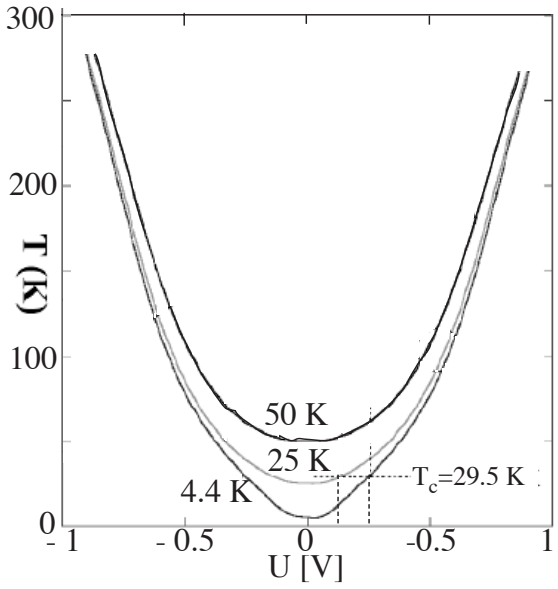

Figure 5.2: Temperatures nearly 10 times as high as T_c were measured with a thermometer close to the stack when a voltage below 1 V was applied over a $Bi_2Sr_{1.6}La_{0.4}CuO_{6+\delta}$ mesa structure (Yurgens *et al.*) [107]. The dI/dV curves which were measured simultaneously (not shown) show peaks and dips for the two measurements taken at a bath temperature below T_c (at 25 K and 4.4 K). The third temperature dependence was measured at a bath temperature of 50 K. T_c is reached close to the voltage of the dip.

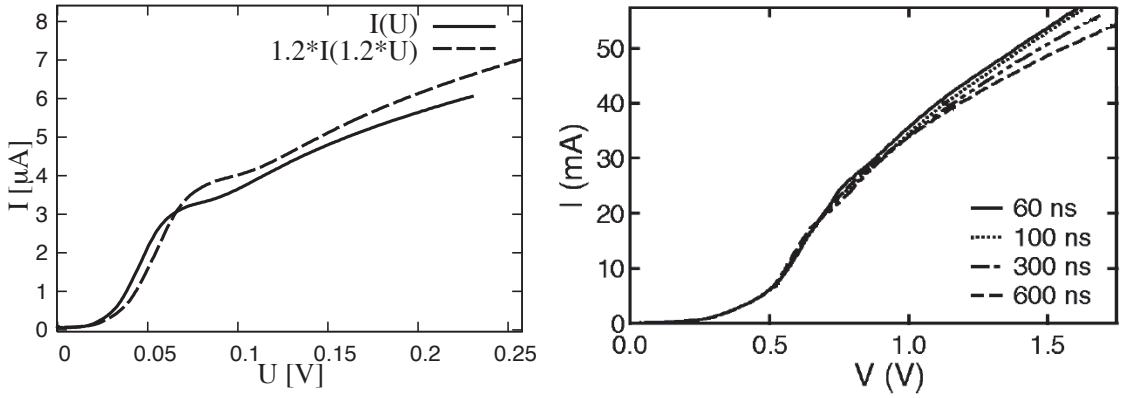

Figure 5.3: Left panel: For a pulsed measurement, in which the temperature changes 1.2 times slower than in the equilibrium measurement, the $I(V)$ curve is reproduced with a simple model (see text). Dashed line: pulsed measurement; full line: measurement at equilibrium. Right panel: The $I(V)$ curve, measured with different pulse lengths in a 10 junctions thick BSCCO-2212 mesa structure at a bath temperature of 10 K (Anagawa *et al.*) [84].

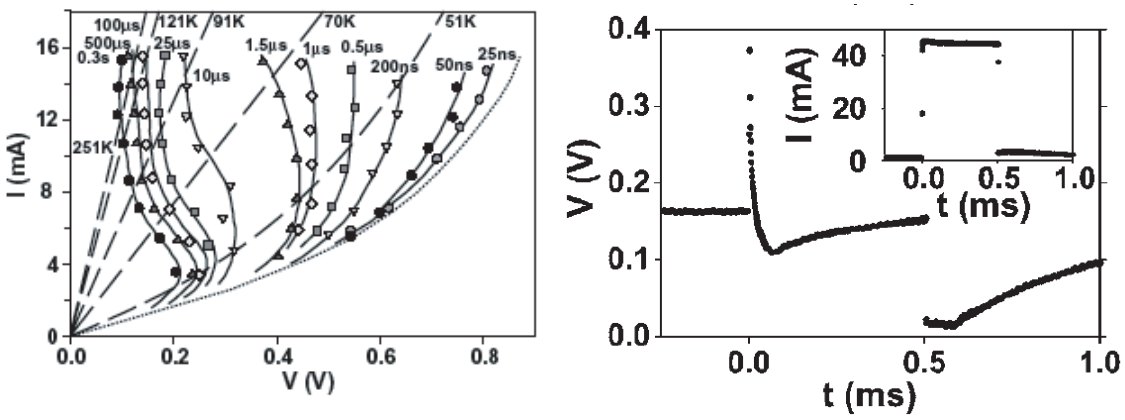

Figure 5.4: Left panel: The upturn in the current that is often associated with the gap, is shifted to higher values, when the pulse length is decreased. The measurements were done in a BSCCO-2212 mesa structure at a bath temperature of 33 K (Fenton *et al.*) [108]. Right panel: The evolution of the voltage with time in the same mesa structure is shown when the current is held constant. Inset: current versus time, recorded in parallel (Fenton *et al.*) [108].

However if we analyse these results with the model described above (see left panel of figure 5.3), we get a different conclusion. Namely, as we can see in the right panel of figure 5.3, at high voltages the resistance decreases with faster pulses, that is with lower temperature. If we have a look to the $R_{V\to 0}(T)$ curve of a mesa (see for example left panel of figure 4.4) we see that dR/dT is only positive for temperatures clearly higher than T_c. We can therefore assume that the effective temperature is above T_c for voltages higher than about 70 mV per junction in this experiment.

The group of Gough made a similar study with different pulse lengths, however in another contact configuration [108]. The 30 junctions counting BSCCO-2212 mesa structure with an area of 30 $(\mu m)^2$ was thicker than the one of Anagawa. They observed that the upturn in the $I(V)$ curve that is associated with the gap shifts to higher voltages when the pulse length is decreased (see figure 5.4, left panel). Still at the fastest measurements of 25 ns, this upturn-voltage depends on the pulse length. In the right panel of figure 5.4, the voltage is shown as a function of time while the current is constant. The strong drop at the beginning and the slow recovery of the voltage is consistent with the assumption that the temperature increases with the time, and that the resistivity as a function of temperature has a shape like the one reproduced from the $I(V)$ curve. This consistency is visible if one compares the curve of the right panel of figure 5.4 with the left panel of figure 4.2.

5.2 Heating effects in STM

In STM, it is often argued that heating effects can be excluded because the resistance, being of the order of $10^9\,\Omega$, is very high. However, one should not forget that the

power that is put into the junctions is probably dissipated in a very small volume in the order of nm^3. Hess *et al.* [109] expects the local tunnelling current densities to be as high as $10^6\,A/cm^2$. This value lies considerably higher than the critical current density in mesa structures, which is normally below $10^3\,A/cm^2$. However, they believe that heating effects could be detected by the thermal smearing of the dI/dV curves. Their fit of the curves with a thermally smeared BCS function does not show any increased temperature. And as the spectra show no noticeable change by varying the tunnelling barrier from $5 \cdot 10^7\,\Omega$ to $5 \cdot 10^9\,\Omega$, they conclude that heating is negligible.

The independence of the STM spectra on the tip-to-sample spacing is often used as an argument against the heating picture. Intuitively one would assume, that the temperature of the junction (if it can be defined at that scale) is higher when the tip is closer to the sample, because the current density is higher. At the moment we do not know however which mechanism is responsible for the resistance in a heating picture. A proof that this mechanism would lead to tip-to-sample spacing dependent spectra in STM and thus cannot be responsible for these non-linearities might give a strong argument against the validity of a heating model for STM experiments.

The question about the critical current density in STM is often discussed in the literature. The critical current density however goes to zero when T_c is reached, thus any current is bigger than I_c at high temperatures. Additionally, the tunnelling current is a one particle current and not a supercurrent. Rather it might be important to know how far the quasiparticles travel before they couple into pairs after having crossed the barrier. I am not aware of a description of this region in which an elevated concentration of unpaired quasiparticles has to be expected.

Conclusions

We measured the well known peak-dip-hump characteristics in the dI/dV curve with a break junction technique in BSCCO. The geometry of the junction is not known in detail, but most probably the two broken pieces touch each other, and the superconducting parts of the sample are separated by a small volume in which the superconductivity is destroyed by a high current density and by heating.

The temperature and doping dependence of the measured peak-dip-hump characteristics interpreted with the semiconductor model gives a result consistent with other tunnelling techniques and ARPES.

The application of this model on our data is however problematic. One of the major problems is for example that it is not clear where we have a tunnelling barrier in our experiment that is a classically forbidden zone for the quasiparticles.

Another problem of the semiconductor model is that it ignores the dissipation of the electrical energy in the junction. Naturally one expects that this dissipation manifests in a temperature rise in the junction region.

An alternative interpretation comes from a heating model, first proposed by Zavaritsky. This model makes clear that the dI/dV curves can be perfectly explained in a simple way by self-heating of the sample. As our measurements do not depend on the contact area of the junction, it was believed that heating could be neglected in our case. In the literature however we found a relation (Kohlrausch relation) that gives the temperature of a metallic contact as a function of the applied voltage. As this result is independent of the contact area and geometry, we could show that we cannot exclude heating in our experiments. Furthermore, this relation predicts a value for the temperature that is close to the temperature needed for explaining all our results by simple heating.

For an exact verification of the applicability of the heating model the temperature dependence of the low bias junction-resistance has to be known. For this check one needs junctions that are mechanically stable under a temperature change, like mesa structures, grain boundary or planar junctions.

Thanks to the data measured in a junction formed by a grain boundary in a thin layer of a cuprate we could test our model: the congruence of the data with the predictions were excellent. These results are striking, already independent of any further interpretation. The occurrence of all the typical features as well as the temperature

and magnetic field dependence are reproduced directly in a randomly chosen material (figures 4.5 to 4.8). That shows clearly that *the heating model is a valid alternative to the semiconductor model.*

Open questions

In order to verify the heating model, the temperature dependence of the junction-resistance has to be known. It is experimentally observed that this resistance increases significantly below T_c. The responsible mechanism for the high resistivity at low temperatures and voltages is however unknown. Has it something to do with the energy gap; with the pairing of electrons; with some interaction of the quasiparticles? Does the manifestation of this mechanism require a direct contact or can it also influence particles that tunnel through a forbidden barrier?

The results of other tunnelling techniques resemble the data of mesa structures or grain boundary junctions. Break junctions and STM are however mechanically not stable enough to test the heating model in the same way as it was done in grain boundaries. In addition, the contact size in STM is too small to estimate the temperature with the Kohlrausch relation. Are there other ways to test the heating model? Is the responsible mechanism for the non-linearities in the $I(V)$ curve the same in mesa structures, grain boundary junctions, break junctions and STM?

Temperature measurements in mesa structures showed that the stacks were strongly overheated. Why does the dI/dV curve from mesa structures resemble so much the data from other tunnelling techniques and ARPES? Which importance has the form of the energy (heat, voltage or light) that enters the sample?

If a tunnelling structure exists, in which excessive heating can be excluded, what is the reason why this structure is heated much less than a metallic contact?

Tunnelling results from planar junctions in low T_c materials show an amazingly good congruence with the predictions from the BCS theory. It is however not clear, why the junction temperature should be lower than in other experiments that seem to be comparable. Planar junction experiments in low temperature superconductor play a highly important role in the theory of superconductivity. A check of the applicability of the heating model by measuring the low voltage junction resistance as a function of temperature is thus worth doing.

Bibliography

[1] H. K. Onnes, Commun. Phys. Lab. Univ. Leiden **124c** (1911).

[2] J. Bardeen, L. Cooper and J. Schrieffer, Phys. Rev. **108**, 1175 (1957).

[3] J. G. Bednorz and K. A. Mueller, Z.Phys. **64**, 189 (1986).

[4] C. W. Chu *et al.*, Nature **365**, 323 (1993). A. Schilling *et al.*, Nature **363**, 56 (1993).

[5] J. L. Tallon *et al.*, Phys. Rev. B **51**, 12911 (1995).

[6] W. S. Corak and C. B. Satterthwaite, Phys. Rev. **102**, 662 (1956).

[7] P. G. de Gennes, *Superconductivity of metals and alloys*, New York : Benjamin (1966).

[8] D. M. Ginsberg and M. Tinkham, Phys. Rev. **118**, 990 (1960).

[9] M. A. Biondi and M. P. Garfunkel, Phys. Rev. **116**, 853 (1959).

[10] R. W. Morse *et al.*, Phys. Rev. Lett. **3**, 15 (1959).

[11] I. Giaever, Phys. Rev. Lett. **5**, 464 (1960).

[12] A. G. Loeser *et al.*, Phys. Rev. B **56**, 14185 (1997).

[13] H. Won and K. Maki, Phys. Rev. B **49**, 1397 (1994).

[14] J. R. Kirtley *et al.*, Nature **373**, 225 (1995).

[15] A. J. Millis *et al.*, Phys. Rev. B **42**, 167 (1990).

[16] J. Ranninger *et al.*, Phys. Rev. B **53**, 11961 (1996); V. J. Emery *et al.*, Nature **374**, 434 (2002).

[17] H. Alloul *et al.*, Phys. Rev. Lett. **63**, 1700 (1989).

[18] W. W. Warren *et al.*, Phys. Rev. Lett. **62**, 1193 (1989).

[19] T. Timusk and B. Statt, Rep. Prog. Phys. **62**, 61 (1999).

[20] B. Bucher *et al.*, Phys. Rev. Lett. **70**, 2012 (1993).

[21] H. Zimmermann *et al.*, Physica C **159**, 681 (1989).

[22] R. J. Birgeneau and G. Shirane, *Physical Properties of High Temperature Superconductors* vol 1, ed Ginsberg, Singapore: World Scientific p 155 (1989).

[23] B. Batlogg *et al.*, Physica C **235-240**, 130 (1994).

[24] Ch. Renner *et al.*, Phys. Rev. Lett. **80**, 149 (1998).

[25] B. D. Josphon, Phys. Lett. **1**, 251 (1962).

[26] E. L. Wolf, Rep. Prog. Phys. **41**, 1439 (1978).

[27] J. Bardeen, Phys. Rev. Lett. **6**, 57 (1961).

[28] R. C. Dynes *et al.*, Phys. Rev. Lett. **41**, 1509 (1978).

[29] P. K. Hansma, *Tunneling Spectroscopy*, New York: Plenum Press p 26 (1982).

[30] I. Giaever, Phys. Rev. Lett. **5**, 147 (1960).

[31] J. Nicol, A. D. Shapiro and P. H. Smith *et al.*, Phys. Rev. Lett. **5**, 461 (1960).

[32] I. Giaever and K. Megerle, Phys. Rev. **122**, 1101 (1961).

[33] J. C. Fisher and I. Giaever, J. Appl. Phys. **32**, 172 (1961).

[34] I. Giaever *et al.*, Phys. Rev. **126**, 941 (1962).

[35] I. Bozovic *et al.*, Physica C **235-240**, 178 (1994).

[36] I. Bozovic *et al.*, Phys. Rev. Lett. **93**, 157002 (2004).

[37] I. Bozovic *et al.*, Nature **422**, 873 (2003).

[38] J. E. Zimmerman and A. H. Silver, Phys. Rev. **141**, 367 (1966).

[39] J. F. Zasadzinski *et al.*, Phys. Rev. Lett. **87**, 067005 (2001).

[40] T. Ekino and J. Akimitsu, Phys. Rev. B **40**, 6902 (1989).

[41] L. Ozyuzer *et al.*, IEEE Trans. Appl. Supercond. **15**, 181 (2005).

[42] I. Maggio-Aprile *et al.*, Phys. Rev. Lett. **75**, 2754 (1995).

[43] Ch. Renner and Ø. Fischer, Phys. Rev. B **51**, 9208 (1995).

[44] S. H. Pan *et al.*, Nature **413**, 282 (2001).

[45] K. M. Lang *et al.*, Nature **415**, 412 (2002).

[46] E. W. Hudson *et al.*, Science **285**, 88 (1999).

[47] S. H. Pan *et al.*, Nature **403**, 746 (2003).

[48] E. W. Hudson *et al.*, Nature **411**, 920 (2001).

[49] J. E. Hoffman *et al.*, Science **295**, 466 (2002).

[50] J. E. Hoffman *et al.*, Science **297**, 1148 (2002).

[51] K. McElroy *et al.*, Nature **422**, 592 (2003).

[52] M. Vershinin *et al.*, Science **303**, 1995 (2004).

[53] R. Kleiner and P. Mueller, Phys. Rev. B **49**, 1327 (1994).

[54] K. Schlenga *et al.*, Phys. Rev. B **57**, 14518 (1998).

[55] A. Yurgens *et al.*, Phys. Rev. Lett. **90**, 147005 (2003).

[56] H. B. Wang *et al.*, Phys. Rev. Lett. **87**, 107002 (2001).

[57] J. Moreland and J. W. Ekin, J. Appl. Phys. **58**, 3888 (1985).

[58] D. Mandrus, L. Forro, D. Koller and L. Mihaly, Nature **351**, 460 (1991).

[59] J. Hartge *et al.*, J. Phys. Chem. Solids **54**, 1359 (1993).

[60] J. Mannhart *et al.*, Phys. Rev. Lett. **77**, 2782 (1996).

[61] D. Beck *et al.*, Appl. Phys. Lett **68**, 3364 (1996).

[62] L. Alff *et al.*, Nature **422**, 698 (2003).

[63] A. Barone and G. Paterno, *Physics and applications of the Josephson effect*, New York a.o. Wiley (1982).

[64] B. D. Josephson, Rev. Mod. Phys. **46**, 251 (1974).

[65] S. Shapiro, Phys. Rev. Lett. **11**, 80 (1963).

[66] D. E. McCumber, J. Appl. Phys. **39**, 3113 (1968).

[67] L. Wang *et al.*, J. Appl. Phys. **49**, 5602 (1978).

[68] T. A. Fulton and L. N. Dunkleberger, J. Appl. Phys. **45**, 2283 (1974).

[69] S. K. Decker and D. W. Palmer, J. Appl. Phys. **48**, 2043 (1977).

[70] K. K. Likharev, Rev. Mod. Phys. **51**, 101 (1979).

[71] A. S. Katz, S. I. Woods and R. C. Dynes, J. Appl. Phys. **87**, 2978 (2000).

[72] P. W. Anderson and A. H. Dayem, Phys. Rev. Lett. **13**, 195 (1964).

[73] H. A. Notarys and J. E. Mercereau, J. Appl. Phys. **44**, 1821 (1973).

[74] L. Ozyuzer *et al.*, Phys. Rev. B **61**, 3629 (2000).

[75] L. Forro, Phys. Lett. A **179**, 140 (1993).

[76] G. E. Blonder, M. Tinkham and T. M. Klapwijk, Phys. Rev. B **25**, 4515 (1982).

[77] A. Yurgens *et al.*, Phys. Rev. Lett. **79**, 5122 (1997).

[78] D. Mandrus *et al.*, Europhys. Lett. **22**, 199 (1993).

[79] M. R. Norman *et al.*, Phys. Rev. B **57**, R11089 (1998).

[80] H. Ding *et al.*, Phys. Rev. Lett. **76**, 1533 (1996).

[81] H. F. Fong *et al.*, Nature **398**, 588 (1999).

[82] K. C. Hewitt and J. C. Irwin, Phys. Rev. B **66**, 054516 (2002).

[83] A. Matsuda *et al.*, Physica C **388-389**, 207 (2003).

[84] K. Anagawa *et al.*, Appl. Phys. Lett. **83**, 2381 (2003).

[85] Y. Yamada *et al.*, Phys. Rev. B **68**, 054533 (2003).

[86] N. Mros *et al.*, Phys. Rev. B **57**, R8135 (1998).

[87] M. Suzuki *et al.*, IEEE Trans. Appl. Supercond. **9 (2)**, 4507 (1999).

[88] F. Kohlrausch, Ann. Phys., Leipzig. **1**, 132 (1900).

[89] R. Holm, Electric Contacts, Theory and Application. New York: Springer (1967).

[90] J. A. Greenwood and J. B. P. Williamson, Proc. Roy. Soc. A **246**, 13 (1958).

[91] R. S. Timsit, IEEE Trans. Comp. Pack. Tech. **22**, 85 (1999).

[92] A. B. McLean, J. Phys. F: Met. Phys. **16**, L249 (1986).

[93] B. I. Verkin *et al.*, Solid State Communications **30**, 215-218 (1979).

[94] Y. G. Naidyuk *et al.*, J. Phys.: Condens. Matter **16**, 3433 (2004).

[95] R. S. Timsit, IEEE Trans. Comp., Hybrids, Manufact. Technol. **6**, 115 (1983).

[96] M. F. Crommie and A. Zettl, Phys. Rev. B **41**, 10978 (1990).

[97] M. F. Crommie and A. Zettl, Phys. Rev. B **43**, 408 (1991).

[98] M. Suzuki *et al.*, Phys. Rev. Lett. **82**, 5361 (1999).

[99] V. M. Krasnov *et al.*, Phys. Rev. Lett. **94**, 077003 (2005).

[100] A. Briceño, M. F. Crommie and A. Zettl, Phys. Rev. Lett. **66**, 2164 (1991).

[101] V. N. Zavaritsky, J. Exp. Theo. Phys. **94**, 802 (2002).

[102] Y. Ando *et al.*, Physica C **282-287**, 240 (1997).

[103] S. Ono *et al.*, Physica C **357-360**, 138 (2001).

[104] A. Yurgens *et al.*, EPAPS Document No. [E-PRLTAO-92-024424] (2003).

[105] V. N. Zavaritsky, Phys. Rev. Lett. **92**, 259701 (2004).

[106] V. N. Zavaritsky, J. Supercond. **15**, 567 (2002); Physica C **404**, 440 (2004); cond-mat/0410069.

[107] A. Yurgens *et al.*, Phys. Rev. Lett. **92**, 259702 (2004).

[108] J. C. Fenton *et al.*, Physica C **388-389**, 341 (2003).

[109] H. F. Hess *et al.*, J. Vac. Sci. Technol. A **8 (1)**, 450 (1990).

Remerciements

László Forró, mon directeur de thèse, pour m'avoir laissé le choix d'étudier la question du réchauffement.

Titusz Fehér, pour les nombreuses heures de discussion, d'explications, de calculs et surtout aussi pour avoir relu ma thèse.

Richard Gaal, pour la résolution des problèmes techniques.

Helmut Berger, pour les échantillons.

Mirko Milas, pour les mesures de microscopie électronique.

Kyumin Lee, pour les mesures de microscopie à force atomique.

Patrick Mayor, pour le soutien linguistique.

Les mécaniciens.

Tous les collègues de l'institut et de l'EPFL.

Bettina Welter, pour les mesures dans des structures de joint de grain.

Les nombreuses personnes qui ont montré de l'intérêt pour la discussion des résultats.

Le programme "Doktorieren an der anderen ETH" pour les financements.

Ma famille.

Et spécialement Mat pour m'avoir donné la pêche pendant ce temps !

Curriculum vitae

Thomas Geiges
Ch. de l'Ochettaz 18
1025 St-Sulpice
thomas.geiges@a3.epfl.ch; thomas.geiges@alumni.ethz.ch
Né le 7 avril 1976 à Winterthur (Suisse)
Etat civil: Marié
Nationalité: Suisse

Études

2004–2005	Étude des "Break junctions" en BSCCO chez Prof. László Forró
2002–2003	Spectroscopie mécanique en LSCO chez Dr. Gianfranco D'Anna
2002–2005	Thèse à l'institut de physique de la matière complexe (IPMC) EPFL Lausanne
2001	Didaktischer Ausweis ETH Zürich (diplôme en didactique)
2001	Travail de diplôme à l' "Institut für Neuroinformatik" à l'ETH Zurich
1998–1999	Année d'échange (Erasmus) à la "Universidad de Granada" (Espagne)
1996–2001	Études de physique à l'ETH Zürich
1996	Maturité type B (latin) à la "Kantonsschule Stadelhofen Zürich"

Divers

Langues:	Allemand, Français, Anglais et Espagnol courants. Base en Italien.
Loisirs:	Sport: cyclisme, alpinisme (hiver et été), course d'orientation, ski de fond, volley-ball, planche à voile Musique: violoncelle